Department of Chemistry

Organic and Isotopic Geochemistry of Source-rocks and Crude Oils from the East Sirte Basin (Libya)

Salem Abdulghni-O-Aboglila

This thesis is presented for the Degree of
Doctor of Philosophy
of
Curtin University of Technology

30 June 2010

Declaration

To the best of my knowledge and belief this thesis contains no material previously published by any other person except where due acknowledgement has been made.

This thesis contains no material that has been accepted for the award of any other degree or diploma in any university.

Salem Aboglila

Perth, October 18, 2010

Abstract

The Sirte Basin is a major oil producing area in Libya, but the understanding of the processes that have led to the petroleum accumulation is still limited. Exploration studies of this area have shown that the oils are mixtures of several charges and may be from different source rocks. The main aims of this thesis are to improve our understanding of the petroleum accumulation history in the East Sirte Basin.

Biomarker ratios, together with stable carbon ($\delta^{13}C$) and hydrogen (δD) isotopic compositions of individual hydrocarbons have been applied to 24 crude oils from the East Sirte Basin to delineate their sources and respective thermal maturities. The crude oil samples are divided into two main families (A and B) based on differences in source inputs and thermal maturity. Using source-specific biomarker parameters based on pristane/phytane (Pr/Ph), hopane/sterane ratios, dibenzothiophene (DBT)/ phenanthrene (P), Pr/*n*-C_{17}, Ph/*n*-C_{18} and the distribution of tricyclic and tetracyclic terpanes, family B oils are ascribed a marine source rock deposited under sub-oxic conditions, whereas family A oils have a more terrestrial source affinity. This source classification is supported by the stable carbon isotopic compositions ($\delta^{13}C$) of the *n*-alkanes. Family A oils were found to be more mature based on differences between the stable hydrogen isotopic compositions (δD) of Pr and Ph and the *n*-alkanes, as well as the $\delta^{13}C$ values of *n*-alkanes.

Within a complex geological setting several potential source rocks have been recognised, ranging in age from Precambrian to Eocene. Biomarker ratios, together with $\delta^{13}C$ and δD of individual hydrocarbons have been applied to 21 source rock extracts from the East Sirte Basin to establish their respective thermal maturity and palaeoenvironmental conditions of deposition. Rock Eval pyrolysis data obtained from the source rocks of the Sirte, Tagrifet, Rakb, Rachmat, Bahi and Nubian Formations show that the organic matter (OM) is mainly dominated by a Type II/III kerogen. Vitrinite reflectance (% R_o range: 0.46 – 1.38) data support variations in thermal maturity and indicate mature to post mature rocks of Sirte and Rachmat Formations and early to mid stage maturities for the rest of the formations. The Sirte Formation in the studied area

was found to be relatively more thermally mature than the Tagrifet, Rakb, Rachmat, Bahi, and Nubian Formations, reflected by δD of Pr and Ph (less depleted in D).

Various unusual steroid biomarkers in the oils and East Sirte source-rocks were identified by gas chromatography- mass spectrometry (GC-MS) and GC-metastable reaction monitoring (MRM) mass spectrometry. These included 24-*nor*cholestanes, dinosteranes, 4α-methyl-24-ethylcholestanes and triaromatic steroids. Diatoms, dinoflagellates and/or their direct ancestors are the proposed sources of these components. These biomarker parameters have been used to establish a Mesozoic oil-source correlation of the East Sirte Basin. This is consistent with the presence of dinoflagellate cysts in the Nubian Formation of Lower Cretaceous age.

Acknowledgements

'My greatest praise to my creator and peace upon all his prophets'.

First a special word of thanks goes to my principal supervisor Professor Kliti Grice. Her scientific guidance, feedback, motivation and continued encouragement have been tremendous. Thanks to Kliti I have had the chance to prepare 3 reviewed international journal articles and present my research at several conferences, as well as achieving my academic aims. I am very fortunate and proud to be a part of the team of PhD students and research fellows supervised by Professor Kliti Grice. I would also like to thank my co-supervisor Dr Katherine Trinajstic, who has given me lots of geological feedback and helped me with writing. I would like to especially thank my wife Eiman for her patience and unlimited encouragement and help.

I extend my thanks to Dr Daniel Dawson. His extensive knowledge, experience and training have been valuable to me over the years and particularly in my first year.

Sincere thanks to my parents, my brothers and sisters and my friends for their encouragement. Thanks also you to Prof Alhadi Almighriby for his help.

Thank you to Mr Geoff Chidlow and Mrs Sue Wang for technical assistance with gas chromatography-mass spectrometry and gas chromatography- isotope ratio mass spectrometry, respectively.

I would also like to thank my PhD colleagues in the WA Organic and Isotope Geochemistry Centre. Special thanks to Amy Bowater for her assistance and a big thank to Tanya Chambers for all her help with administration and travel. Thank you to my friend Muhammad Asif from Lahore University for his useful discussions. I thank Curtin University of technology for a scholarship for my final year of my study. I am grateful to the staff of the National Oil Corporation (NOC) in Tripoli, and staff of the Libyan Petroleum companies (Waha – Veba - Gulf) for providing me with samples. A final big thank you to all staff and students in the Department of Chemistry and in the WA Organic and Isotope Geochemistry Centre at Curtin.

I also thank my external PhD examiners (Dr Ameed Ghori from Geological Survey WA and Assistant Professor Joseph Werne (University of Minnesota, Duluth, US) for reviewing my PhD thesis and providing helpful feedback.

Primary Publications

This thesis is assembled by publications, either *in press*, or submitted, which form the individual chapters and are listed below.

CHAPTER 2

S. Aboglila, K. Grice, K. Trinajstic, D. Dawson, K. H. Williford (2010). Use of biomarker distributions and compound specific isotopes of carbon and hydrogen to delineate hydrocarbon characteristics in the East Sirte Basin (Libya) *Organic Geochemistry*. ERA A.

CHAPTER 3

S. Aboglila, K. Grice, K. Trinajstic, D. Dawson, K. H. Williford (2010). A geochemical evaluation of thermal maturity and depositional palaeoenvironments of seven Cretaceous formations from the East Sirte Basin (Libya), *Libyan Petroleum Institute Journal*. *In Press.*

CHAPTER 4

S. Aboglila, K. Grice, K. Trinajstic, C. Snape and K. H. Williford (2010). The significance of 24-norcholestanes, 4-methylsteranes and dinosterane in oils and source-rocks from East Sirte Basin (Libya), *Applied Geochemistry*. ERA A. *In Press.*

Contribution of others

The work presented in this thesis was primarily designed, experimentally executed, interpreted, and the individual manuscripts were prepared by the first author (Salem Aboglila). Contributions by co-authors are described below.

CHAPTER 2

Salem Aboglila, Kliti Grice, Kate Trinajstic**,** Daniel Dawson and Ken Williford contributed to the writing of the paper. Salem Aboglila performed experiments, interpreted results, and wrote the paper. Salem Aboglila, Kliti Grice, Kate Trinajstic and Daniel Dawson provided intellectual input through discussions on the interpretation of results. Kliti Grice provided analytical facilities.

CHAPTER 3

Salem Aboglila, Kliti Grice, Kate Trinajstic**,** Daniel Dawson and Ken Williford contributed to the writing of the paper. Salem Aboglila performed experiments, interpreted results, and wrote the paper. Salem Aboglila, Kliti Grice, Kate Trinajstic and Daniel Dawson provided intellectual input through discussions on the interpretation of results. Kliti Grice provided analytical facilities.

CHAPTER 4

Salem Aboglila, Kliti Grice and Kate Trinajstic contributed to the writing of the paper. Salem Aboglila performed experiments, interpreted results, and wrote the paper. Salem Aboglila, Kliti Grice and Kate Trinajstic provided intellectual input through discussions on the interpretation of results. Ken Williford extracted and separated the coral sample. Colin Snape performed hydropyrolysis experiments on the coral extract. Kliti Grice provided analytical facilities.

Contents

Chapter 2.

Chapter 3.

List of Figures

Chapter 1.

Chapter 2.

Chapter 3.

Chapter 4.

List of Tables

Chapter 1.

Chapter 2.

Chapter 3.

Chapter 4.

Chapter 1 Introduction

1.1. Sediments and organic matter (OM)

1.1.1. Origin of sedimentary organic matter (SOM)

Sedimentary organic matter (SOM) originates from biologically-derived material from the three-domains of life i.e. Archaea, Prokaryotes and Eukaryotes (Woese et al., 1990). Carbon is the basic element of life on Earth. It is the major constituent of OM spanning from simplistic hydrocarbons to complex molecules like DNA (i.e. a component that controls genetic reproduction). Carbon constantly alternates between the biosphere, hydrosphere, geosphere and atmosphere. Carbon accumulates in extant and deceased organisms in the biosphere, exists as gaseous carbon dioxide (CO_2) in the atmosphere, exists as OM in water, soils and the lithosphere, forms petroleum, and sedimentary inorganic rock accretions as well as existing in a dissolved form as inorganic carbon in oceans and lakes. Calcified deposits are also made by certain marine organisms (Tissot and Welte, 1978).

A number of organisms are photoautotrophic and use CO_2 as their only carbon source. With water and sunlight, these organisms carry out photosynthesis to fix the CO_2 into basic biochemical units. Eventually these units lead to proteins, cellulose and amino acids through biosynthesis (Peters et al., 2005). OM produced by photoautotrophic organisms can be passed onto other organisms through the food-chain. When organisms die, their OM under certain conditions can be transported and buried in sediments. Sediments are thus described as being comprised of unconsolidated minerals with OM or pre-existing rocks that can either be transported by water, wind or glaciers. Sedimentary rocks arise from the deposition (sedimentation, Fig. 1.1) and consolidation of OM in the subsurface. Parent rock lithology is determined by the kinds of minerals present, whereas, the OM in sediments comes predominantly from the lipid remains of Prokaryotes, Eukaryotes and Archeae. Fine-grained sediments (≥1% OM) and ≥0.5 wt.% total organic carbon TOC) can potentially lead to rocks offering fair petroleum potential if they are buried adequately.

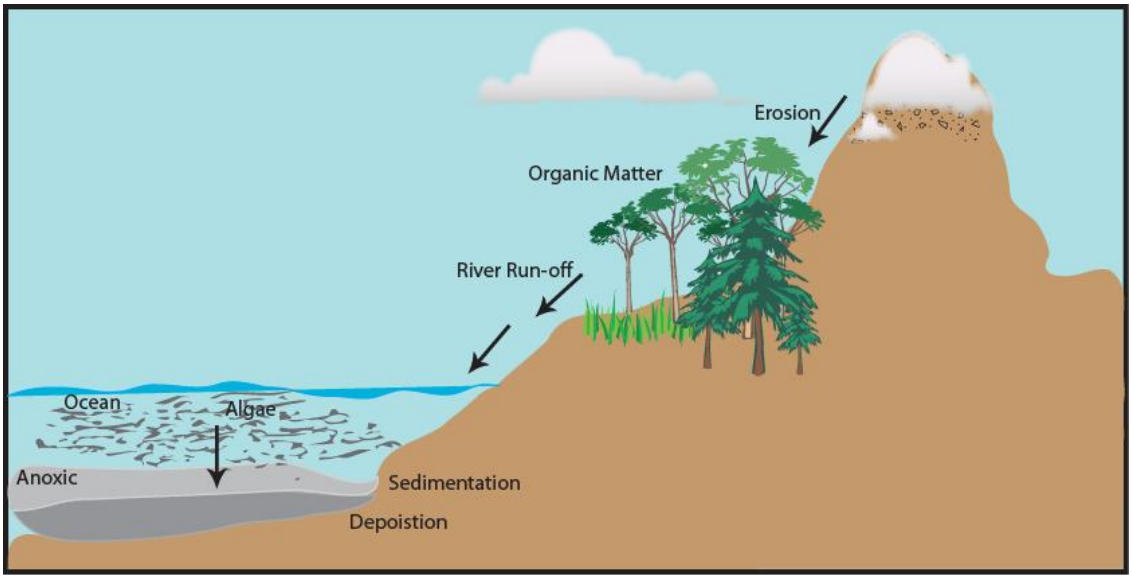

Fig. 1.1 Deposition of terrestrial and marine OM

1.1.2. Preservation of SOM

During sedimentation and initial burial, quite a few processes lead to almost total destruction of OM. < 0.1% of carbon produced by organisms (i.e. biomass) generally gets preserved in sediments. In order to lead to the formation of OM-rich sediments, the OM needs to be incorporated into the sediments and preserved under very special conditions (e.g. Berner, 1982; Emerson et al., 1987). It is best preserved under low oxygen conditions (i.e. reducing) < 0.1% of OM is preserved under oxygenated conditions and > 10% of OM can be preserved under reducing conditions (Hedges and Keil, 1995). Large amounts of OM are best conserved in stagnant water bodies (i.e. lakes and/or restricted marine basins (i.e. less oxygen is mixed with the bottom waters). Stagnant water bodies can either be stratified (temperature or salinity gradients). In addition to the redox conditions, other factors are important such as high algal productivity sustained with elevated nutrient inputs (i.e. phosphate, nitrate) and with oxygen available for photosynthesis, allowing for algae to bloom.

1.1.3. Molecular composition of SOM

SOM consists of bitumen and kerogen (see below). Biomarkers or molecular fossils carry a wealth of information concerning the composition, ecology and diversity of microbial and land plant communities. Many of the biomarkers

reported in sediments and petroleum have been related to lipids and other biochemicals of extant organisms, thus allowing their biomarker-precursor relationship to be established (Brocks and Grice, 2010 and references therein). Lipids are the molecular components of cell membranes including, sterols, hopanols, alcohols, phospholipids and ether-lipids. Maleimides are an important biochemical class that can also be formed through oxidation of chlorophylls and bacteriochlorophylls in various photoautotrophs (Grice et al., 1996a).

The sedimentary biomarkers of sterols are steranes which have become an important molecular tool for paleontologists because of a resistance to microbial attack over significant periods of time. Thus, they are well represented biomarkers in the rock record. The sedimentary discovery of many diverse steranes reflects considerable taxonomic and/or physiological specificity and has stimulated a search for unique naturally occurring sterols in many branches of the Eukaryotic domain of life. For example, ergosterol is a precursor of the biomarker ergostane occurring in fungi and several groups of algae, including coccolithophorids and diatoms, while sterols with the stigmastane skeleton are very widespread in higher plants, eustigmatophytes, chrysophytes and green algae (Chlorophyceae). The biomarker 24-*iso*propylcholestane has been suggested as a marker for sponges or their direct ancestors due to its high relative abundance in pre-Ediacaran-Early Cambrian sedimentary rocks and oils (Love et al., 2009). Recently the oldest evidence for early metazoan evolution in the fossil record has come from demosponge-derived biomarkers and which pushed the date for the earliest-known animal life back by at least 100 million years (Love et al., 2009).

Biomarkers in solvent extracts are traditionally detected by gas chromatography-mass spectrometry GC-MS (MS) or by their distinctive stable isotopic values now measurable with the advent of compound specific isotope analysis (CSIA) - see below. The identity, isomeric arrangement and stable isotopic composition of biomarkers have been widely used in studies of petroleum and SOM to assess the source of OM, palaeoenvironmental depositional information and for a source correlation of oil and rock samples (Grice and Brocks, 2010 and references therein).

1.1.4. Formation of petroleum

1.1.4.1. Kerogen

Kerogen is a complex high-molecular-weight material, insoluble in common organic solvent and it is the major starting material of oil and gas. It is also the most abundant form of organic carbon on Earth. Kerogen forms during the early stages diagenesis, *via* polycondensation and defunctionalisation mechanism (Tissot and Welte, 1978) or from the selective preservation pathway (e.g. Gelin et al., 1996; Zonneveld et al., 2009). Kerogens are characterised into four types based on the composition of the OM and the depositional environments of the sediments which led to their formation. The four types are I, II, III and IV, whereas II-S is part of II type in Fig. 1.2 (Killops and Killops, 2005). Kerogens also have different atomic ratios (i.e. Oxygen to carbon: O/C and hydrogen to carbon: H/C. The type of kerogen is represented in the Van Krevelen (1961) diagram (Fig. 1.2).

Type I kerogen is exceptional and is formed from OM of freshwater/lacustrine algae such as *Botryococcus braunii* and has the potential to generate a high grade oil. Type I contains less aromatic and hetero components. The H/C can extend up to 1.9. This kerogen is often associated with fine-grained, organic-rich silts that are deposited under low oxygen conditions and in shallow water (Tissot and Welte, 1978). Type II kerogen consists of a mixture of terrestrial and marine derived OM deposited under marine conditions and can potentially yield oil and gas. The kerogen consists predominantly of aromatic and ketone structures and can contain organosulfur compounds between 8-14% and are referred to as Type II-S kerogens (Killops and Killops, 2005). The H/C ratio extends up to 1.4. Type III kerogen has the potential to yield gas and is derived from terrestrial OM deposited in a deltaic/ marine setting. This kerogen also contains polyaromatic and ketone compounds (Tissot and Welte, 1978; Killops and Killops, 2005). The H/C ratio is usually less than 1. Type IV kerogen is probably derived from higher plant material that has been transported and highly oxidised. These kerogens have virtually no oil or gas generative potential (Killops and Killops, 2005).

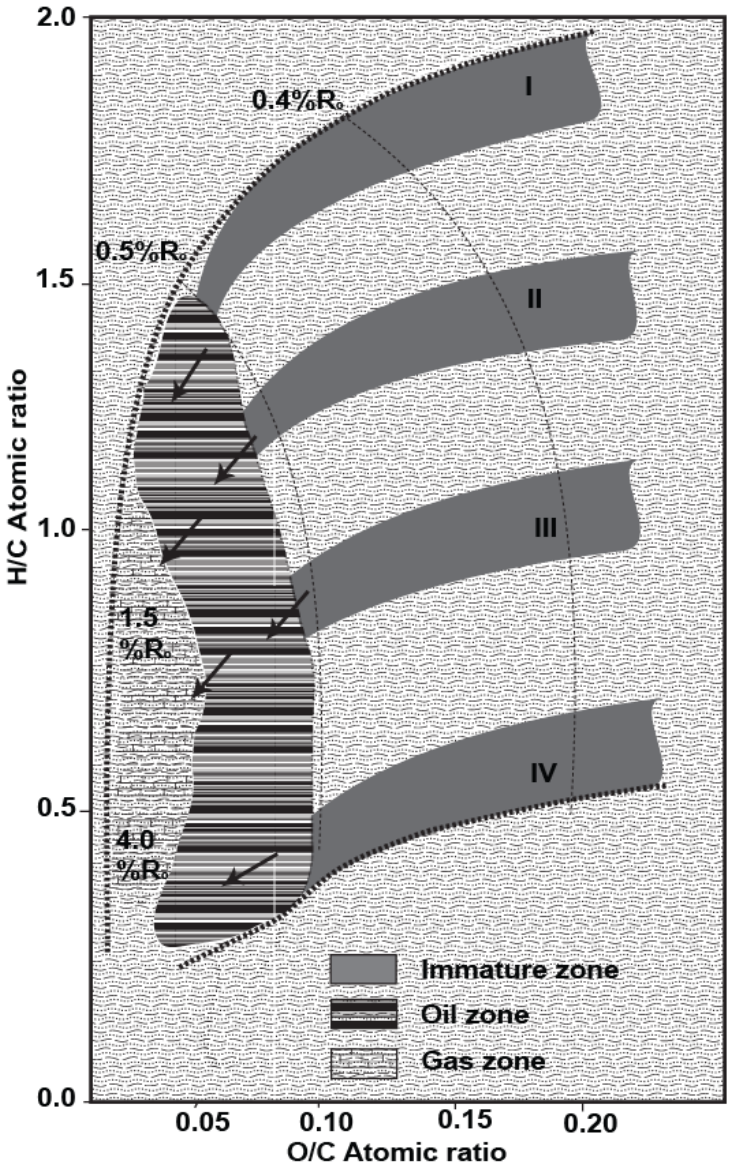

Fig. 1.2 Types and chemical evolution of kerogen in response to increased levels of burial and thermal maturity presented on Van Krevelen's diagrams (arrows indicate increasing maturity) (Maslen et al., 2010).

1.1.4.2. Thermal Maturity

Increasing temperature and pressure during deeper burial of sediments causes thermal breakdown of kerogen, thus producing petroleum (Fig 1.3, Hunt, 1996). The quantity of hydrocarbon generated by a potential source rock is controlled not just by the amount of the SOM but also by the level of thermal maturity. Maturation of SOM can be influenced by temperature, pressure and time (Tissot and Welte, 1978).

The temperature range during catagenesis is considered a significant process to delineate hydrocarbons from the oil window, gas window and oil and gas window (Speight, 1999). Expulsion is a process of the petroleum migrating away from its source rock. Immature source rocks are described as containing OM that has undergone diagenetic effects without a significant effect from temperature. Mature source rocks contain OM that has undergone significant thermal breakdown. This generally occurs during catagenesis and represents the major zone of oil production. Post-mature source rocks contain OM matter that has undergone thermal destruction yielding graphite capable of only generating gas, brought about by the stage of metagenesis. Various maturity parameters that are used to describe the thermal evolution of SOM, include, thermal alteration indicators (vitrinite reflectance), bulk geochemical parameters (Rock-Eval pyrolysis) and molecular parameters (various biomarker ratios). Thermal Alteration Index (TAI) is based on the change of colour of spores and pollen with maturity (Tissot and Welte, 1978), vitrinite particles from land-plants reflect light. The rreflectance increases with maturity as the molecular structure changes. Such changes are predictable and consistent.

The reflectivity of at least 30 individual grains of vitrinite from a rock sample is measured under a microscope. The measurement is given in units of reflectance, % R_o, with typical values ranging from 0% R_o to 3% R_o. $R_o < 0.6$ is indicative of immaturity, $0.6\% < R_o > 1\%$ falls within the oil window and $R_o >$ 1% over mature. TAI, Rock Eval pyrolysis parameters and vitrinite reflectance cannot be applied to crude oils. Thus many molecular parameters have been developed to estimate maturity levels of crude oils. These are in turn also used to estimate maturity of SOM, and are often related back to the bulk parameters. Molecular parameters generally include ratios of selected compounds. Ideally they reflect the extent of the chemical reactions that these compounds are involved in. Often there is a decrease in abundance of a compound relative to its more stable isomerisation product. The decreasing compound usually has a configuration derived directly from a natural product, and is inherently less stable (Fig. 1.4).

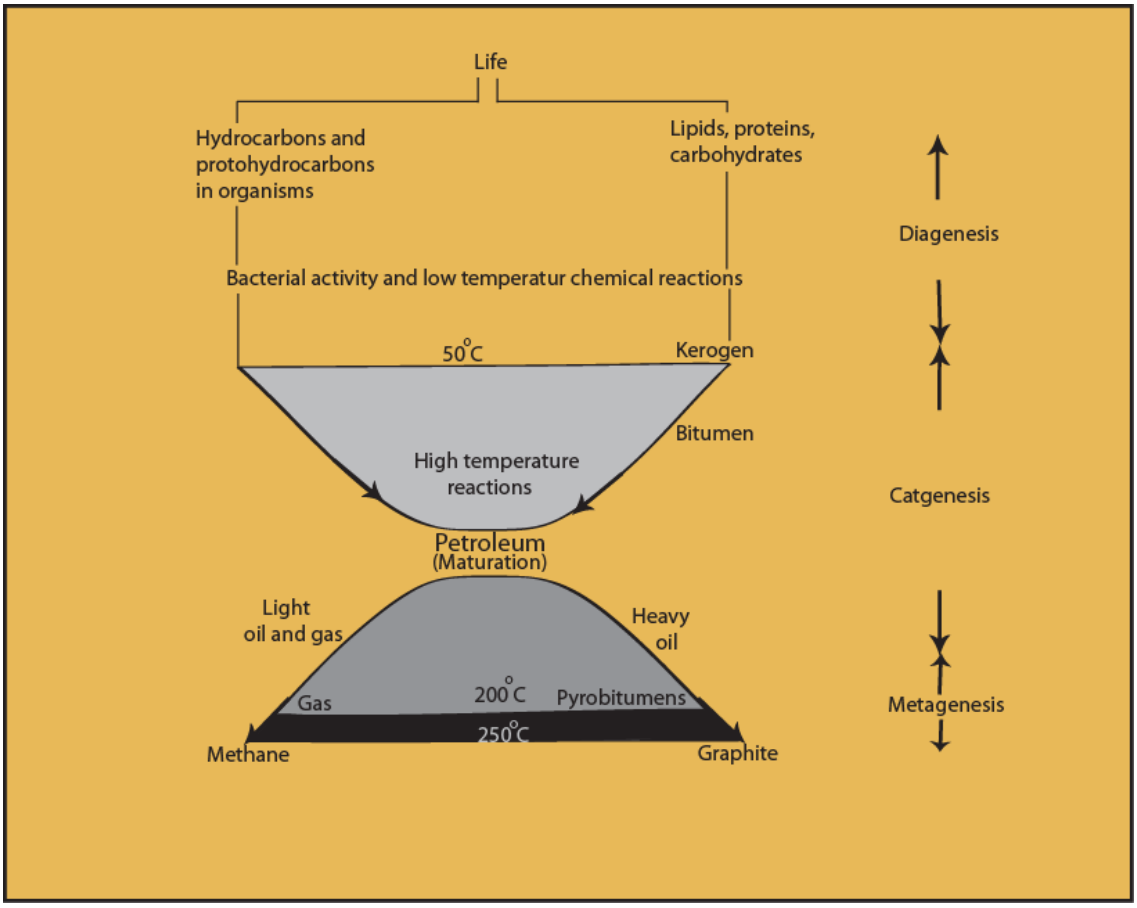

Fig. 1.3 Stages of kerogen transformation and hydrocarbon formation pathways in geological situations (from Hunt, 1996).

Maturity Model

Molecular maturity parameter A/A+B
Increases when:

1. B → A
2. Kerogen → A > Kerogen → B
3. B →Products > A → Products

1. Interconversion - direct isomerisation in the bitumen
2. The relative rates of generation from kerogen or another non-hydrocarbon fraction
3. Relative rates of cracking - i.e. thermal degradation, reliant upon the relative stabilities of the compounds.
4. All of the above

Fig. 1.4 Model thermal maturity estimate maturity of from kerogen and bitumen fraction.

Various maturity parameters based on abundance of saturated compounds and include, (i) Steranes ααα, αββ, diasteranes, 20*S*/*R* and (ii) Hopanes Ts, diahopanes, 22*S*/*R*. Parameters based on aromatic hydrocarbon distributions, include various ratios of alkylnaphthalene, alkylphenanthrene and dibenzothiophenes. *20S/(20S + 20R); Sterane isomerization; 20S/(aaa20S + aaa20R)].* E.g. Isomerization at C-20 in the C_{29} 5α (H), 14α (H), 17α (H)-steranes causes the 20*S*/(20*S* + 20*R*) ratio to rise from 0 to about 0.5 (0.52 to 0.55 = equilibrium; Seifert and Moldowan, 1986) with increasing maturity (Fig. 1.5).

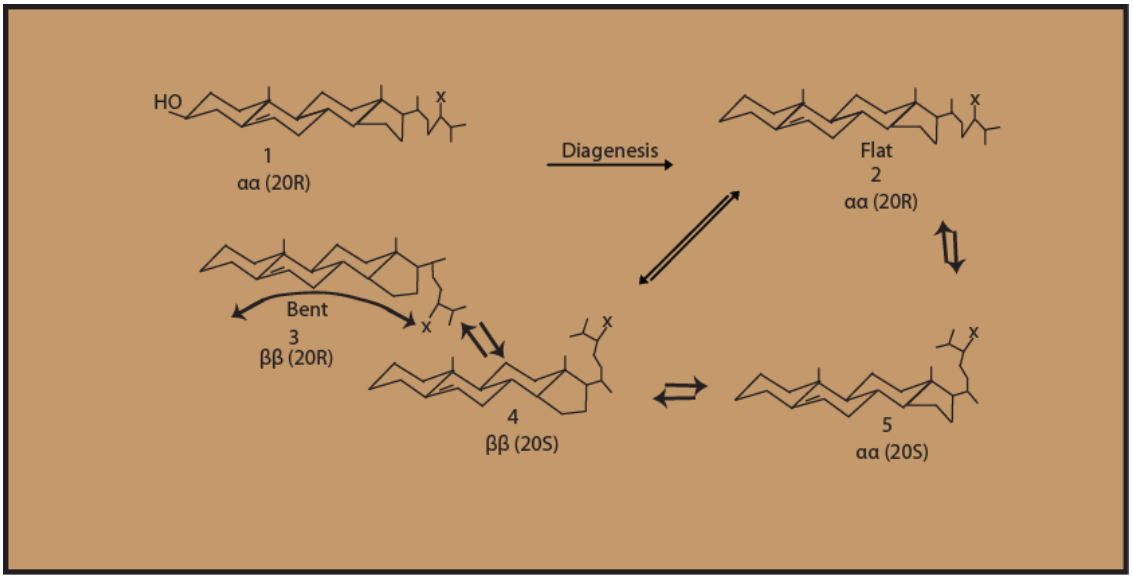

Fig. 1.5 Sterane maturity (*20S/(aaa20S + aaa20R)*

1.1.4.3. Source to Reservoir

The processes that kerogen undergoes in a source rock to a reservoir rock involves expulsion, migration and eventually it becomes trapped in a reservoir by a seal (Fig. 1.6). A number of geological structures in sedimentary basins must be in place for the accumulation of petroleum, such as a source rock enough OM to generate hydrocarbons, followed by a mechanism for the petroleum to move or migrate. A reservoir rock with a configuration to constitute a trap and be covered by a seal with low-permeability prevents further migration.

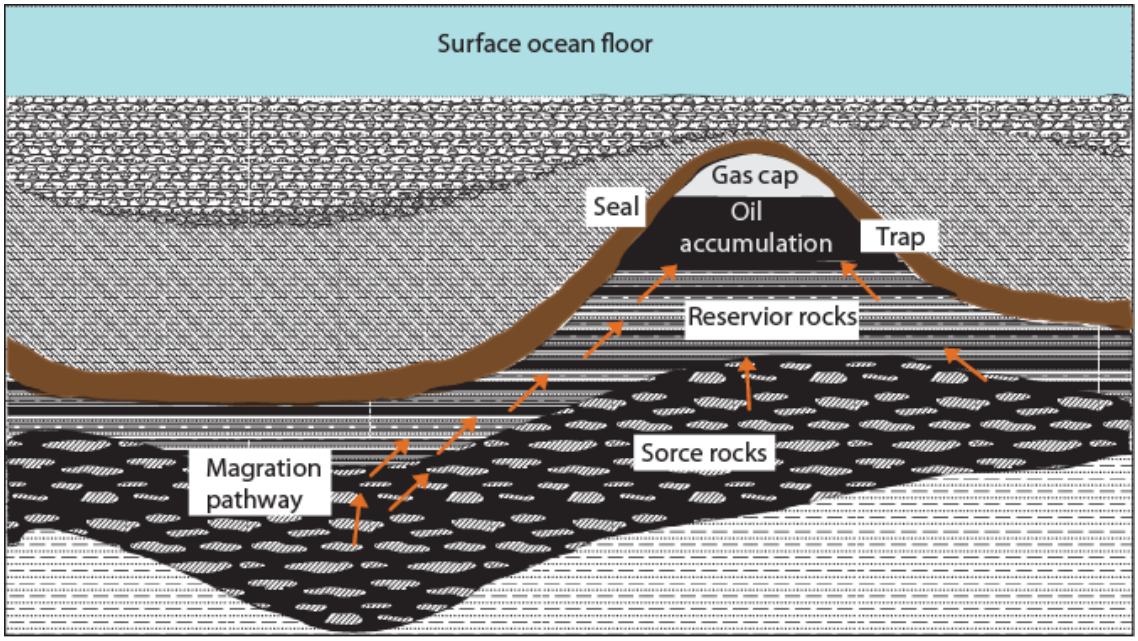

Fig. 1.6 Depicting structural styles of hydrocarbon migration pathways and entry pathways into reservoirs and traps (Speight, 1999)

1.1.4.4. Composition of Petroleum

Petroleum is a complex assortment of hydrocarbons i.e. saturated hydrocarbons, aromatic hydrocarbons, NSO compounds and metal porphyrins containing mainly vanadium and nickel (Hunt, 1996). Saturated hydrocarbons include, normal and branched alkanes, cycloaliphatic hydrocarbons (e.g. alkylcyclohexanes) and polycyclic compounds (e.g. hopanes). Aromatic hydrocarbons consist of benzene and polycyclic aromatic hydrocarbons-PAHs), as well as their methylated and alkylated counterparts, and aromatics with heteroatoms (N, S and O). NSO compounds also contain heteroatomic elements (mainly N, S and O) phenols, fatty acids, alcohols and asphalthenes. Some petroleum compounds are directly derived from the macromolecular kerogen, and can be directly related to their biological precursors. Other petroleum components are formed in the subsurface and are often referred to as geosynthetic products.

1.1.5. Analysis of Petroleum

1.1.5.1. Gas-Chromatography-Mass Spectrometry (GC-MS)

In order to identify biomarkers in sediments and petroleum GC-MS fingerprinting analysis techniques are applied (Peters et al., 2005). Certain ions diagnostic (usually the base peak of the mass spectrum) of the biomarker are used in identification along with their relative retention time and mass spectral data. *m/z* 191 is a diagnostic ion of hopane biomarkers (Table 1.1).

Table 1.1 Diagnostic ions for compounds identified by GC-MS

Compound name	Diagnostic ion
C_{19} Tricyclic terpane	191
C_{23} Tricyclic terpane	191
C_{24} Tetracyclic terpane	191
Trisnomeohopane, Ts, (C_{27})	191
Hopane (C_{30})	191
Pentakishomohopane (C_{35})	191
Diacholestane (C_{27})	217
Cholestane (C_{27})	217
Cholestane (C_{28})	217
Cholestane (C_{29})	217
Naphthalene	128
Triaromatic Steroid	245
Phenanthrene	178
Dibenzothiophene	184

1.1.5.2. Stable Isotopes

Carbon and hydrogen both have two stable isotopes, ^{12}C and ^{13}C and ^{1}H and ^{2}D, respectively. 98.899 weight % of ^{12}C is present in nature, whereas ^{13}C only accounts for 1.111 weight % of the total pool of carbon (Tissot and Welte, 1984). 99.985 weight % of ^{1}H and 0.0105 weight % of ^{2}D is present in the total pool of hydrogen. Isotope fractionation leads to changes in the relative abundance of isotopes and occurs naturally within chemical, biochemical and physical processes (Hoefs, 1987). Stable isotope composition is expressed as a ratio calculated by the δ (delta) notation and is presented in per mil (‰):

$$\delta_{sample} = [(R_{sample} - R_{standard})/R_{standard}] \times 1000\ ‰$$

For carbon, R is the measured ratio of ^{13}C to ^{12}C for a sample and a standard, respectively, relative to an international marine carbonate standard (i.e. Vienna Pee Dee Belemnite, VPDB)(Hoefs, 1987). For hydrogen, R is the measured ratio of D to H in a sample and a standard, respectively, relative to the international Vienna Mean Ocean Water (VSMOV) standard (Werner and Brand, 2001). Two

stable isotope methods are often used to measure samples. These include bulk stable isotope analysis and CSIA.

Bulk stable isotope analysis allows measurement of the stable isotopic composition of the total carbon (C) and hydrogen (H) in a sample. Thus it is used to assess the isotopic composition of all compounds in a mixture and thus only provides an average value for all components in a mixture. CSIA allows the measurement of individual compounds (e.g. hydrocarbons) in a complex matrix (e.g. petroleum and bitumen extracts from sediments) leading to specific data and is carried out with a gas chromatograph - isotope ratio monitoring - mass spectrometer (GC-irm-MS). The GC is attached to an irm-MS *via* a combustion interface to allow the $^{13}C/^{12}C$ measurement of individual organic components (Matthews and Hayes, 1978). The Micromass furnace interface used in this work either consisted of a quartz tube containing CuO pellets (850°C) allowing the production of CO_2 and H_2O for each GC-separated component. H_2O is removed with a liquid N_2 trap at -100°C. The irm-MS measures the abundances of the ions *m/z* 44 ($^{12}CO_2$), 45 ($^{13}CO_2$) and 46 ($^{12}C^{18}O^{16}O_2$). For D/H CSIA the GC is linked to the irm-MS *via* a pyrolysis furnace containing a catalyst of Cr (e.g. Prosser and Scrimgeour, 1995). The irm-MS measures the abundances of the ions *m/z* 3 (^2DH) and 2 ($^1H_2$). Contributions from H^{3+} ions in ppm produced in the ion source are corrected following *m/z* 3 analyses at two variable pressures of the H_2 reference gas (Dawson et al., 2004; Grice et al., 2008).

1.1.5.3. Carbon Isotope Composition

The $\delta^{13}C$ values of crude oils or rock extracts, their fractions, and individual compounds, have been employed to find out origin, age and the environmental deposition of the source (e.g. Sofer, 1984; Andrusevich et al., 1998). Thermal maturation is one of many factors that can affect stable carbon isotopes, leading to heavier values (Dawson et al., 2007). The maturation leads to enrichment in ^{13}C in the source rocks due to the release of ^{13}C-depleted components in the generated hydrocarbon (Clayton, 1991). Biodegradation has effects on the $\delta^{13}C$ which leads steadily to enrichment of ^{13}C values in remaining compounds with increasing molecular weight (e.g. George et al., 2002; Asif et al., 2009).

1.1.5.4. Hydrogen Isotope Composition

Typically, SOM derived from marine source rocks has δD value close to -150‰ with a significant alteration through isotopic exchange can occur by thermal maturity (Santos Neto and Hayes, 1999). In meteoric waters in hot-arid environments, high δD in OM is incorporated by aquatic organisms due to the intense evaporation of water. δD of OM in terrestrial plants is determined by evapo-transpiration, δD of meteoric water, leaf morphology and plant physiology (e.g. Grice et al., 2008). Typically, OM from a terrestrial source shows more negative δD values compared to marine sourced OM due to the fact that meteoric water is often depleted in D compared to marine-sourced water (Craig, 1961) (Dawson et al., 2007). Although, a wide difference in δD values have been reported in terrestrial derived OM (Schimmelmann et al., 2004; Xiong et al., 2005).

The water in the world's oceans contains the major natural reservoir of hydrogen, and is important in the global hydrological cycle. In marine and terrestrial environments, ocean water, and/or meteoric water formed by operation of the hydrological cycle is taken up by biota. Therefore, the distribution of D/H in present day environments is mostly inhibited by the natural processes of the hydrological cycle. The Vienna Standard Mean Ocean Water (VSMOW) has an isotopic composition of 0±5‰ (Craig and Gordon, 1965). The first stage of the hydrological cycle results from the evaporation of ocean water to form clouds with the largest amount of water evaporating in tropical provinces according to the Rayleigh model. Consequently, when the water vapour is transported to lower temperature regions (i.e. higher latitudes) condensation takes place leading to rain-fall (Fig. 1.7).

The δD of petroleum, particularly using CSIA is used in correlation studies for petroleum and source rocks. It is also useful parameter of thermal maturity, as well as biodegradation (e.g. Rigby et al., 1981; Li et al., 2001; Pedentchouk et al., 2006; Asif et al., 2009). The δD of sedimentary saturated hydrocarbons has been used to assess thermal maturity of sediments and petroleum from the Perth Basin in Western Australia and the Vulcan-sub Basin in the Timor Sea (Dawson et al. 2004 and 2007). The application of δD for thermal maturity has been extended back to the Devonian in samples that lack vitrinite (Maslen et al.,

2010).

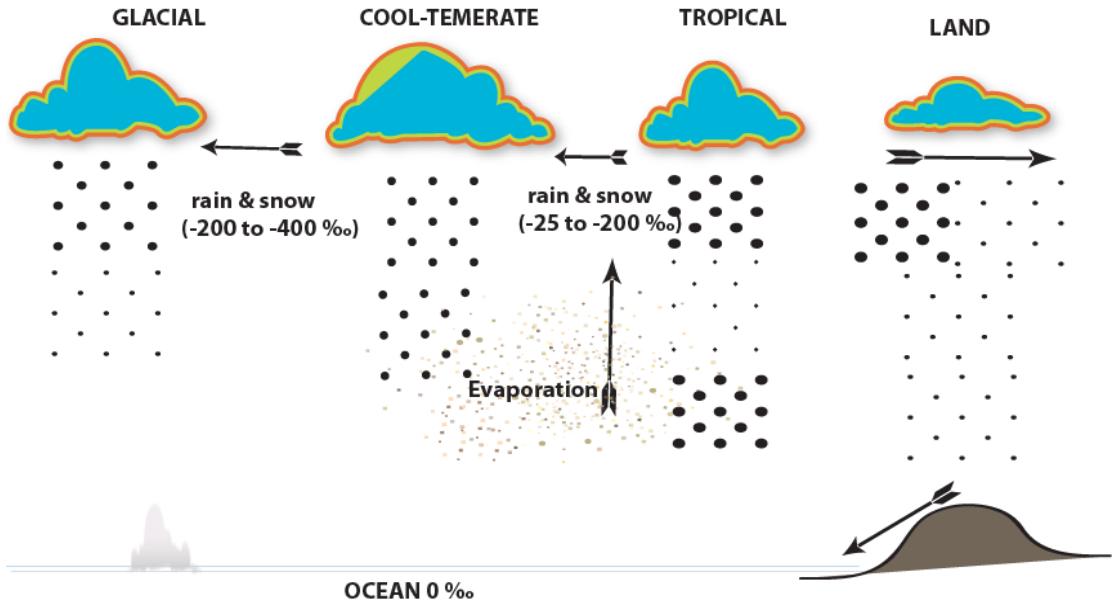

Fig. **1.7** Variation in the stable hydrogen isotopic composition of water in the hydrological cycle from the ocean to the land

1.2. Geology and Petroleum Systems of the Sirte Basin

1.2.1. Introduction to the geology of Libya

The northern coast of Libya is located along the south Mediterranean Sea in the centre of the North African Margin and its geology reflects a polyphone tectonic history, which has been ongoing since the Precambrian. Within Libya there are five sedimentary basins, the evolution of which has been controlled by seven major tectonic events common across the northern margin of Africa: the compressional Pan African orogeny, which joined proto-continental segments into an early Gondwanaland; the Infracambrian extension, a period of alternating extension and compression throughout the Cambrian to Carboniferous; the Late Carboniferous Hercynian Orogeny, which effected southern and central Europe in addition to North Africa; rifting events in the Late Triassic to Early Jurassic and again in the Early Cretaceous and final rifting event in the Oligocene-Miocene and the Cretaceous compression events associated with the breakup of Gondwana and the evolution of the Mediterranean Sea from the Tethys (Craig et al, 2004). These tectonic phases,

originated in the Precambrian, and controlled subsequent sedimentation in all of the Libyan basins.

The Palaeozoic Ghadames, Murzuk and Kuffra Basins are sag basins and are located onshore (Fig. 1.8) within a tectonically stable region of the country whereas the Late Mesozoic – Cenozoic Sirte Basin lies in a more tectonically active area in the north-central region of the country and the Cyrenaica Basin, which is divided into the tectonically stable Cyrenaica Platform, and the more tectonically active Al Jabal al Akhdar Uplift which is located along the north-east coast of Libya (Gumati et al., 1996) (Fig. 1.9). Offshore, also in a tectonically active area along the north-western coastline, lies the Tripolitana Basin. All of these basins have yielded petroleum deposits of economic importance with onshore, production is primarily oil however, offshore increased thermal gradient and deeper burial indicates a greater potential for gas production (Ahlbrandt, 2001).

The intracratonic Ghadames Basin is separated from Murzak Basin by the Qarqaf uplift and both basins extend across Libya's western border into Algeria, the more southern Murzak Basin also extends into Niger and Chad. The oils of the Ghadames Basin are sourced from Middle Devonian and basal Silurian shales while Lower Devonian and Upper Silurian deposits form reservoirs. The Murzak Basin has sediments fills ranging in age from Cambrian to Quaternary with the Silurian Tanzuft shale the major charge in terms of source rock. The major reservoirs are in Ordovician Sandstones; however, there are also some Upper Silurian and Lower Devonian reservoirs. The geological setting of the Al Kufra Basin is similar to the Murzak with both basins located on the northern African craton with sediment fills dominantly composed of clastics overlying basement. This basin is underexplored and to date no commercial discoveries of oil have been made; although, Lower Silurian Shales and Upper Ordovician Sandstone appear prospective. The Cyrenaica Platform within the Cyrenaica Basin contains several potential reservoir and seal rocks with Upper Cretaceous and Tertiary sediments. The Sirte Basin is the major source for the petroleum industry of Libya, notably the east arm of the basin, which has proved to be the most productive (Ahlbrandt, 2001). The only offshore basin of Libya is the Tripolitania Basin and this basin contains the largest oils field discovered in the

Mediterranean Sea. The major source rock is organic shale of Early Eocene Age. The geological framework of Libya has been described by Burwood, 1996; Gumati and Nairne, 1991; Gumati and Schamel, 1988; El-Alami, 1996; Ghori and Mohammed, 1996; Mansour and Magairhy, 1996; Macgregor and Moody, 1998; Ahlbrandt, 2001. It is the aim of this section to present a brief geological overview in order to place the geochemistry within the context of the basin geology.

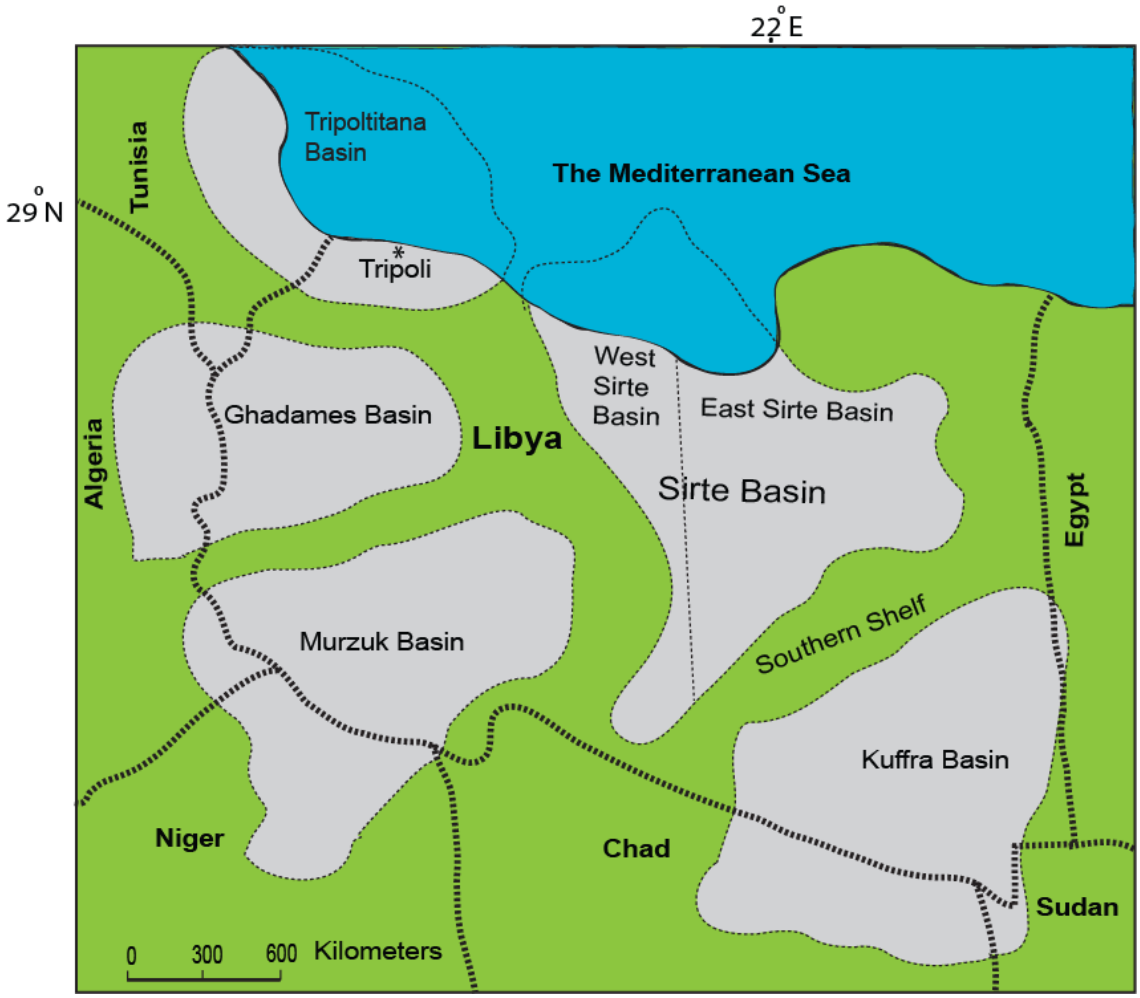

Fig. 1.8 The geological basins of Libya (modified from Gumati et al., 1996, Burwood et al., 2003 and Aboglila et al., 2010a).

1.2.2. Geology of the Sirte Basin

1.2.2.1. Geological setting

The Sirte Basin is an extensional rift basin covering an area of approximately 230,000 km^2 making it Libya's largest basin. It is considered to be the most

important of the Libyan Basins containing approximately 320 petroleum fields 16 of which are giant oil fields and estimated to have recoverable reserves of 44 billion barrels of oil and 33 trillion cubic feet of gas (Montgomery, 1994; Macgregor and Moody, 1998; Ahlbrandt, 2001). The Sirte Basin (Fig. 1.10) extends offshore to the 200th metre bathymetric line into the Sirte Gulf and is separated from the Tripolitana Basin by the Medina Bank. Onshore the Sirte Basin is bounded in the east to north-east by the Cyrenaica Shelf, to the west the Ghadames Basin, and to the south the Kufra Basin (Burwood, 1996; Macgregor and Moody, 1998; Ahlbrandt, 2001). The current basin margins have been identified by surface geology and subsurface tectonic mapping prepared by UNESCO (Persits et al 1997) alternate basin outlines have been presented by Montgomery (1994). The Sirte Basin has a complex tectonic history of Cretaceous to Eocene rift structures (Abadi, 2002), which differs, significantly from the broad and generally un-faulted Murzak and Kufra Basin. This has resulted in the formation of multiple reservoirs through structural features such as tilted faults, which also support hydrocarbon generation, migration and accumulation, principally adjacent to horst blocks (Ahlbrandt, 2001). Onshore the structures are relatively well explored; however, offshore the area is largely unexplored and the petroleum potential is unknown; although, Eocene source rocks show potential (Ahlbrandt, 2001).

The Sirte Basin is asymmetric and divided into the West Sirte Basin and the East Sirte Basin, which are separated by the Zelton platform also referred to as the Central Sirte Basin (Hallett, 2002). In respect of recoverable oil, this area is regarded as the economic centre, hosting the largest fields such as Amal, Nafoora, Gialo and Sarir (e.g. Hallet, 2002; Burwood et al., 2003). The main faults, which divide the basin into a series of platforms and troughs, trend in a north-west to south-east direction except in the East Sirte Basin where fault trends occur in an east-west direction and it is this faulting which is thought to have contributed to the structural traps which have resulted in the East Sirte Basin being most productive for the petroleum industry of Libya. The Creataceous and Palaeocene sediments show an increased thickness across the major faults bounding the horst and graben structures (Abadi, 2002). The major troughs and platforms, which formed during the Late Cretaceous and

Palaeocene are common to both areas and these geological features show comparable source intervals, reservoirs and oil production (Rusk, 2001).

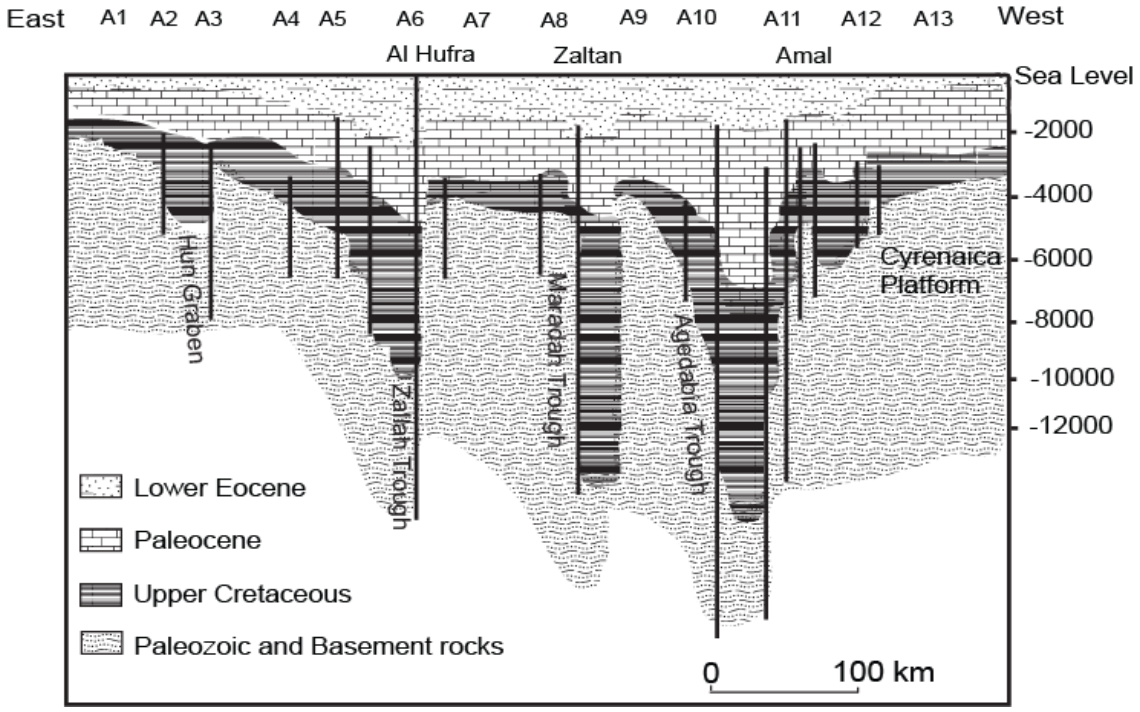

Fig. 1.9 East-West cross section of Sirte Basin, showing the burial depths in the Agedabia Trough are the greatest relative to burial depths in Zallah Trough and Maradah Graben (modified from Roohi, 1996).

The depths within the Sirte Basin are quite variable, deepening to the east with Agedabia Trough being the deepest part of the basin (Fig. 1.9), and the relative relief of the horst and graben slabs raises to the east coincident with major thinning of sediments across the Sirte Basin (Ahlbrandt, 2001).

1.2.2.2. Tectonic History of the Sirte Basin

Four tectonic phases of basin evolution are commonly recognised which describe the geological history of the Sirte Basin (cf. Gumati and Nairn, 1991; Baird et al., 1996). A complex series of horst and grabens began to develop in the latest Jurassic (Abadi et al, 2008). From the Mid Jurassic the basin structure began to evolve as a rifted embayment along the North African plate as a result of tectonic sequences leading to the breakup of Pangea. The current configuration of the Sirte Basin was formed through Early-Mid Cretaceous

rifting with the fragmentation of the pre-existing Sirte Arch (Fig. 1.10), which represented a period of tectonic instability in the region (Burke and Dewey, 1974; Gumati and Kanes, 1985; Gumati and Nairn, 1991; Baird et al., 1996; Rusk 2001; Hallett, 2002). The tectonism gave rise to a series of troughs and platforms (Fig. 1.9). The structure of the troughs and platform controlled the entire sedimentary sequence of the basin and their formation was followed by successive phases of subsidence (Ahlbrandt, 2001). Subsidence and extensional fault reactivation continued into the Tertiary with maximum subsidence occurring in the Late to Middle Eocene (Rusk 2001; Hallett, 2002). Many of the hydrocarbon discoveries in the Sirte Basin are linked to tectonic features such as tilted fault blocks and associated folding along the eastern basin margin, and sedimentary features such as carbonate reefs and bioherms which have accumulated on low amplitude drapes formed over horst blocks, between grabens, in the centre and western rift margins of the basin (Ahlbrandt, 2001).

1.2.3. Stratigraphic Framework

Correlation of stratigraphic units between the sediments of the platform and troughs has proved difficult due to the rapid lateral changes in facies type and sediment thickness. In addition historically different formation names have been used and operating oil companies again use different formation names in their log charts (Barr and Weeger, 1972; Ahlbrant 2001; Hallett, 2002). Here we use the stratigraphic nomenclature according to Barr and Weegar, 1972).

Five basin-fill sequences are preserved within the Sirte Basin, and together they from a classic rift complex resting on Precambrian basement (Abadi, 2002). Pre-rift sediments comprise clastic sediments of Cambrian to Ordovician Age (e.g. Amal Formation (Fig 1.11). The first Mesozoic rift sequence comprises of continental-marine clastics of the Nubian and Sarir sandstones. This cycle was followed by deposition of Upper Cretaceous marine clastics and carbonates. The sediment fills of the Upper Cretaceous are characterised by extensive lateral and vertical facies changes attributed to the tectonic instability of this period (Abadi., et al 2008). The Upper Cretaceous-aged Bahi, Lidam, Etel, Maragh, Rachmat, Tagrifet, Rakb, Sirte and Kalash Formations comprise the second basin fill sequence (Fig. 1.11) (Barr and Weegar, 1972). During this stage deposition

within the troughs is characterised by fine siliciclastic whereas the highs are characterised by shallow marine carbonates (Abadi., et al 2008).

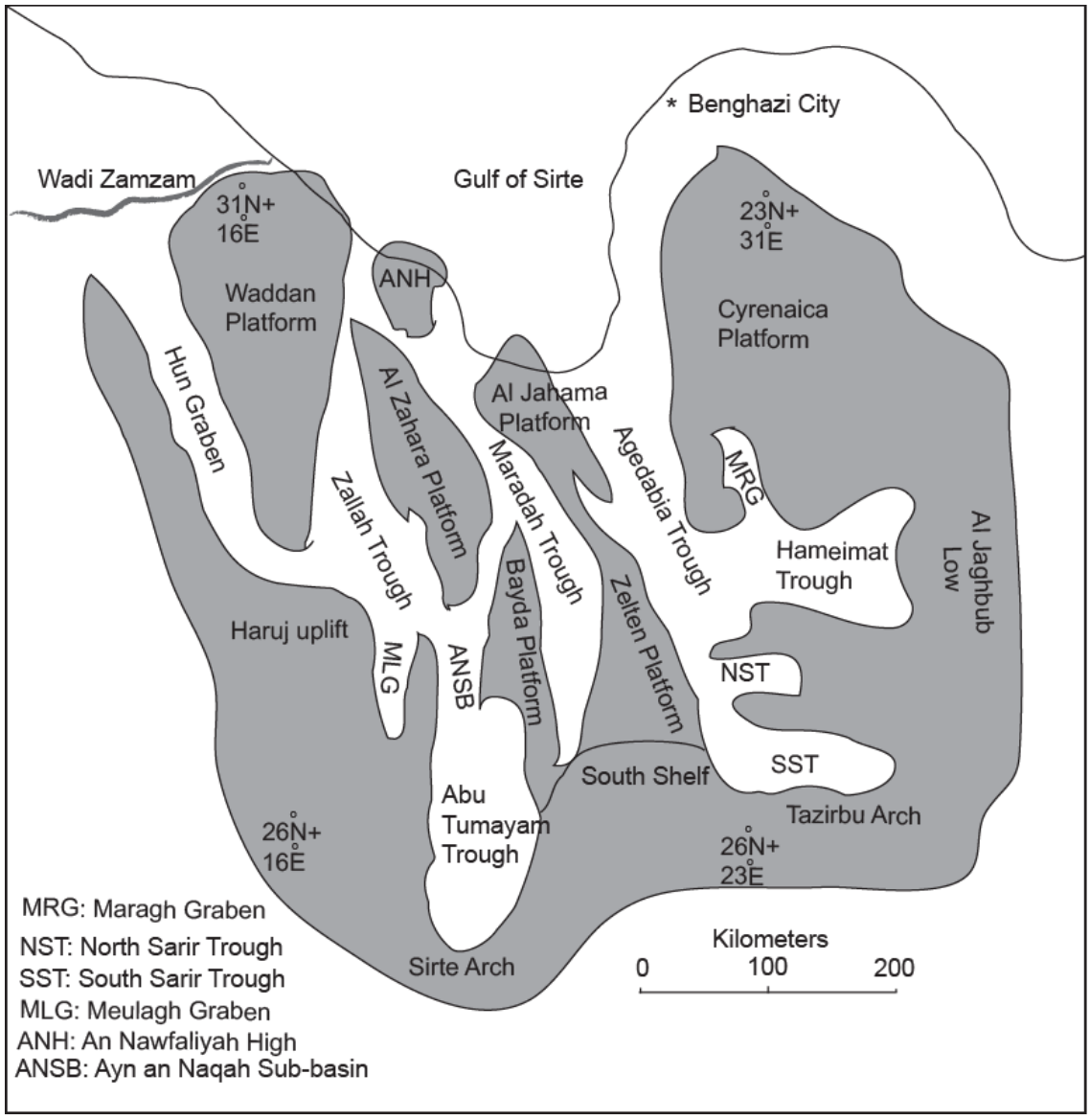

Fig. 1.10 Sirte Basin: main tectonic structures of the platforms, troughs and grabens. (modified from Hallett, 2002 and references therein).

The Bahi Formation (Fig. 1.11) was deposited in a littoral or very shallow marine environment during the Cenomanian. The Lidam Formation represents the first marine unit for the majority of the basin and comprises mainly of dolomite and shale with thin beds of anhydrite in the higher part of formation (Fig. 1.11) (Rusk, 2001; Hallett, 2002). The Etel Formation is limited to the central and southern parts of the Sirte Basin but even in those areas it is absent

on the highs. The marine Sirte Formation consists of a shale sequence with thin interbedded limestones and is widely distributed throughout the basin grabens reaching depths of 500m in the Zallah Trough and 700m in the Agedabia Trough (Barr and Weeger, 1972; Hallet, 2002). There was a shallowing of the depositional environment during the Maastrichtian with the shaley limestones of the Kalash Formation deposited under shallow marine conditions (Barr and Weeger, 1972). The third fill sequences, corresponding to the main Sirte rifting events of Palaeocene to Eocene Age, were carbonates, with minor evaporates. The onset of rifting corresponded to a deepening in the basin with thick, deep marine sections (e.g. Khalifa Formation) deposited in troughs and carbonate buildups on the platforms (e.g. Lower Sabil and Defa Formations). These carbonate platforms extended across the western part of the basin indicating an open marine environment. The rift fill sequence was complete in Middle Eocene with deposition of mixed carbonates and siliciclastics followed by continental clastics, which are fairly uniform throughout the basin (Fig 1.11). The Gir Formation limestone and anhydrite form reliable seals for the Facha Formation (dolomite). Post rift deposition of shallow marine carbonates occurs from the Middle Eocene to the Oligocene across the Sirte Basin with the exception of the northwest where there are minor units of shale (Barr and Weegar, 1972).

The Oligocene regression resulted in different environmental conditions within the basin reflecting the different lithologies of continental sandstone in the south and marine carbonates and shales in the central and eastern parts of the basin (Fig. 1.11) (Barr and Weegar, 1972; Hallet, 2002). During the Miocene the deposition environment in the East Sirte Basin was fluvial along the basin margins, marginal marine towards the north and a marine shelf in the north-east. The Miocene Marada Formation consists of anhydrite, sandstone, and sandy limestone, which are an interfingering of assorted continental, littoral, and distal/marine facies (Barr and Weegar, 1972; Ahlbrandt, 2001; Hallett, 2002). The exploration for new sources is ongoing in the Sirte Basin. In addition, there is also an increased interest in enhancing oil recovery from existing reservoirs. The geology of the basin is complex due to a multi pattern of horsts and grabens as well several potential source rocks, ranging from the Precambrian to Eocene in age (Parsons et al., 1980).

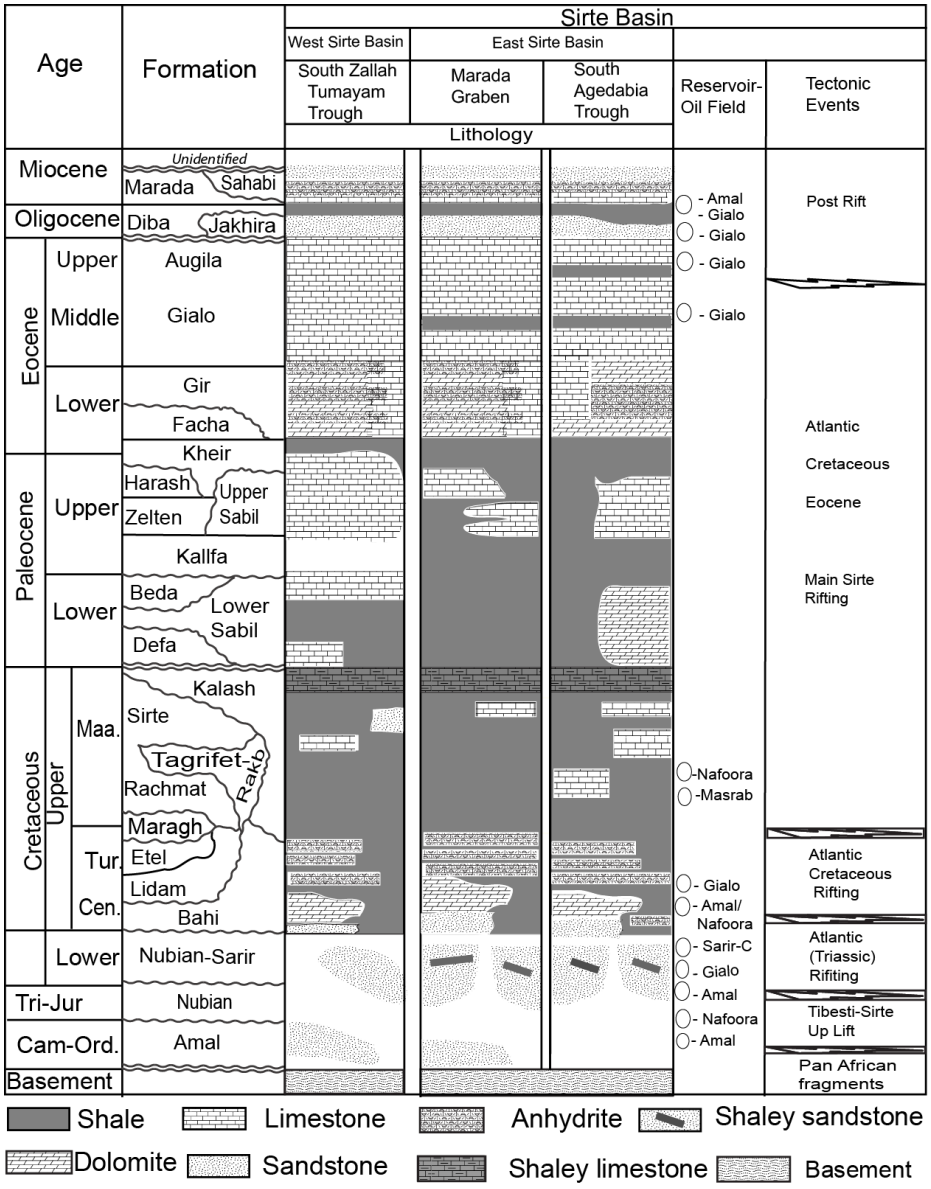

Fig. 1.11 Stratigraphic column of the Sirte Basin highlighting the lithologies of the formations, the reservoir units of the oil fields demonstrates age, formations, lithology, main reservoir-oil fields and its tectonic events (modified from Barr and Weeger (1972), Rusk (2001) and Burwood et al. (2003).

1.2.4. Petroleum Systems

1.2.4.1. Petroleum Systems of the East Sirte Basin

The Sirte Basin contains multiple petroleum systems; however, the Sirte-Zelten, principally sourced by the Upper Cretaceous Sirte Shale (Fig. 1.11) is considered to be the dominant total petroleum system, (Gumati and Schamel, 1988; El-Alami, 1996; Ghori and Mohammed, 1996; Mansour and Magairhy,

1996; Burwood, 1996; Macgregor and Moody, 1998; Ahlbrandt 2002). Recent geochemical petroleum studies confirmed the domination of the Sirte Shale in Upper Cretaceous as the source of hydrocarbon (Ghori and Mohammed, 1996). The Sirte shales occur across the basin in varying thicknesses and have total organic carbon contents (TOC) ranging from 0.5-1.9% (Parsons et al, 1980). Maturation levels can be explained by geothermal gradients with maturation depth trends slightly higher in the West Sirte Basin compared with the east. The oil window is reached at depths of 2000m in the West Sirte Basin compared with 2700m and 3400m in the east and central Sirte Basin (Gumati and Schamel, 1988; Ahlbrandt, 2001). Shallow marine clastics and carbonates deposited on adjacent horst blocks ranging in age and rock type comprise the primary reservoir (El-Alami, 1996).

Additional reservoirs include cracked Precambrian basement, the Upper Jurassic – Lower Cretaceous Nubian Formation, which provides reservoir having maximum porosities exceeding 20% in the Ajdabiya Trough and 12-13% in the Maragh Graben. The Sabil reef also has high porosity levels due to the reefal fabric comprising of corals providing a porosity of around 40% in the Ajdabiya Trough. In the Maragh Graben the reefal sediments of the Zelton Formation are considered equivalent to the Sabil Formation (Fig. 1.11). These are charged along transfer, relay or wrench fault zones adjacent to the horsts and graben (Guiraud and Maurin; 1991). It is generally accepted that the Sirte Basin is an example of a vertical migration system and oils from variously aged reservoirs are genetically related to each other (El-Alami, 1996). Peak oil expulsion occurred from the Late Eocene to the Late Pliocene in the Agedabia Trough. The Eocene age anhydrite and shales, in addition to carbonates of Upper Cretaceous/Tertiary age (Fig. 1.11) are major structures forming important seals in the Sirte Basin area (Gumati et al., 1996; Hallett, 2002). The seal thickness changes in depth between the troughs, reaching approximately 600m in Zallah Trough, a maximum of 1305m in the Maradah Trough, while in the Agedabia Trough the reservoirs are sealed by thickness more than 1000m along the trough (Hallett, 2002). The dominant trap style is structural with traps formed from horsts and tilted fault blocks. Some stratigraphic traps occur in the

Sarir and Messla fields are superimposed on structure and a combination of trap style occurs in some parts of the East Sirte Basin (e.g. Gumati et al., 1996).

Recent geochemical studies on crude oils from the Sirte Basin have indicated the presence of mixed oils from different source rocks. To date, at least 12 oil families have been recognised in the Sirte Basin, based on differences in their composition (e.g. Burwood et al., 2003). Various additional potential source rock horizons have been recognised in Palaeogene, Cretaceous, Triassic, Cambrian and Precambrian-aged sediments (Burwood, 1996; Ahlbrandt, 2001). The Upper Cretaceous Etal Formation occurs throughout the Sirte Basin, although is only considered as source rock in the southern Ajdabiya Trough and Maragh Graben in the East Sirte Basin where it reaches sufficient depths (Rusk, 2001). A third potential source is the Cretaceous middle shale member of the Nubian formation deposited in a lacustrine to lagoonal palaeoenvironment (El-Hawat, 1996). It has a TOC of 3% and has been identified as a minor source in the Ajdabiya Trough; however is a more significant source for the Maragh Graben (Burwood et al., 2003; Rusk, 2001). The Tertiary petroleum systems might exist in the deeper parts and in offshore areas of Agedabia Trough, where oils were found in lower Tertiary reservoirs. Recently a Triassic source has been confirmed (Baird et al., 1996). In the Ajdabiya Trough the seal for the Nubian Sandstone is the Etal shale and anhydride. However the occurrence of an unconformity and the thinness of the Bahi Formation may mean the Nubian Sandstone effectively lacks a seal. The seal thickness changes in depth between the troughs, reaching over 600m in Zallah Trough, a maximum of 1305m in the Maradah Trough, while in the Agedabia Trough the reservoirs are sealed by thickness more than 1000m along the trough (Hallett, 2002).

Samples for this study comprise oils from three northwest-southeast trending areas of the giant oil fields of the Zelton Platform and from the Gialo High, a horst block in the north east of the East Sirte Basin.

1.3. Aims and scope of this study

The Sirte Basin is a major oil producing area in Libya, but the understanding of the processes that have led to the petroleum accumulation is still limited.

Exploration studies of this area have shown that the oils are mixtures of several charges and may be from different source rocks. This geochemical study is to increase understanding history of petroleum accumulation and help to promote oil exploration activities in this basin, where there is a need to better understand potential hydrocarbon plays. The main aims of this study are to improve understanding of the petroleum accumulation history in the East Sirte Basin.

Objectives are:

To characterisate the hydrocarbon sources and maturities based on specific biomarker parameters, together with compound-specific stable carbon and hydrogen isotopes and to determine different oil families in the East Sirte Basin.

To improve the on-going characterisation of hydrocarbon sources in the East Sirte Basin, notably from Cretaceous shales and to determine their thermal maturities and paleoenvironments of deposition of the source-rocks

Use gas chromatography- mass spectrometry (GC-MS) and GC-metastable reaction monitoring (MRM) analyses of several crude oils and source rocks to establish an oil-source correlation and an age prediction of the source-rock of the oils. New analytical approaches that are not yet used in the studied area, such as using profiles of CSIA, biomarkers from saturated fractions of oils and cuttings, particularly compound specific hydrogen isotopes from isoprenoids, were measured to establish the sources and thermal maturities of hydrocarbons in the studied area. In addition, various parameters have been used to establish the number of oil families. The results of this study are compared with previous research and provide organic geochemical expertise to research organizations.

1.4. References

Abadi, A., 2002. Tectonics of the Sirte Basin. PhD Dissertation. Vrije Universiteit, Amsterdam, ITC, Enschede, pp. 187.

Abadi, A.M., van Wees, J.D., van Dijk, P.M., Cloetingh, S.A., 2008. Tectonics and subsidence evolution of the Sirte Basin, Libya. AAPG Bulletin. 8, p. 993-1027.

Aboglila, S., Grice, K., Trinajstic, K., Dawson, D., Williford, K., 2010. Use of biomarker distributions and compound specific isotopes of carbon and hydrogen to delineate hydrocarbon characteristics in the East Sirte Basin (Libya). Organic Geochemistry. Presented at the 15th Australian Organic Geochemistry Conference, Adelaide, September 2008. *In press*.

Ahlbrandt, T.S., 2001. The Sirte Basin is Province of Libya-Sirte-Zelten Total Petroleum System. US Geological Survey Bulletin 2202-F. <http:// geology.cr.usgs.gov/pub/bulletins/b2202-f/> (accessed 20.4.2009).

Andrusevic, V.E., Engel, M.H., Zumberge, J.E., Brothers, L.A., 1998. Secular, episodic changes in stable carbon isotope composition of crude oils. Chemical Geology, 152, 59-72.

Asif, M. Grice, K. Fazeelat, T., 2009. Assessment of petroleum biodegradation using stable hydrogen isotopes and polycyclic aromatic hydrocarbons Organic Geochemistry, 40, 301-311.

Baird, D.W., Aburawi, R.M., Bailey, N.J.L., 1996. Geohistory and petroleum in the central Sirte Basin. In: Salem, M.J., El-Hawat, A.S., Sbeta, A.M. (Eds.), Geology of Sirte Basin II, Elsevier, Amsterdam, p.3–56.

Barr, F.T., Weegar, A.A., 1972. Stratigraphic Nomenclature of the Sirte Basin, Libya. Petroleum Exploration Society of Libya, Tripoli. p. 179.

Berner, R.A., 1982. Burial of organic carbon and pyrite sulfur in the modern ocean: Its geochemical and environmental significance. American Journal of Science, 282, 451-473.

Brocks J.J., Grice K., 2010. Biomarkers (Ancient biomolecules end evolution) Encyclopedia of Geobiology. *in press*.

Burke, K., Dewey, J., 1974. Two plates in Africa during the Cretaceous?: Nature, 249, p. 313–316.

Burwood, R., 1996. Geochemical evaluation of east Sirte Basin petroleum systems and oil provenance Proceedings of First Magrebian Conference on Petroleum Exploration, Benghazi, GSPLAJ, November 28, 18-20.

Burwood, R., Redfern, J., Cope, M., 2003. Geochemical evaluation of East Sirte Basin (Libya) petroleum systems and oil provenance. In: Burnham, T., MacGregor, D.S., Cameron, N.R. (Eds.), Petroleum Geology of Africa. Geological Society Special Publication, London, 207 p.203–214.

Clayton, C., 1991. Effect of maturity on carbon isotope ratios of oils and condensates. Organic Geochemistry 17, 887–899.

Craig, J., Rizzi, C., Said, F., Thusu, B., Lüning, S., Asbali, A.I., Keely, M.L., Bell, J.F., Durham, M.J., Eales, M.H., Beswetherick, S. and Hamblett, C. 2004. Structural Styles and Prospectivity in the Precambrian and Palaeozoic Hydrocarbon Systems of North Africa. Abstract: III Symposium Geology of East Libya, November 21-23 2004, Binghazi, GSPLAJ; extended Abstract, PETEX 2004, London, 23rd-25th November 2004.

Craig, H., 1961 isotopic variations in meteoric waters. Science, 133, 1702-1703.

Craig, H., Gordon, L.I., 1965. Deuterium and oxygen 18 variations in the ocean and the marine atmosphere. Symposium on Marine Geochemistry, Narraganset Marine Laboratory, University of Rhode Island Publication, 3, 277-374.

Dawson, D., Grice, K., Wang, S. X., Alexander, R., Radke, J., 2004. stable hydrogen isotopic composition of hydrocarbons in torbanites (Late Carboniferous to Late Permian) deposited under various climatic conditions. Organic Geochemistry, 35, 189-197.

Dawson, D., Grice, K., Alexander, R., Edwards, D., 2007. The effect of source and maturity on the stable isotopic compositions of individual hydrocarbons in sediments and crude oils from the Vulcan Sub-basin, Timor Sea, Northern Australia. Organic Geochemistry, 38, 1015–1038.

El-Alami, M., 1996. Habitat of oil in Abu Attiffel area, Sirte Basin, Libya, in Salem, M.J., El-Hawat, A.S., and Sbeta, A.M., eds. The geology of Sirte Basin: Amsterdam, Elsevier, v. II, p. 337-348.

El-Hawat, A.S., Missallati, A.A., Bezan, A.M., Taleb, T.M., 1996. The Nubian Sandstone in Sirte Basin and its correlatives. In: Salem, M.J., El-Hawat, A.S., Sbeta, A.M. (Eds.), The Geology of Sirte Basin II, Elsevier, Amsterdam, 3–30.

Emerson, S., Stump, C., Grootes, P.M., Stuiver, M., Farwell, G.W., Schmidt, F.H., 1987. Estimates of degradable organic organic carbon in deep-sea sediments from 14C concentrations. Nature, 329, 51-53.

Gelin, F., Boogers, I., Noordeloos, A. A. M., Hatcher, P.G., Sinninghe Damste, J. S., de Leeuw, J. W., 1996. Novel, resistant microalgal polyethers: an important sink of organic carbon in the marine environments. Geochimica et Cosmochimica Acta, 60, 1275-1280.

George, S. C., Boreham, C. J., Minifie, S. A., Teerman, S. C., 2002. The effect of minor to moderate biodegradation on C_5 to C_9 hydrocarbons in crude oils. Organic Geochemistry, 33, 1293-1317.

Ghori, K.A.R., Mohammed, R.A., 1996. The application of petroleum generation modelling to the eastern Sirte Basin, Libya. In: Salem, M.J., El-Hawat, A.S., Sbeta, A.M. (Eds.), The Geology of Sirte Basin II, Elsevier, Amsterdam, p.529–540.

Grice, K., Brocks J.J., 2010. Biomarkers (organic, compound specific isotopes) Encyclopedia of Geobiology. *in press*.

Grice, K., de Mesmay, R., Glucina, A., Wang, S., 2008. An improved and rapid 5A molecular sieve method for gas chromatography isotope ratio mass spectrometry of *n*-alkanes (C_8-C_{30}). Organic Geochemistry, 39, 284-288.

Grice K., Schaeffer P., Schwark L., Maxwell J. R. (1996) Molecular indicators of palaeoenvironmental conditions in an immature Permian shale (Kuperschiefer, Lower Rhine Basin, north-west Germany) from free and S-bound lipids. Organic Geochemistry, 25, 131-147.

Guiraud, R., Maurin, J.C., 1991. Early Cretaceous rifts of Western and Central Africa: an overview. Tectonophysics, 213, 153–168.

Gumati, D., and Schamel, S., 1988 Thermal maturation history of the Sirte basin, Libya. Journal of Petroleum Geology, 2, 529-540.

Gumati, D., and Nairn, A.E.M., 1991. Tectonic subsidence of the Sirte Basin, Libya. Journal of Petroleum Geology, 69, 39-52.

Gumati, D., Kanes, W.H., and Schamel, S., 1996. An evaluation of the hydrocarbon potential of the sedimentary basins of Libya: Journal of Petroleum Geology, 19, 95–112.

Harding, T.P., 1984. Graben hydrocarbon occurrences and structural styles: American Association of Petroleum Geologists Bulletin, 68, 333–362.

Hallett, D., 2002. Petroleum Geology of Libya. Elsevier, Amsterdam, 1, 265-321.

Hedges, J.I., and Keil, R.G., 1995. Sedimentary organic matter preservation: an assessment and speculative synthesis. Marine Chemistry, 49, 81–115.

Hoefs, J., 1987. Stable Isotope Geochemistry, third edition. Springer-Verlag, Berlin, p. 254.

Hunt, J.M., 1996. Petroleum Geochemistry and Geology. New York, 394-743.

Killops, S., Killops, V., 2005. Introduction to Organic Geochemistry. Blackwell publishing, p. 64-67.

Li, M., Huang, Y., Obermajer, M., Jiang, C., Snowdon, L.R., Fowler, M.G., 2001. Hydrogen isotopic compositions of individual alkanes and a new approach to petroleum correlation: case studies from the Western Canada Sedimentary Basin. Organic Geochemistry, 32, 1387–1399.

Love, G.D., Grosjean, E., Stalvies, C., Fike, D.A., Grotzinger, J.P., Bradley, A.S., Kelly, A.E., Bhatia, M., Meredith, W., Snape, C.E., Bowring, S.A., Condon, D.J., Summons, R.E., 2009. Fossil steroids record the appearance of Demospongiae during the Cryogenian period. Nature, 457, 718–721.

Macgregor, D. S., and Moody, R. T. J., 1998. Mesozoic and Cenozoic petroleum systems of North Africa ,in MacGregor. Petroleum geology of North Africa : Geological Society, 132, 201-216.

Mansour, A. T., Magairhy, I. A., 1996. Petroleum geology and stratigraphy of the southeastern part of the Sirte Basin, Libya. The geology of Sirte Basin: Amsterdam, Elsevier, 2, 485-528.

Maslen, E., Grice, K., Dawson, D., Le Metayer, D., 2010. Stable carbon isotopic compositions of individual aromatic hydrocarbons as source and age indicators in oil from Western Australian Basins. Organic Geochemistry. Submitted.

Matthews, D.E, Hayes, J.M., 1978. Isotope-ratio-monitoring gas chromatography-mass spectrometry. Analytical Chemistry, 50,1465–1473.

Montgomery, S., 1994, Sirte Basin, North-Central Libya, prospects for the future: Petroleum Frontiers, Petroleum Information Corporation, 11, p. 94 .

Parsons, M.B., Azgaar, A.M., and Curry, J.J., 1980, Hydrocarbon occurrences in the Sirte Basin, Libya, in Miall, A.D., ed. Canadian Society Petroleum Geologists Memoir, 6, 723–732.

Pedentchouk, N., Freeman, K.H., Harris, N.B., 2006. Different response of δD values of *n*-alkanes, isoprenoids, and kerogen during thermal maturation. Geochimica et Cosmochimica Acta, 70, 2063–2072.

Persits, F., Ahlbrandt, T.S., Tuttle, M., Charpentier, R., Brownfield, M., Takahashi, K., 1997. Map showing geology, oil and gas fields and geological provinces of Africa: U. S. Geological Survey Open-File Report, 97-470A (CD-ROM).

Peters, K.E., Walters, C.C., Moldowan, J.M., 2005. The biomarker guide vol 1: biomarkers and isotopes in the environment and human history. Cambridge University Press, Cambridge, p. 471.

Prosser, S.J., Scrimgeour, C.M., 1995. High-precision determination of H/H in H2 and H2O by continuous-flow isotope ratio mass spectrometry. Analytical Chemistry, 67, 992-1997.

Rigby, D., Batts, B.D., Smith, J.W., 1981. The effect of maturation on the isotopic composition of fossil fuels. Organic Geochemistry, 3, 29–36.

Roohi, M., 1996. A geological view of source-reservoir relationships in the western Sirte Basin, in Salem, M.J., El-Hawat, A.S., and Sbeta, A.M. eds., Geology of the Sirte Basin: Amsterdam, Elsevier, 2, 323–336.

Rusk, D. C., 2001. Libya: Petroleum potential of the underexplored bas centers-A twenty-first-century challenge, in M.W. Downey, J. C. Threet, and W. A. Morgan, eds., Petroleum provinces of the twenty-first century: AAPG Memoir, 74, 429–452.

Santos Neto, E. V., Hayes, J.M., 1999. Use of hydrogen and carbon stable isotopes characterizing oils from the Potiguar Basin (onshore), Northeastern Brazil. AAPG Bulletin, 83, 496-518.

Seifert, W.K., Moldowan, L. M., 1986. Use of biologicaI markers in petroleum exploration. In: Biological Markers in the Sedimentary Record (E& R.B. Johns), Methods in Geochemistry and Geophysics 24, Elservier, New York, 26 1-290.

Schimmelmann, A., Sessions, A.L., Boreham, C.J., Edwards, D.S., Logan, G.A., Summons, R.E., 2004. D/H ratios in terrestrially sourced petroleum systems. Organic Geochemistry, 35, 1169–1195.

Sofer, Z., 1984. Stable carbon isotope compositions of crude oils: Applications to source depositional environments and petroleum alteration. Occurrence of hydrocarbons in the Vivian Formation, northern Peruvian Oriented. Paper presented at Geological Symposium in Bogota, Colombia. AAPG Bull, 68, 31-49.

Speight, G., 1999. The Chemistry and Technology of Petroleum. Marcel Dekker. p.215-216.

Tissot B.P., Welte D.H., 1978. Petroleum Formation and Occurrence. a new approach to oil and gas exploration. Springer-Verlag, New York, p. 538.

Tissot B. P., Welte, D.H., 1984. Petroleum Formation and Occurrence. 2nd Edition. Springer Verlag. New York, p. 699.

Van Krevelen, D.W., 1961. Coal. Elsevier, New York, p. 514.

Werner, R.A., Brand, W.A., 2001. Referencing strategies and techniques in stable isotope ratio analysis. Rapid Communications in Mass Spectrometry, 15, 501-519.

Woese, C.R., Kandler, O.و Wheelis, M.L., 1990. Towards a natural system of organisms: Proposal for the domains Archaea, Bacteria, and Eucarya. Proceedings of the National Academy of Science, USA, 87, 4576-4579.

Xiong, Y., Geng, A., Pan, C., Liu, D., Peng, P., 2005. Characterization of the hydrogen isotopic composition of individual *n*-alkanes in terrestrial source rocks. Applied Geochemistry, 20, 455–464.

Zonneveld, L., Chen, J., Mobius, M.S., 2009. Environmental significance of dinoflagellate cysts from the proximal part of the Po-river discharge plume (off southern Italy, Eastern Mediterranean), Journal of Sea Research, 62, 189–213.

Chapter 2

Use of biomarker distributions and compound specific isotopes of carbon and hydrogen to delineate hydrocarbon characteristics in the East Sirte Basin (Libya)

S. Aboglila, K. Grice, K. Trinajstic, D. Dawson, K. H. Williford

Organic Geochemistry

Abstract

Biomarker ratios, together with stable carbon ($\delta^{13}C$) and hydrogen (δD) isotopic compositions of individual hydrocarbons have been applied to a suite of crude oils (n = 24) from the East Sirte Basin to delineate their sources and respective thermal maturities. The crude oil samples are divided into two main families (A and B) based on differences in source inputs and thermal maturity. Using source-specific biomarker parameters based on pristane/phytane (Pr/Ph) ratios, hopane/sterane ratios, dibenzothiophene (DBT)/ phenanthrene (P), Pr/*n*-C_{17}, Ph/*n*-C_{18} and the distribution of tricyclic and tetracyclic terpanes, family B oils are ascribed a marine source rock deposited under sub-oxic conditions, while family A oils have a more terrestrial source affinity. This source classification is supported by the stable carbon isotopic compositions (^{13}C) of the *n*-alkanes. Using biomarker maturity parameters such as the abundance of Pr and Ph relative to *n*-alkanes and the distribution of sterane and hopane isomers, family A oils are more thermally mature than family B oils. The higher maturity of family A oils is supported by differences between the stable hydrogen isotopic compositions (D) of Pr and Ph and the *n*-alkanes, as well as the ^{13}C values of *n*-alkanes.

Keywords: East Sirte Basin, Libya, biomarkers, stable carbon isotopes, stable hydrogen isotopes

2.1. Introduction

The Sirte Basin, in north central Libya, is one of Africa's most productive petroleum basins and the world's 13th largest petroleum province, with reserves estimated at 43 billion barrels of oil equivalent (recoverable) within 16 giant oil fields and 23 relatively large oil fields (Ahlbrandt, 2001) (Fig. 2.1). The Sirte Basin covers an area of 600,000 km^2, stretching from the 2,000 km bathymetric line offshore in the Mediterranean coast to the Chad border in the south (Abadi, 2002) (Fig. 2.1). It comprises offshore and onshore provinces, with the former largely unexplored and representing a major opportunity for reserves to be added (Ahlbrandt, 2001). Reservoirs range from Precambrian to Miocene in age (Figs. 2.1 and 2.2) and production is approximately equally divided between clastic and carbonate reservoirs, both producing low-sulfur and in some fields highly waxy oils (Burwood et al., 2003). In the Eastern Sirte Basin, significant stratigraphic traps superimposed on structural highs principally occur in Mesozoic clastic reservoirs, such as those of the Sarir and Massla fields (Abadi, 2002) (Fig. 2.1). Geochemical data on the crude oils form East Sirte Basin indicates a diverse petroleum provenance (Burwood et al., 2003). The East Sirte Basin oils have low sulfur contents (<0.6%), similar specific gravities (30 to 39°API), low gas-to-oil ratios, (e.g. Amal and Nafoora) and variable wax contents (e.g. Sarir-C) (Burwood et al., 2003). Using biomarker parameters, multivariate statistical analysis and bulk stable isotope analysis, Burwood et al. (2003) delineated 12 end-member oil families, which they interpreted as contributing to mixed-system hybrid oils.

In many cases the oils were discovered to comprise two or more end-members (e.g. of marine, lacustrine and/or terrestrial affinity), resulting in at least eight unique petroleum systems. Biomarker characteristics, such as sterane/hopane and C_{27}/C_{17} *n*-alkane ratios, indicated segregation between lacustrine/terrestrial waxy and marine crude oil end-members (Burwood et al., 2003). The ethylcholestane content and the $n\text{-}C_{27}/n\text{-}C_{17}$ alkane ratio together confirmed a contribution from terrestrial OM to the waxy petroleum.

Burwood et al. (2003) also found that organic facies variability within the Late Cretaceous Sirte and Rachmat Formations (Fig. 2.2) was insufficient to cause the observed diversity of the East Sirte Basin petroleums and predicted a

significant contribution from Paleocene sources. The present study continues the characterisation of hydrocarbon sources in the East Sirte Basin. Source and maturity-specific biomarker parameters, together with compound-specific carbon and hydrogen isotopes (especially for the *n*-alkanes and Pr and Ph) in the crude oils have been used to distinguish source(s) and thermal maturity levels.

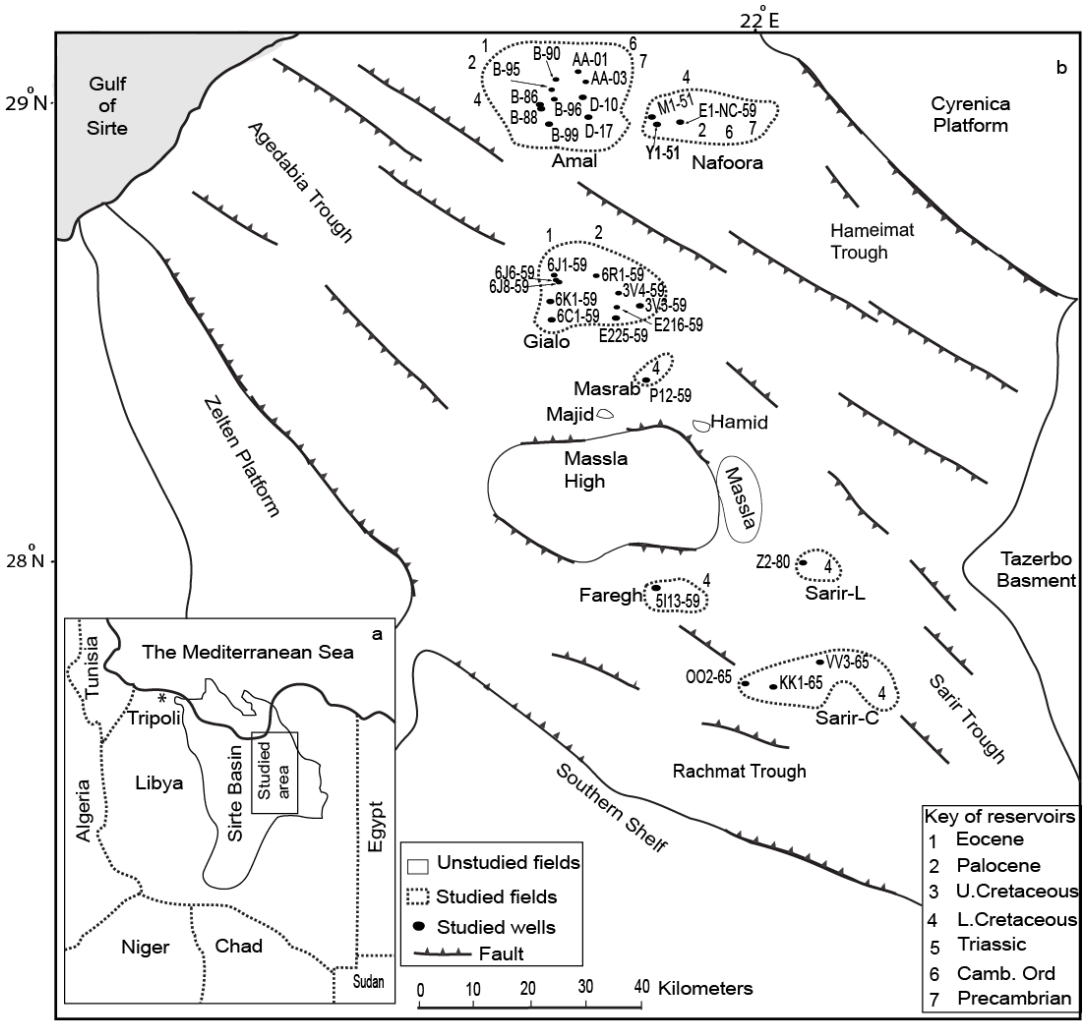

Fig. 2.1 Map showing the location of the Sirte Basin and its structural elements in the studied area. Camb and Ord = Cambrian and Ordovician. (modified from Ahlbrandt (2001) and Burwood et al. (2003*).*

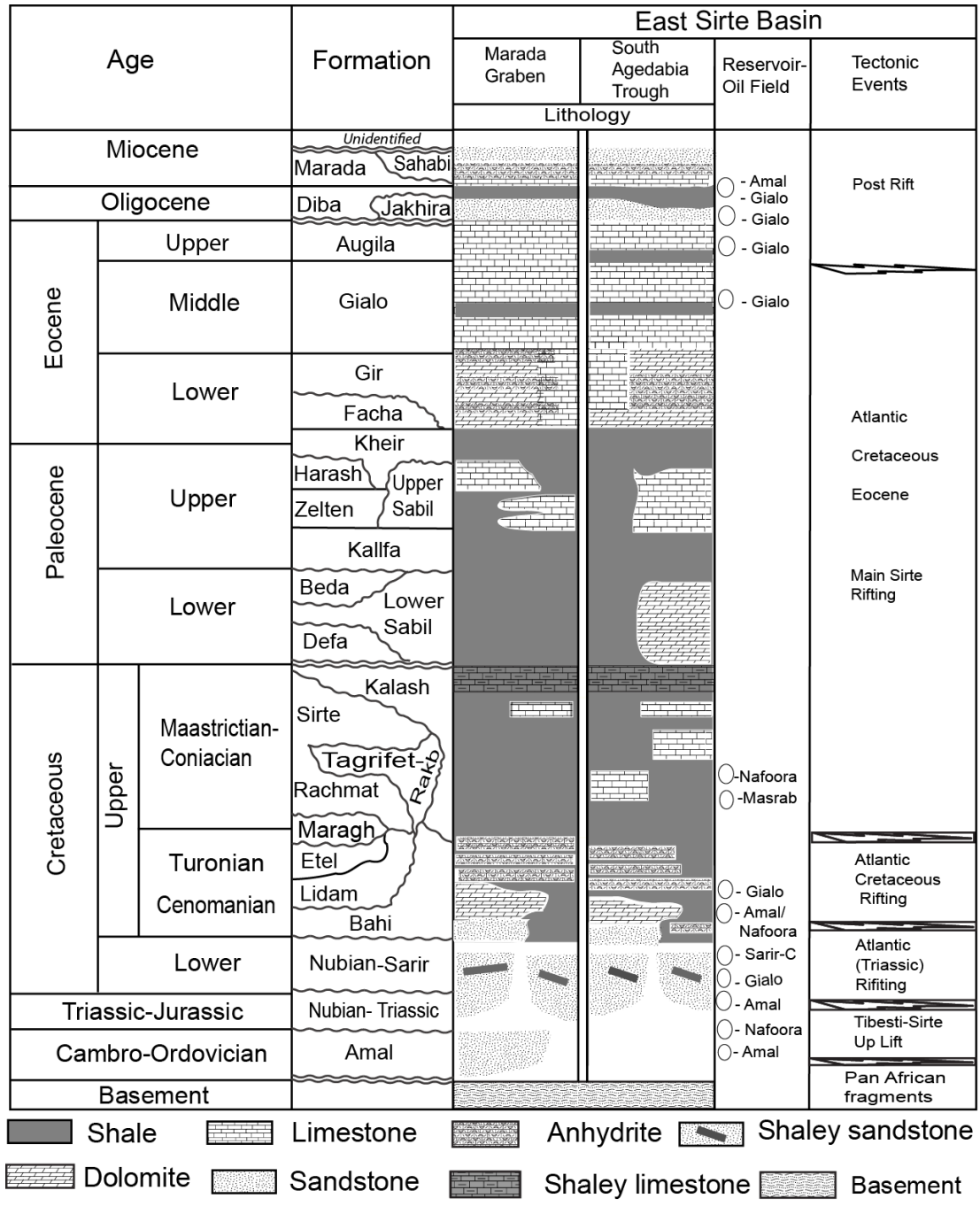

Fig. 2.2 Stratigraphic column of the Sirte Basin highlighting the lithologies of the formations, the reservoir units of the oil fields and its tectonic events. Modified from Barr and Weeger (1972), Rusk (2001) and Burwood et al. (2003).

2.2. Materials and methods

2.2.1. Geological setting

The Sirte Basin is one of Africa's oldest Hercynian structural provinces (Gras, 1996) with the geology having being well described (Parsons et al., 1980; El-Alami et al., 1989; Macgregor, 1996; Ghori and Mohammed, 1996). The structure of the Sirte rift began in the Early Cretaceous, and the dominant basin architecture resulted from Late Cretaceous rifting, which reactivated pre-existing Palaeozoic tectonic lineaments (Ahlbrandt, 2001; Burwood et al., 2003). The east-west trending structures of the Sarir and Hameimat Troughs of the Sirte Basin (Fig. 2.1) were formed during this period (Guiraud and Maurin, 1991) with the East Sirte Basin separated from the West Sirte Basin by the Southern Shelf and the Zelten Platform (Fig. 2.1). The province contains one dominant total petroleum system, the Sirte-Zelten, based on geochemical data. Following the active phase of rifting, major subsidence is recorded in the basin during the Paleocene (Gumati and Nairne, 1991). The resulting basin fill sequence buried older Mesozoic basin-fill sediments and this is thought to have provided source potential predominantly within the Cretaceous Sirte Shale (Fig. 2.2). The Upper Cretaceous Sirte Shale is the primary hydrocarbon source bed with other marine sourced oils been recently attributed to the Tagrifet, Rachmat and Gialo Formations based on carbon isotope oil-source correlation (Burwood et al 2003). Reservoirs range in rock type and age from fractured Precambrian basement, clastic reservoirs in the Cambrian-Ordovician Gargaf sandstones, and Lower Cretaceous Nubian (Sarir) Sandstone to Paleocene Zelten Formation and Eocene carbonates commonly in the form of bioherms (Fig. 2.2).

2.2.2. Samples

The oil samples were obtained directly the well heads of 24 different wells in the Nafoora, Amal, Gialo, Masrab, Faregh, Sarir-L and Sarir-C fields (Fig. 2.1), by the National Oil Corporation (NOC) in Tripoli.

2.2.2. Fractionation of crude oils

Crude oils were fractionated using a small-scale column chromatographic method (Bastow et al., 2007). In brief, the sample (crude oil, about 10–20 mg) was applied to the top of a small column (5.5 cm x 0.5 cm i.d.) of activated silica gel (120ºC, 8 h). The aliphatic hydrocarbon (saturated) fraction was eluted with *n*-pentane (2 mL); the aromatic hydrocarbon fraction with a mixture of *n*-pentane and DCM (2 mL, 7:3 v/v,); and the polar (NSO) fraction with a mixture of DCM and MeOH (2 mL, 1: 1 v/v).

2.2.4. 5A Molecular sieving

Aliphatic fractions of oils were subjected to 5A molecular sieving as described by Grice et al. (2008). In brief, a portion of the aliphatic fraction in cyclohexane was added to a 2 mL vial, filled with activated sieves (7 g). The vial was sealed and placed into a pre-heated aluminum block (85ºC, 8 h). The solution was then cooled and decanted through a small column of silica plugged with cotton wool and pre-rinsed with cyclohexane (2 mL). The sieves were subsequently rinsed well with cyclohexane and the washings filtered through the same silica column. The combined filtrates yielded the branched/cyclic fraction. The *n*-alkanes were recovered by hydrofluoric acid (HF) digestion of the sieve as described previously (Dawson et al., 2005).

2.2.5. Gas chromatography–mass spectrometry (GC-MS)

Aliphatic and aromatic fractions were analysed by GC-MS using a Hewlett Packard (HP) 5973 mass-selective detector (MSD) interfaced to a HP6890 gas chromatograph (GC). A HP-5MS (J and W Scientific) GC column (5% phenylmethylsiloxane stationary phase) was used with helium as the carrier gas. The GC oven was programmed from 40°C to 310°C at a rate of 3°C/min, after which it was held isothermal for 30 min. Samples were dissolved in *n*-hexane and introduced by the HP6890 autosampler into a split-splitless injector operated in the pulsed-splitless mode. Biomarker data were acquired in full-scan mode (*m/z* 50-500). The ion source was operated in the electron ionization (EI) mode at 70 eV. Selective ion monitoring (SIM) was used to identify the terpanes, steranes and triaromatic steroids by monitoring *m/z* 191, 217, 218 and 231 ions. Selected aromatic compounds were identified using *m/z* 178

(phenanthrene), *m/z* 156 (dimethylnaphthalenes) and *m/z* 184 (dibenzothiophene) ions and relative retention time data reported in the literature.

2.2.6. GC–isotope ratio mass spectrometry (GC-ir-MS)

A HP6890 gas chromatograph (GC) equipped with a HP6890 autosampler was used in tandem with a Micromass isotope ratio mass spectrometer (ir-MS) for carbon and hydrogen isotope measurements. The GC-ir-MS conditions used were those detailed by Dawson et al. (2005). In brief, the GC oven was programmed from 50°C to 310°C at 3°C/min for analysis with initial and final hold times of 1 and 20 min, respectively. The same type of capillary column used in GC-MS analysis was employed for GC-ir-MS. The carrier gas was He at a flow rate of 1mL/min. The $\delta^{13}C$ data were obtained by integrating the masses 44, 45 and 46 ion currents of the CO_2 produced from oxidation of each chromatographically separated component, after passing through a quartz furnace packed with copper oxide pellets heated at 850°C. The accuracy and precision of $\delta^{13}C$ measurements were monitored by analysing a mixture of organic reference compounds with known $\delta^{13}C$ values. Each sample was analysed at least three times, and the average $\delta^{13}C$ values and standard deviations are reported in per mil relative to a CO_2 reference gas calibrated to Vienna Peedee Belemnite (VPDB). The δD values were obtained by integration of the masses 2 and 3 ions derived from H_2 produced from pyrolysis of each chromatographically separated component, after passing through a quartz furnace packed with chromium particles (350-400 μm particle size), heated at 1050°C. The H_3^+ correction was performed by measuring mass 3 at two different H_2 reference gas pressures. Each sample was analysed at least three times, and average D values and standard deviations are reported in per mil relative to a H_2 reference gas calibrated to Vienna Standard Mean Ocean Water (VSMOW).

2.3. Results and Discussion

2.3.1. Crude oil characteristics

The oils analysed in this study are non-biodegraded based on a high relative abundance of *n*-alkanes and Pr and Ph, and the absence of 25-norhopanes and an obvious unresolved complex mixture (UCM). This is consistent with the findings of a previous study of the Sirte Basin crude oils by Burwood et al. (2003). The following sections therefore focus on the thermal maturity and the source of organic matter (OM) of the East Sirte Basin crude oils.

2.3.2. Thermal maturity

Thermal maturity parameters based on selected biomarker ratios (i.e. Pr/*n*-C_{17} and Ph/*n*-C_{18}, ααα C_{29} sterane 20*S*/(20*S*+20*R*) and Ts/(Ts+Tm) for the Sirte Basin crude oils are shown in Table 2.1. In non-biodegraded crude oils the isoprenoid to *n*-alkane ratios, Pr/*n*-C_{17} and Ph/*n*-C_{l8}, are useful indicators of thermal maturity (Lijmbach, 1975; Radke et al., 1980). The oils of the East Sirte Basin show obvious differences based on these ratios (Fig. 2.3) and fall into two major families (A and B). Those in family A are from the Sarir-L, Nafoora, Faregh and Sarir-C fields. They have the lowest values for Pr/*n*-C_{17} and Ph/*n*-C_{l8} (0.22-0.30 and 0.09-0.30), likely due to their higher thermal maturity. Oils from the Amal, Gialo and Masrab fields are assigned to family B and have the highest values of Pr/*n*-C_{17} and Ph/*n*-C_{l8} (0.40-0.84 and 0.29-0.74), consistent with their lower thermal maturity. A plot of ααα C_{29} sterane (20*S*/20*S*+20*R*) against Ts/Ts+Tm (Seifert and Moldowan, 1978; Fig. 2.4) confirms that the family A oils are the most mature, and family B the least mature.

2.3.3. Molecular indicators of source rock depositional environment

According to Hughes et al. (1995), the dibenzothiophene (DBT)/ phenanthrene (P) and Pr/Ph ratios of crude oils can be used to identify their source lithofacies. These parameters for the Sirte Basin oils analysed in this study (Table 2.2), when plotted in Fig. 2.5, identify two principal source rock types. All of the family B oils appear to have originated from marine shales deposited under sub-oxic conditions (DBT/P <1, Pr/Ph = 1–2). The higher Pr/Ph values of the family A oils (>2) and DBT/P <1 indicate deposition of the source rock under more oxic conditions (Fig. 2.5). Two of the family A oils have Pr/Ph values <3 (from the Sarir-L, Nafoora fields) which may indicate a source

rock deposited in a relatively less oxic environment, or they may be hybrid crudes that are the result of in-reservoir mixing of family A and family B oils.

Table 2.1 Selected thermal maturity biomarker parameters of the crude oils from the East Sirte Basin.

Well	Field	Formation	Depth (m)	Pr/n-C_{17}	Ph/n-C_{18}	Ts/Ts+Tm	αααC_{29} S/S+R	Pr/Ph
Family A								
Z2-80	Sarir-L	Nubian	3167	0.29	0.30	0.48	0.60	2.22
Y1-51	Nafoora	Nubian	3036	0.30	0.22	0.62	0.67	2.53
5I13-59	Faregh	Nubian	3006	0.22	0.09	0.56	0.69	2.13
VV3-65	Sarir-C	Nubian	2667	0.26	0.10	0.58	0.70	2.28
Family B								
3V3-59	Gialo	Lidam	3102	0.57	0.45	0.40	0.55	1.51
3V4-59	Gialo	Nubian	3121	0.76	0.58	0.45	0.58	1.57
6C1-59	Gialo	Gialo	979	0.75	0.61	0.41	0.54	1.40
E225-59	Gialo	Jakhira	3290	0.72	0.59	0.40	0.49	1.64
E216-59	Gialo	Augila	3182	0.70	0.56	0.44	0.50	1.71
6J6-59	Gialo	Nubian	3430	0.48	0.42	0.40	0.59	1.73
6J8-59	Gialo	Nubian	3290	0.48	0.41	0.41	0.56	1.62
6K1-59	Gialo	Lidam	3364	0.55	0.43	0.40	0.58	1.85
5R1-59	Gialo	Lidam	3458	0.72	0.52	0.43	0.59	1.75
P-12	Masrab	Gialo	3329	0.84	0.74	0.44	0.54	1.78
B-90	Amal	Amal	3090	0.40	0.29	0.40	0.53	1.88
B-95	Amal	Amal	3092	0.42	0.31	0.45	0.46	1.70
B-99	Amal	Maragh	3053	0.45	0.32	0.46	0.51	1.98
D-10	Amal	-	824	0.49	0.45	0.48	0.57	1.76
D-17	Amal	-	808	0.53	0.44	0.48	0.54	1.64
B-86	Amal	Amal	2996	0.42	0.30	0.46	0.51	1.83
B-88	Amal	Amal	3000	0.42	0.30	0.47	0.45	1.84
AA-01	Amal	Sahabi	3824	0.55	0.44	0.47	0.49	1.75
AA-03	Amal	Sahabi	3848	0.54	0.42	0.47	0.52	1.91
B-96	Amal	Amal	3261	0.44	0.34	0.47	0.50	1.93

Pr= pristane/Ph= phytane; Ts/Ts+Tm= 18α (H)-22, 29, 30-trisnorhopane/18α(H)-22, 29,30-trisnorhopane+17α(H)-22,29,30-trisnorhopane; $S/S+R$=C_{29}ααα20S/C_{29}ααα20S + C_{29}ααα20R.

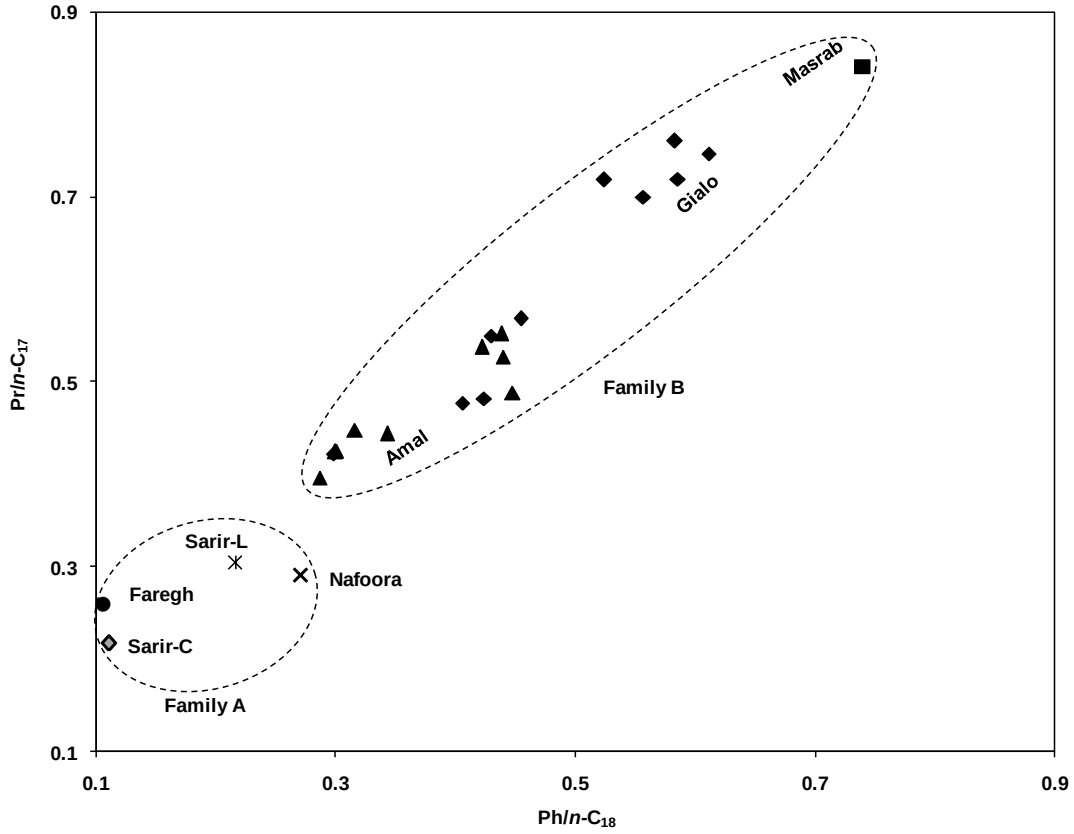

Fig 2.3 Cross-plot of Ph/*n*-C_{18} versus Pr/*n*-C_{17} showing the varying thermal maturity levels for two families of crude oil (A and B), source and depositional environments.

The family A oils contain a high relative abundance of prokaryotic biomarkers relative to eukaryotic biomarkers (Table 2.2) having much higher hopane/sterane ratios (12–13 for crudes from the Faregh and Sarir-C fields and 0.66–2.18 from Sarir-L, Nafoora) than do the oils of family B (0.07–2). In family A oils C_{29} steranes are generally more abundant relative to C_{27} steranes (Table 2.2) compared to family B (Fig. 2.6). The high abundance of the C_{24} tetracyclic terpane (TeT) relative to C_{19} – C_{24} tricyclic terpanes (TT) in some Australian crude oils has been suggested to reflect their origin from terrigenous OM (Philp and Gilbert, 1986). Therefore, the high ratio of C_{24} TeT to C_{23}TT in family A oils (0.71: Table 2.2) may indicate a predominantly terrigenous source for their organic matter (OM). In contrast, the family B oils are characterised by lower ratios of C_{24}TeT to C_{23}TT and C_{19} to C_{23} TT (Table 2.2) and an extended TT series up to carbon number 45 (Fig. 2.6) indicating a dominantly marine source.

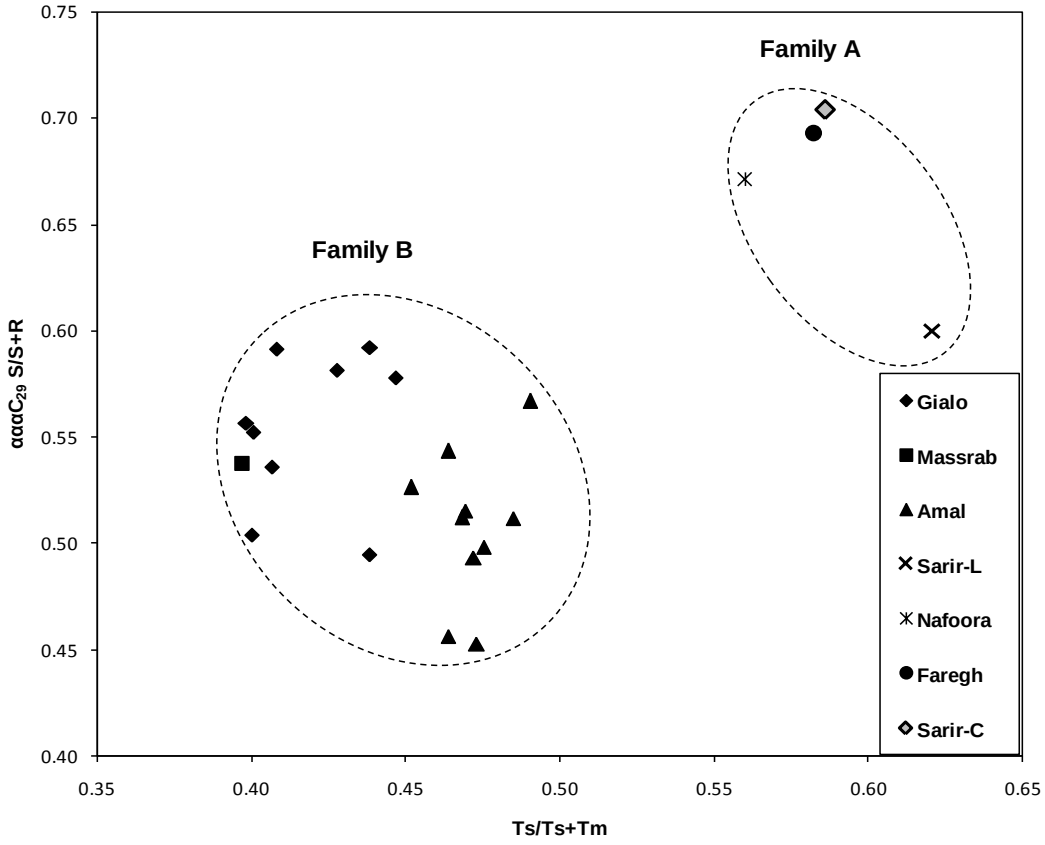

Fig. 2.4 Cross-plot of Ts/Ts+Tm versus ααα C_{29} sterane (20S/ 20S+20R) for the East Sirte Basin oils. Two oil families are defined (A and B) according to their thermal maturity levels.

Table 2.2 Source-specific parameters of the crude oils from the East Sirte Basin

Well	Field	Formation	Depth (m)	Source-specific parameters			
				C_{29}/C_{27} Ste	Hop /Ste	C_{24}TeT/C_{23}TT	C_{19}TT/C_{23}TT
Family A							
5I13-59	Faregh	Nubian	3006	1.36	12.98	0.71	0.74
VV3-65	Sarir-C	Nubian	2667	1.39	12.50	0.71	0.71
Family AB							
Z2-80	Sarir-L	Nubian	3167	1.25	0.66	0.38	0.05
Y1-51	Nafoora	Nubian	3036	1.28	2.18	0.45	0.21
Family B							
3V3-59	Gialo	Lidam	3102	1.11	0.53	0.29	0.09
3V4-59	Gialo	Nubian	3121	1.18	0.99	0.29	0.08
6C1-59	Gialo	Gialo	979	1.05	1.15	0.29	0.07
E225-59	Gialo	Jakhira	3290	0.96	1.62	0.37	0.09
E216-59	Gialo	Augila	3182	1.17	1.71	0.31	0.08
6J6-59	Gialo	Nubian	3430	0.86	0.20	0.28	0.11
6J8-59	Gialo	Nubian	3290	0.73	0.09	0.30	0.15
6K1-59	Gialo	Lidam	3364	0.94	0.37	0.31	0.07
5R1-59	Gialo	Lidam	3458	1.11	0.47	0.26	0.07
P-12	Masrab	Gialo	3329	0.98	1.13	0.28	0.06
B-90	Amal	Amal	3090	1.08	2.14	0.28	0.12
B-95	Amal	Amal	3092	1.07	2.15	0.40	0.12
B-99	Amal	Maragh	3053	1.09	1.92	0.24	0.11
D-10	Amal	-	824	0.95	0.94	0.24	0.15
D-17	Amal	-	808	0.96	1.39	0.26	0.11
B-86	Amal	Amal	2996	1.11	1.89	0.27	0.11
B-88	Amal	Amal	3000	1.15	1.75	0.40	0.13
AA-01	Amal	Sahabi	3824	0.60	0.07	0.29	0.12
AA-03	Amal	Sahabi	3848	0.77	0.07	0.29	0.12
B-96	Amal	Amal	3261	1.18	2.03	0.40	0.13

Pr= pristane/Ph= phytane; DBT= dibenzothiophene/P= phenanthrene; C_{29}/C_{27} Ste = C_{29} and C_{27} regular sterane; Hop/ Ste = Hopane / sterane; where hopanes=17α (H), 21β (H)-hopane and steranes= 14α, 17α-cholestane (20*S*); C_{24}TeT/C_{23}TT= C_{24} tricyclic terpane/C_{24} tetracyclic terpane +C_{23} tricyclic terpane; C_{19}TT/C_{23}TT= C_{19} tricyclic terpane/C_{19} tricyclic terpane + C_{23} tricyclic terpane.

2.3.4. δD of *n*-alkanes and isoprenoids

The average D value of *n*-alkanes and the D values of Pr and Ph from the crude oils are summarised in Table 2.2. The *n*-alkane D profiles are shown in Fig 2.7. The average D values of the *n*-alkanes range from -98‰ to -130‰ and show no obvious distinction between families A and B. However, the D values of Pr and Ph are significantly more enriched in D for the family A oils (with the exception of Pr for Sarir-L) compared to the family B oils probably reflecting higher thermal maturity (cf. Dawson et al., 2005; 2007).

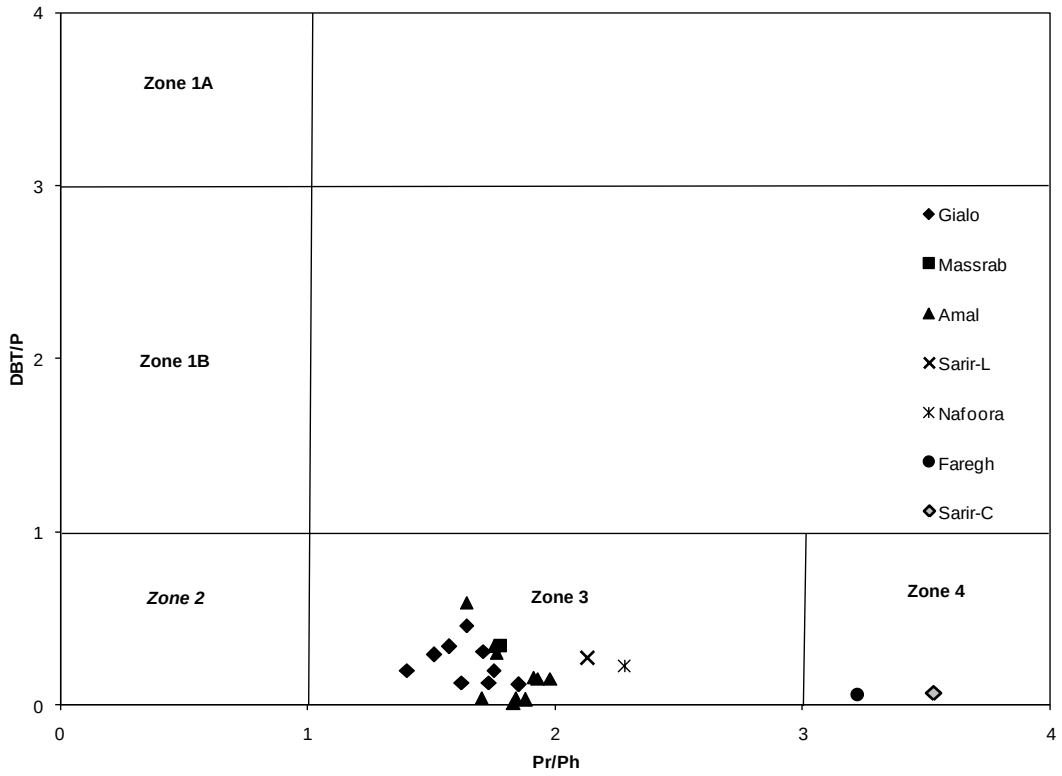

Fig 2.5 Cross-plot of DBT/P versus Pr/Ph for East Sirte Basin crude oils showing their source-rock depositional environments and lithologies. Zone 1A = marine carbonate; Zone 1B = marine carbonate and marl; Zone 2 = marine hypersaline; Zone 3 = marine shale and lacustrine; Zone 4 = fluvio-deltaic shale (after Hughes et al., 1995).

The thermal maturity of the crude oils can also be assessed based on the differences between the δD values of Pr and Ph and the average δD values of the *n*-alkanes (δD, Dawson et al., 2005; 2007). The family A oils have δD values of 31 to 60 ‰ reflecting higher thermal maturity, while the less mature family B oils have δD values of -3 to 26 ‰ (Table 2.3). These results are also consistent with the thermal maturities assessed by traditional biomarker parameters (see above).

Interestingly the δD value of Pr for Sarir-L (family A) is more negative than Ph, suggesting perhaps a contribution here for Pr from tocopherol E derived from terrestrial organisms (Goosens et al., 1984). This is further evidence for a terrestrial contribution to this family A oil. All oils show a trend of more positive D values with increasing carbon number for *n*-alkanes between C_{23} and $C_{30,}$ reflecting in part contributions to these compounds from higher-plant waxes (Fig. 2.5).

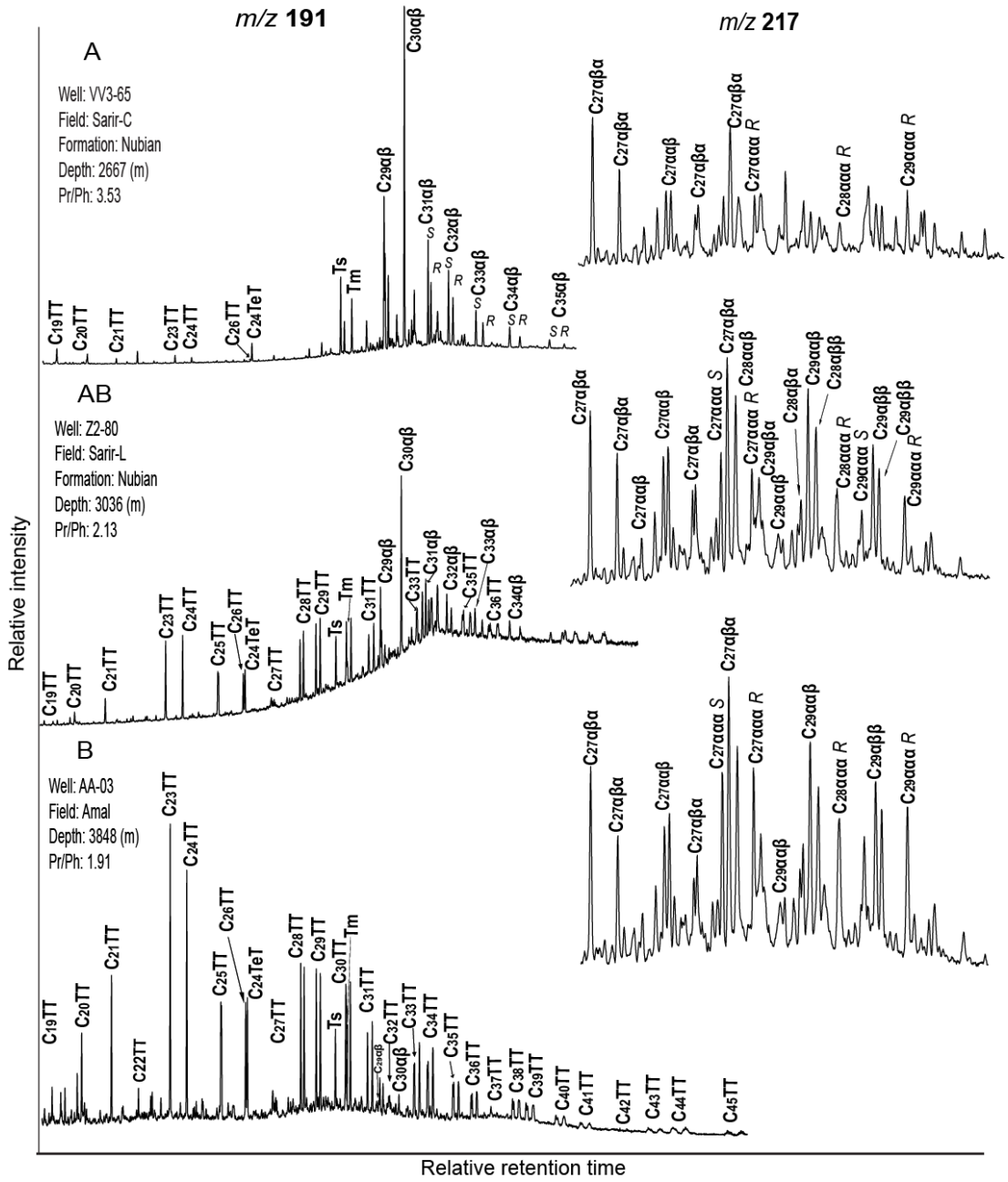

Fig. 2.6 Partial mass chromatograms showing distributions of tricyclic and tetracyclic terpanes and hopanes (*m/z* 191) and steranes (*m/z* 217) in various oils from the East Sirte Basin

Table 2.3 Stable hydrogen and carbon isotopic data for crude oils from the East Sirte Basin.

Well	Field	Formation	Depth(m)	Pr(δD‰)	Ph(δD‰)	$\delta^{13}C$‰	δD‰	ΔδD‰
Family A								
Z2-80	Sarir-L	Nubian	3167	-101	-93	-28.6	-128	31
Y1-51	Nafoora	Nubian	3036	-78	-70	n.d.	-112	38
5I13-59	Faregh	Nubian	3006	-76	-65	-27.3	-129	59
VV3-65	Sarir-C	Nubian	2667	-75	-65	-29.0	-130	60
Family B								
3V3-59	Gialo	Lidam	3102	-108	-103	-29.9	-127	22
3V4-59	Gialo	Nubian	3121	-103	-100	-30.6	-127	26
6C1-59	Gialo	Gialo	979	n.d.	n.d.	-31.1	-126	n.d
E225-59	Gialo	Jakhira	3290	-111	-109	n.d	-107	-3
E216-59	Gialo	Augila	3182	-107	-105	n.d	-110	4
6J6-59	Gialo	Nubian	3430	n.d.	n.d.	n.d	-109	n.d
6J8-59	Gialo	Nubian	3290	-101	-99	n.d.	-104	4
6K1-59	Gialo	Lidam	3364	n.d.	n.d.	-31.2	-116	n.d
5R1-59	Gialo	Lidam	3458	-110	-95	-30.8	-124	22
P-12	Masrab	Gialo	3329	n.d.	n.d.	-33	-115	n.d
B-90	Amal	Amal	3090	-112	-100	-32.7	-114	8
B-95	Amal	Amal	3092	-114	-97	-32.3	-110	5
B-99	Amal	Maragh	3053	-111	-96	-32.3	-109	6
D-10	Amal	-	824	-109	-100	n.d	-117	13
D-17	Amal	-	808	n.d.	n.d.	-30.1	-116	n.d
B-86	Amal	Amal	2996	n.d.	n.d.	-32.2	-128	n.d
B-88	Amal	Amal	3000	n.d.	n.d.	-32.1	-113	n.d
AA-01	Amal	Sahabi	3824	-103	-94	n.d	-98	-1
AA-03	Amal	Sahabi	3848	-102	-100	-30.8	-102	1
B-96	Amal	Amal	3261	-108	-103	n.d	-126	21

δD‰ = the average of δD values of *n*-alkanes (C_{15} – C_{30}); $\delta^{13}C$‰ =the average of $\delta^{13}C$‰ values of *n*-alkanes (C_{15} – C_{30}); ΔδD: Difference between average δD value of Pr and Ph and average δD value of *n*-alkanes and n.d.: not determined.

2.3.5. $\delta^{13}C$ of *n*-alkanes

The average $\delta^{13}C$ values of *n*-alkanes (C_{15}-C_{30}) for the East Sirte Basin oils range from -27.3‰ to -32.7‰ (Table 2.3). All the oils show relatively flat $\delta^{13}C$ profiles for the *n*-alkanes (C_{15}-C_{30}, Fig. 2.8). Family A oils have average *n*-alkane $\delta^{13}C$ values ranging from -27.3‰ to -29.0‰, while family B oils have average *n*-alkane ^{13}C values ranging from -29.9‰ to -32.7‰. Family A oils are more thermally mature than family B oils based on biomarker and D results (see above).

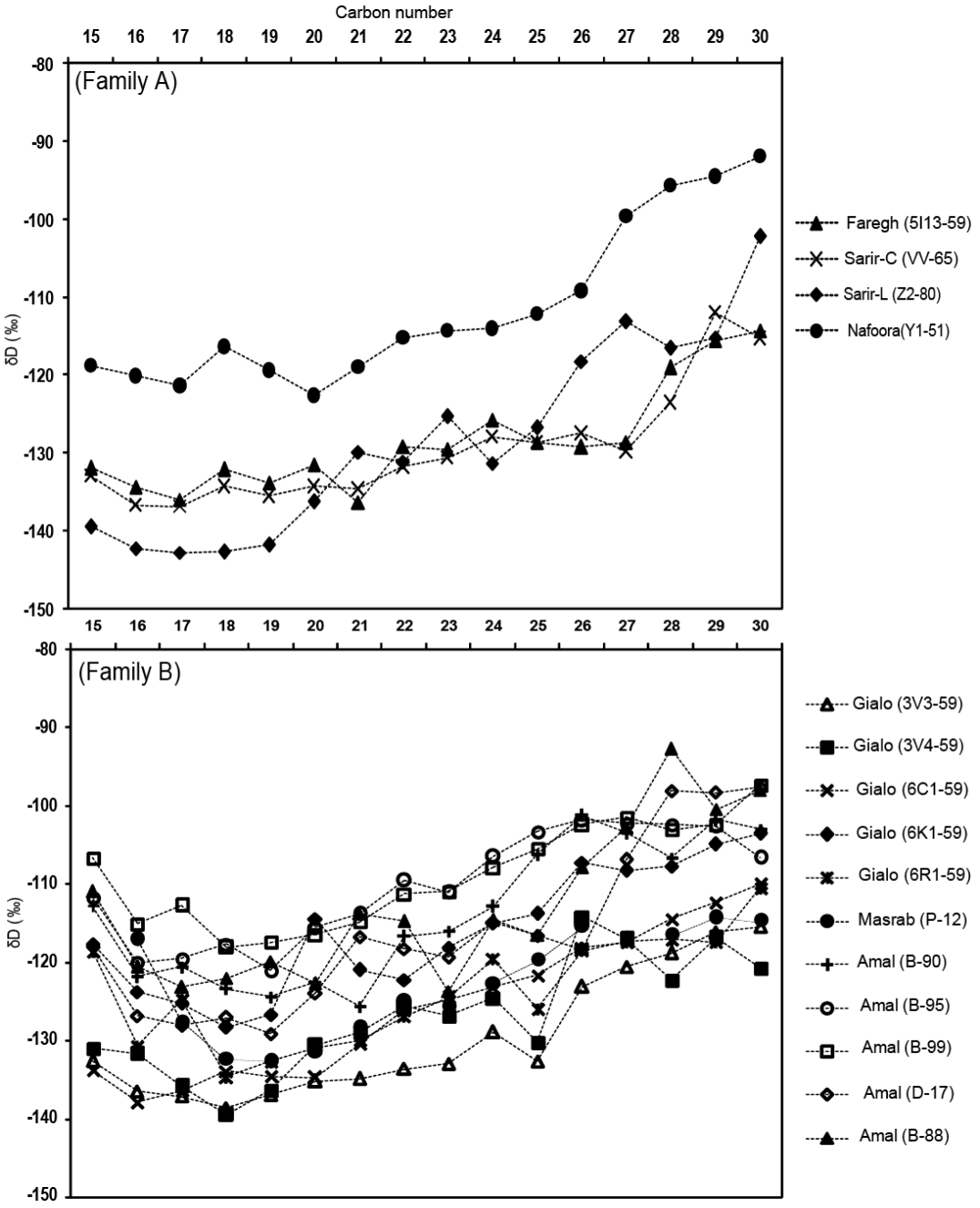

Fig 2.7 Stable hydrogen isotopic (δD ‰) profiles of *n*-alkanes in East Sirte Basin oils: (A) family A and (B) family B.

The relatively more positive ^{13}C values of *n*-alkanes in family A oils are consistent with their higher thermal maturities. However the extent of ^{13}C enrichment cannot be attributed to maturity alone because the differences between A and B families are generally greater than 2‰ (Clayton, 1991; Summons et al., 1994; Peters et al., 2005). ^{13}C values for the *n*-alkanes therefore largely reflect source. The more negative ^{13}C values for most of the Family B oils

are consistent with a marine source (Murray et al., 1994), whereas the more positive values for the family A oils are indicative of a terrestrial contribution.

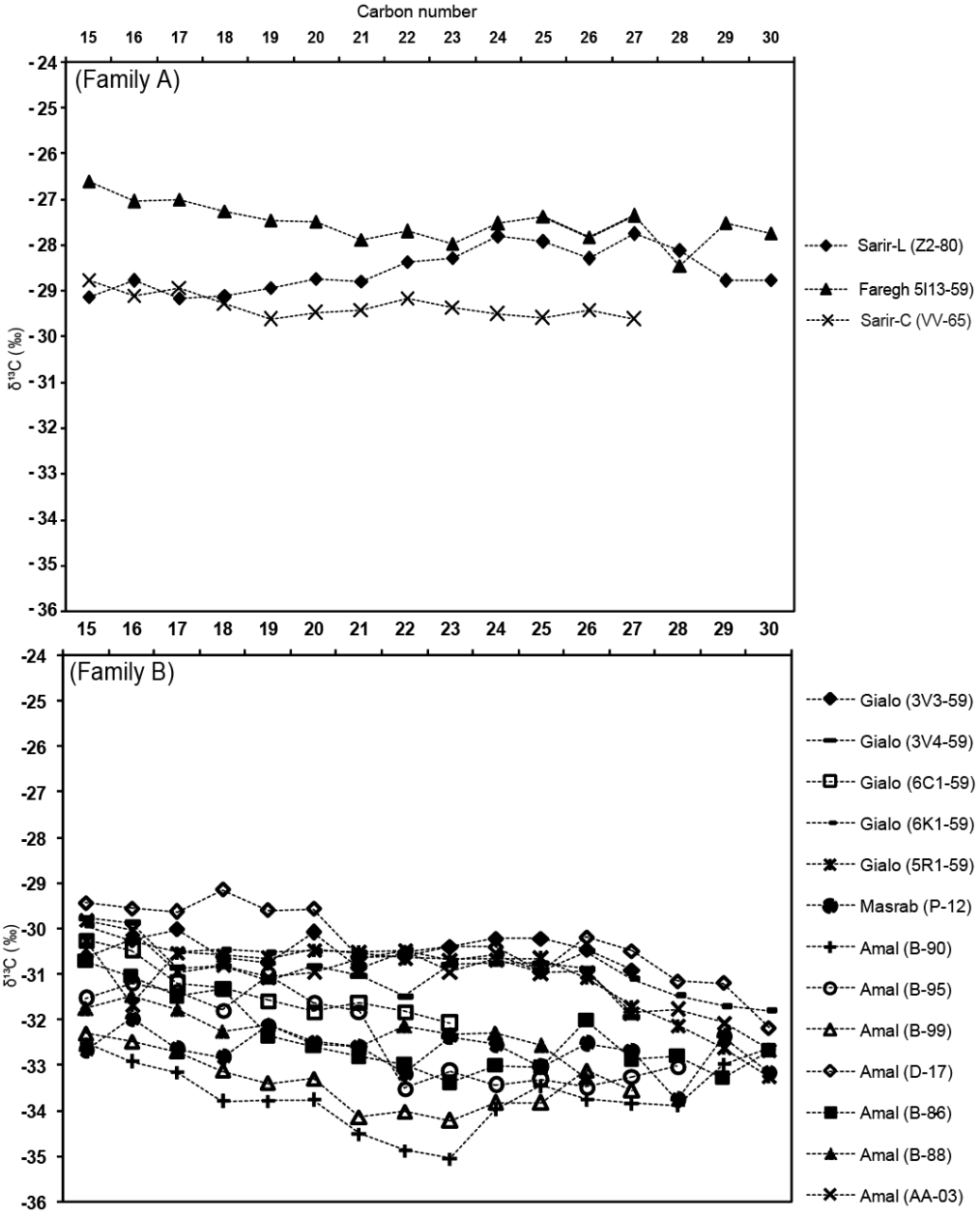

Fig. 2.8 Stable carbon isotopic ($\delta^{13}C$ ‰) profiles of *n*-alkanes in East Sirte Basin oils: (A) family A and (B) family B.

2.4. Conclusions

(i) A variety of organic geochemical analyses were applied to large a set of oils from the East Sirte Basin (Libya). The thermal maturity and

palaeoenvironment of deposition was established, using biomarker ratios and compound specific hydrogen and carbon isotopes of individual hydrocarbons from crude oils.

(ii) Various biomarker maturity parameters separated the oils from the East Sirte Basin into two main families (A and B). The family A oils (Sarir-L, Nafoora, Faregh and Sarir-C fields) were found to be relatively more mature having higher ratios of Pr/n-C_{17}, Ph/n-C_{18}, ααα C_{29} 20S/20S+20R and Ts/Ts+Tm than the family B oils (Amal, Gialo and Masrab fields). The D values of Pr and Ph were found to be significantly more enriched in D for the family A oils, compared to the family B oils reflecting the higher thermal maturity of family A oils.

(iii) Source-specific biomarker parameters indicate that family B oils are derived from a marine source rock deposited under sub-oxic conditions, based on Pr/Ph ratios, sterane/hopane ratios and the distribution of tricyclic and tetracyclic terpanes. Family A oils have a more terrestrial source affinity.

(iv) Family A oils have relatively more positive ^{13}C values of n-alkanes than family B oils, consistent with the higher thermal maturity of family A oils and their derivation from a terrestrial source rock. The more negative ^{13}C values for the family B oils are consistent with a marine source.

Acknowledgements

The authors thank Geoff Chidlow and Sue Wang for their assistance with GC-MS and GC-ir-MS analysis, respectively. We are grateful to the staff of the National Oil Corporation (NOC) in Tripoli and staff of the Libyan Petroleum companies (Waha, Veba and Gulf) for providing samples. We thank Dr Khaled R. Arouri and an anonymous reviewer for their constructive and very helpful comments on this manuscript. Aboglila thanks Curtin University for a fee waiver and scholarship.

2.5. References

Abadi, A., 2002. Tectonics of the Sirte Basin. PhD Dissertation. Vrije Universiteit, Amsterdam ITC. Enschede, p. 187.

Ahlbrandt, T.S., 2001. The Sirte Basin is Province of Libya-Sirte-Zelten Total Petroleum System. US Geological Survey Bulletin 2202-F. <http://geology.cr.usgs.gov/pub/bulletins/b2202-f/> (accessed 20.4.2009)

Barr, F.T., Weegar, A.A., 1972. Stratigraphic Nomenclature of the Sirte Basin, Libya. Petroleum Exploration Society of Libya, Tripoli, p. 179.

Bastow, T.P., van Aarssen, B.G.K., Lang, D., 2007. Rapid small–scale separation of saturate, aromatic and polar components in petroleum. Organic Geochemistry, 38, 1235–1250.

Burwood, R., Redfern, J., Cope, M., 2003. Geochemical evaluation of East Sirte Basin (Libya) petroleum systems and oil provenance. In: Burnham, T., MacGregor, D.S., Cameron, N.R. (Eds.), Petroleum Geology of Africa. Geological Society Special Publication, London, 207, 203–214.

Clayton, C., 1991. Effect of maturity on carbon isotope ratios of oils and condensates. Organic Geochemistry, 17, 887–899.

Dawson, D., Grice, K., Alexander, R., 2005. Effect of maturation on the indigenous D signatures of individual hydrocarbons in sediments and crude oils from the Perth Basin (Western Australia). Organic Geochemistry, 36, 95–104.

Dawson, D., Grice, K., Alexander, R., Edwards, D., 2007. The effect of source and maturity on the stable isotopic compositions of individual hydrocarbons in sediments and crude oils from the Vulcan Sub-basin, Timor Sea, Northern Australia. Organic Geochemistry, 38, 1015–1038.

El-Alami, M., Rahouma, S., Butt, A., 1989. Hydrocarbon habitat in the Sirte Basin northern Libya. Petroleum Research Journal, 1, 17–28.

Ghori, K.A.R., Mohammed, R.A., 1996. The application of petroleum generation modelling to the eastern Sirte Basin, Libya. In: Salem, M.J., El-Hawat, A.S., Sbeta, A.M. (Eds.), the Geology of Sirte Basin II, Elsevier, Amsterdam, p. 529–540.

Goosens, H., de Leeuw, J.W., Schenck, P.A., Brassell, S.C., 1984. Tocopherols as likely precursors of pristine in sediments and crude oils. Nature, 312, 440-442.

Gras, R., 1996. Structural style of the southern margin of the Messlah High. In: Salem, M.J., El-Hawat, A.S., Sbeta, A.M. (Eds.). The Geology of Sirte Basin II, Elsevier, Amsterdam, 201–210.

Grice, K., de Mesmay, R., Glucina, A., Wang, S., 2008. An improved and rapid 5A molecular sieve method for gas chromatography isotope ratio mass spectrometry of n-alkanes (C_8-C_{30}). Organic Geochemistry, 39, 284-288.

Guiraud, R., Maurin, J.C., 1991. Early Cretaceous rifts of Western and Central Africa: an overview. Tectonophysics, 213, 153–168.

Gumati, Y.D., Nairn, A.E.M., 1991. Tectonic subsidence of the Sirte Basin, Libya. Pet. Geol, 14**,** 93–102.

Hughes, W., Holba, A.G., Dzou, L., 1995. The ratios of dibenzothiophene to phenanthrene and pristane to phytane as indicators of depositional environment and lithology of petroleum source rock. Geochimica et Cosmochimica Acta, 59, 3581–3598.

Lijmbach, M., 1975. On the origin of petroleum. In: Proceedings 9th World Petroleum Congress, 2, 357-369.

Macgregor, D.S., 1996. The hydrocarbon systems of North Africa. Marine and Petroleum Geology, 13, 32-340.

Murray, A.P., Summons, R.E., Boreham, C.J., Dowling, L.M., 1994. Biomarker and *n*-alkane isotope profiles for Tertiary oils: relationship to source rock depositional setting. Organic Geochemistry, 22, 521-542.

Parsons, M.G., Zagaar, A.M., Curry, J.J., 1980. Hydrocarbon occurrence in the Sirte Basin, Libya. Canadian Society of Petroleum Geologists Memoirs, 6, 723-732.

Peters, K.E., Walters, C.C., Moldowan, J.M., 2005. The biomarker guide vol 1: biomarkers and isotopes in the environment and human history. Cambridge University Press, Cambridge, 471.

Philp, R.P., Gilbert, T.D., 1986. Biomarker distributions in Australian oils predominantly derived from terrigenous source material. Organic Geochemistry, 10, 73–84.

Radke, M., Willsch, H., Welte, D.H., 1980. Preparative hydrocarbon group type determination by automated medium liquid chromatography. Analytical Chemistry, 52, 406–411.

Rusk, D.C., 2001. Libya: Petroleum potential of the underexplored basin centers—A twenty-first-century challenge. In: Downey, M.W., Threet, J.C., Morgan, W.A. (Eds.), Petroleum Provinces of the Twenty-first Century. American Association of Petroleum Geologists Memoir, 74, 429–452.

Seifert, W.K., Moldowan, J.M., 1978. Applications of steranes, terpanes and monoaromatics to the maturation, migration and source of crude oils. Geochimica et Cosmochimica, Acta, 42, 77–95.

Summons, R.E., Jahnke, L.L., Roksandic, Z., 1994. Carbon isotopic fractionation in lipids from methanotrophic bacteria: Relevance for interpretation of the

geochemical record of biomarkers. Geochimica et Cosmochimica Acta, 58, 2853-2862.

Chapter 3

A geochemical evaluation of thermal maturity and depositional palaeoenvironments of seven Cretaceous formations from the East Sirte Basin (Libya)

S. Aboglila, K. Grice, K. Trinajstic, D. Dawson, K. Williford

LPI Petroleum Research Journal, Libya

In Press

Abstract

The Sirte Basin is Libya's most important petroleum province and the world's 13th largest petroleum-producing region. Within a complex geological setting several potential source rocks have been recognised, ranging in age from Precambrian to Eocene. Biomarker ratios, together with stable carbon ($\delta^{13}C$) and hydrogen (δD) isotopic compositions of individual hydrocarbons have been applied to source rock extracts (n = 21) from the East Sirte Basin to establish their respective thermal maturity and palaeoenvironmental conditions of deposition. Rock Eval pyrolysis (OI range: 3 - 309 units and HI range: 115 – 702 units) data obtained from the source rocks of the Sirte, Tagrifet, Rakb, Rachmat, Bahi and Nubian Formations show that the organic matter (OM) is mainly dominated by a Type II/III kerogen. Vitrinite reflectance (% R_o range: 0.46 – 1.38) data support variations in thermal maturity and indicate mature to post mature rocks of Sirte and Rachmat Formations and early to mid stage maturities for the rest of the formations. The Sirte Formation in the studied area was found to be relatively more thermally mature than the Tagrifet, Rakb, Rachmat, Bahi, and Nubian Formations, reflected by δD of pristane (Pr) and phytane (Ph) (less depleted in D). A contribution of terrestrial material to the organic matter for all formations except the Sirte Formation is evident from δD of the higher-molecular-weight *n*-alkanes. OM depositional conditions under anoxic and suboxic of the source rocks identified via the pristane to phytane (Ph/Ph range 0.65 – 1.25) and dibenzothiophene to phenanthrene (DBT/P range 0.04 – 0.47) values.

Keywords: East Sirte Basin, Libya, biomarkers, stable carbon isotopes, stable hydrogen isotopes, Cretaceous source rocks.

3.1. Introduction

The Petroleum Sirte Basin is one of Africa's most productive oil provinces, located in north-central Libya. It occupies an area of 600,000 km^2 (Abadi, 2002). In the world it has classified as the 13th largest petroleum region (Ahlbrandt, 2001), with oil equivalent recoverable in reserves of approximate 43 billion barrels (Burwood et al., 2003) (Fig. 3.1). Reviews of reserves, stratigraphical structure and petroleum geological description have been attained by many authors (e.g. Ghori and Mohammed, 1996; Baric et al., 1996; Ahlbrandt, 2001; Burwood et al., 2003, Aboglila et al., 2010)

Several petroleum systems have been identified, marginal to the horsts and the deeper Agedabia grabens in the offshore areas of the basin (Baird et al., 1996). In the Eastern Sirte Basin, significant stratigraphic traps superimposed on structural highs principally occur in Mesozoic clastic reservoirs, such as those of the Sarris and Massla fields (Abadi, 2002) (Fig. 3.1). The main structural features of the habitat are the Late Mesozoic–Cenozoic Agedabia and the slightly older Lower Cretaceous age Hameimat, Maragh and Sarir Troughs (Burwood et al., 2003) (Fig. 3.1). Subsidence throughout the Mesozoic has resulted in basin-fill sediments hosting source rocks (Burwood et al., 2003). Sediments decrease in thickness from 7 km offshore in the northern Gulf or Sirte province to around 1 km near the Nubian uplift in the south (Ahlbrandt, 2001). The grabens, particularly those in the southern part of the Zallah (Abu Tumayam), Maragh (Marada) and Sirte grabens, have recently been identified as potential hydrocarbon kitchens (Hallett and El-Ghoul, 1996).

Hydrocarbons generated by Late Eocene carbonate source rocks, particularly offshore, offers another possible additional hydrocarbon potential (Gruenwald, 2001). Traditionally the Upper Cretaceous marine shales of the Sirte and Rachmat sediments have been identified as the main sources of hydrocarbons in the Sirte Basin (Ghori and Mohammed, 1996; Baric et al., 1996) (Fig. 3.2), with total organic carbon (TOC) contents ranging between 1 and 5% (El-Alami et al., 1989). The main depocentre in the East Sirte Basin is the Agedabia Trough (Fig. 3.1) and due to the thickness of the section (>1400 m) there is considerable difference in the source rock maturity between the basal and uppermost shales (Burwood et al., 2003). Vitrinite reflectance (R_o) data indicate that the main

source rocks have reached at least three levels of thermal maturity (Hallett, 2002). Basin modelling has shown that in the southern part of the Agedabia Trough the Rachmat Formation entered the oil window during the Mid Eocene, whereas the Sirte Shale started generating oil in the Late Eocene. In the north of the Agedabia Trough (Fig. 3.1), where it plunges steeply the sediments are post-mature and have generated gas (Burwood et al., 2003). Additionally the Upper Cretaceous marine shales of the Rakb Formation and the carbonates of the Tagrifet Formation (Fig. 3.2) have been identified as source rock candidates in the Hameimat Trough; and the Rakb Formation is believed also to act as the seal for a number of the Sarir fields. The Nubian Formation (Triassic and Lower Cretaceous) (Fig. 3.2) comprises mostly continental sandstones, although some lacustrine shale horizons, located in the Faregh and Massla field of the Hameimat Trough (Fig. 3.1), may also act as source for minor inputs of waxy oils in the southern part of the Agedabia Trough (El-Hawat et al., 1996; Burwood et al., 2003).

This paper is to improve the on-going characterisation of hydrocarbon sources in the East Sirte Basin (Fig. 3.1), notably its Cretaceous shales (Fig. 3.2). An organic geochemical assessment of 99 source rock samples (n = 99) was performed on seven Cretaceous formations. Twenty one of these samples were subjected to more detailed biomarker and compound-specific stable carbon and hydrogen isotopes analyses. From these data the relative thermal maturities and paleoenvironments of deposition of the source-rocks was established.

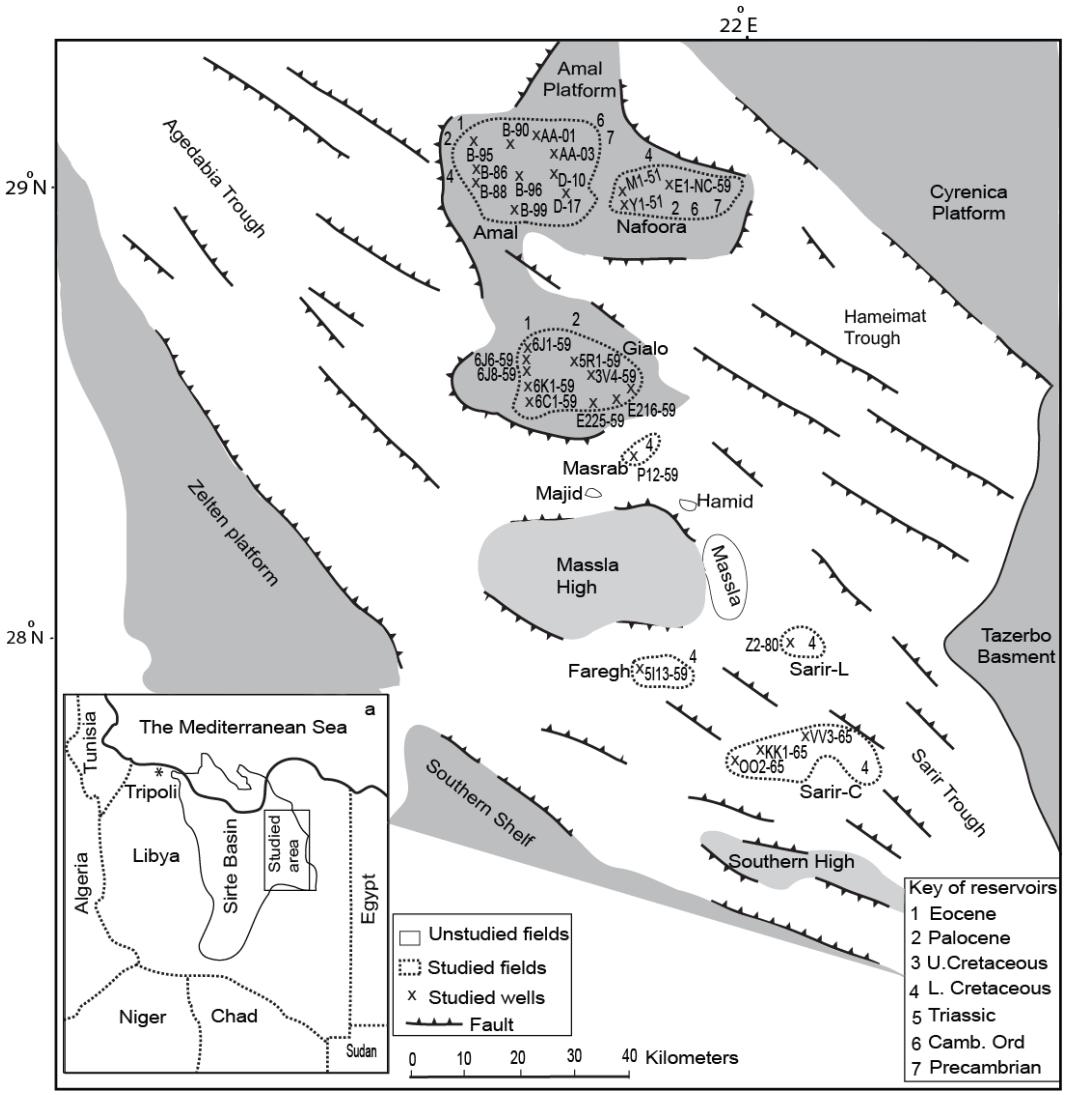

Fig. 3.1 Map shows the location of the Sirte Basin and its structural elements illustrate regional faults, high troughs and well samples in the studied area. Modified from Ahlbrandt (2001) and Aboglila et al. (2010).

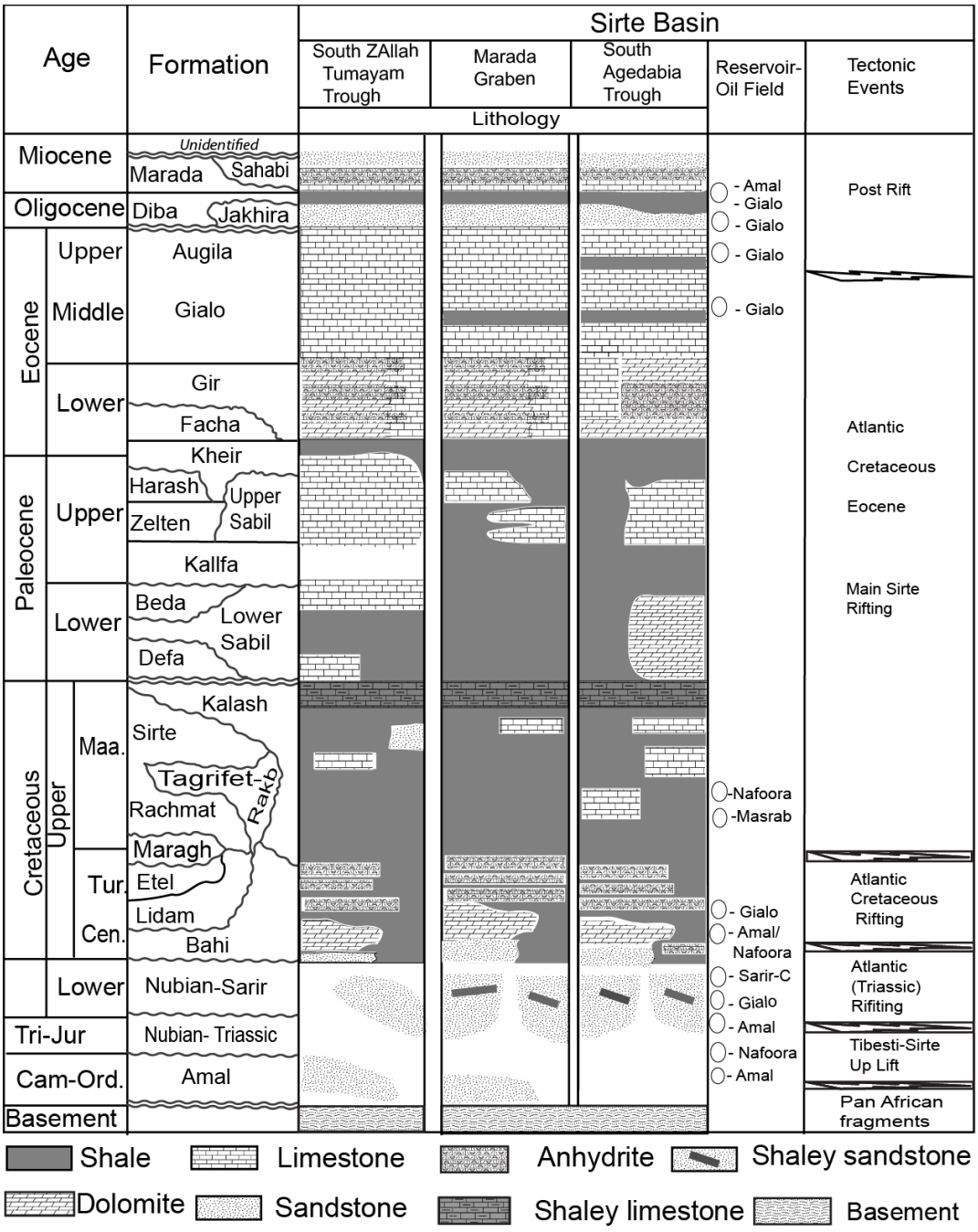

Fig. 3.2 Stratigraphic column of the Sirte Basin highlighting the lithologies of the formations, the reservoir units of the oil fields demonstrates age, formations, lithology, main reservoir-oil felids and its tectonic events. Modified from Barr and Weeger (1972), Rusk (2001) and Burwood et al. (2003).

3.2. Materials and methods

3.2.1. Geological setting

The Sirte Basin is part of one of Africa's oldest Hercynian structural provinces (Gras, 1996). Alternating episodes of uplift and subsidence commenced in the Neoproterozoic with the Pan-African orogeny that consolidated a number of proto-continental fragments into an early Gondwanaland (Kroner, 1993). Rifting began in the Early Cretaceous, peaked in the Late Cretaceous, and ended in the Early Tertiary, resulting in the triple junction within the basin (Ahlbrandt, 2001). During the Late Jurassic and Early Cretaceous, the central Atlantic Ocean opened between northwest Africa and North America, which led to a westward shift of the African plate relative to the European plate. At this time, continental rifting was active in Africa, affecting the Northeast Brazil-Gulf of Guinea domain, southern Chad, Sudan, Kenya, the north and east of Niger, the western desert of Egypt and the southern Sirte Basin in Libya (Coward and Ries, 2003). The east-west trending structures of the Sarir and Hameimat Trough of the Sirte Basin were formed during this period (Guiraud and Maurin, 1991). Most important information in previous reviews have attained in chapter 2.

3.2.2. Sample

Ninety nine samples of drill cuttings were collected by the National Oil Corporation (NOC) in Tripoli from 11 different wells (Fig. 3.1), located in the Amal, Galio, Nafoora, and Sarir Fields. The units sampled were the Upper Cretaceous Kalash Sirte, Rakb, Tagrifet Rachmat and Bahi Formations (Fig. 3.2) and the Lower Cretaceous Nubian (Sarir) Formation (Fig. 3.2). The terms Nubian Sandstone and Sarir Formation have been used by many authors for all or part of the non-marine Lower Cretaceous units (c.f. Hallett, 2002).

3.2.3. Preparation of cutting samples

The cutting samples were washed with doubly distilled water and dried at room temperature prior to analysis. Following Rock Eval pyrolysis and TOC analysis (see below), a suite of representative samples was selected for more detailed organic geochemical examination. These samples were ground to a fine powder (particle size of <150 μm) using a ring-mill (Rocklabs).

3.2.4. Rock Eval pyrolysis and total organic carbon (TOC) measurements

Rock Eval pyrolysis of powdered rock (10-50 mg) was carried out on a Girdel Rock Eval instrument, while the TOC was measured on a Leco instrument. Samples with low TOC values (< 0.5%) were considered unsuitable for Rock Eval pyrolysis and therefore not subjected to any further analyses.

3.2.5. Solvent extraction and isolation of the maltenes

Twelve cuttings samples from representative formations were selected for solvent extraction based on their TOC values (> 0.3%). About 10-20 g of ground sediment was extracted in an ultrasonic bath for two hours using a 9:1 mixture of dichloromethane (DCM) and methanol (MeOH). The solvent extract was then filtered and excess solvent removed by carefully heating on a sand bath (60°C) to obtain the bitumen. Asphaltenes were precipitated by mixing the bitumen with an excess of chilled *n*-heptane. The mixture was left (1 h) to settle for 1 h and later centrifuged at 2500 rpm for 5 min. The supernatant solution containing the maltenes was carefully removed and decanted. This procedure was repeated (5x) by adding fresh *n*-heptane to precipitate the asphaltenes. Maltenes from the bitumens were fractionated using a small-scale column chromatographic method (Bastow et al., 2007). In brief, the sample (maltenes, about 10–20 mg) was applied to the top of a small column (5.5 cm x 0.5 cm i.d.) of activated silica gel (120°C, 8 h). The aliphatic hydrocarbon (saturated) fraction was eluted with *n*-pentane (2 mL); the aromatic hydrocarbon fraction with a mixture of *n*-pentane and DCM (2 mL, 7:3 v/v,); and the polar (NSO) fraction with a mixture of DCM and MeOH (2 mL, 1: 1 v/v).

3.2.6. 5A Molecular sieving

Aliphatic fractions of maltenes were subjected to 5A molecular sieving as described by Grice et al. *(*2008). In brief, a portion of the aliphatic fraction in cyclohexane was added to a 2 mL vial, filled with activated sieves (7 mg). The vial was sealed and placed into a pre-heated aluminum block (85°C, 8 h). The solution was then cooled and decanted through a small column of silica plugged with cotton wool and pre-rinsed with cyclohexane (2 mL). The sieves were

subsequently rinsed well with cyclohexane and the washings filtered through the same silica column. The combined filtrates yielded the branched/cyclic fraction. The *n*-alkanes were recovered by hydrofluoric acid (HF) digestion of the sieve as described previously (Dawson et al., 2005).

3.2.7. Gas chromatography–mass spectrometry (GC-MS)

Aliphatic and aromatic fractions were analysed by GC-MS using a Hewlett Packard (HP) 5973 mass-selective detector (MSD) interfaced to a HP6890 gas chromatograph (GC). A HP-5MS (J and W Scientific) GC column (5% phenylmethylsiloxane stationary phase) was used with helium as the carrier gas. The GC oven was programmed from 40°C to 310°C at a rate of 3˚C/min, after which it was held isothermal for 30 min. Samples were dissolved in *n*-hexane and introduced by the HP6890 autosampler into a split-splitless injector operated in the pulsed-splitless mode. Biomarker data were acquired in a full-scan mode (*m/z* 50-500). The ion source was operated in the electron ionization (EI) mode at 70 eV. Selective ion monitoring (SIM) was used to identify the terpanes, steranes and triaromatic steroids by monitoring *m/z* 191, 217, 218 and 231 ions. Selected aromatic compounds were identified using *m/z* 178 (phenanthrene), *m/z* 156 (dimethylnaphthalenes) and *m/z* 184 (dibenzothiophene) ions and relative retention time data reported in the literature.

3.2.8. GC–isotope ratio mass spectrometry (GC-ir-MS)

A HP6890 gas chromatograph (GC) equipped with a HP6890 autosampler was used in tandem with a Micromass isotope ratio monitoring mass spectrometer (ir-MS) for stable carbon and hydrogen isotope measurements. The GC-ir-MS conditions used were those detailed by Dawson et al. (2005). In brief, the GC oven was programmed from 50°C to 310ºC at 3ºC/min with initial and final hold times of 1 and 20 min, respectively. An identical capillary column to that used in GC-MS analysis was employed for GC-ir-MS. The carrier gas was He at a flow rate of 1mL/min. The ^{13}C data were obtained by integrating the masses 44, 45 and 46 in the ion currents of the CO_2 reference. CO_2 was produced from oxidation of each chromatographically separated component, after being

passed through a quartz furnace packed with copper oxide pellets (heated at 850°C). The accuracy and precision of $\delta^{13}C$ measurements were monitored by analysing a mixture of organic reference compounds with known $\delta^{13}C$ ratios. Each sample was analysed at least three times, and the average $^{13}C/^{12}C$ values and standard deviations are reported in ‰ relative to a CO_2 reference gas calibrated to the Vienna Peedee Belemnite (VPDB). The δD values were obtained by integration of the masses 2 and 3 ions derived from H_2 reference, produced from pyrolysis of each chromatographically separated component, after passing through a quartz furnace packed with chromium particles (350-400 μm particle size, heated at 1050°C). The H_3^+ correction was performed by measuring mass 3 at two different H_2 reference gas pressures. Each sample was analysed at least three times, and average δD values and standard deviations are reported in ‰ relative to a H_2 reference gas calibrated to Vienna Standard Mean Ocean Water (VSMOW).

3.3. Results and Discussion

3.3.1. Bulk geochemical parameters

The data obtained from Rock Eval pyrolysis and TOC (%) measurements for the East Sirte Basin sediments show quite diverse values (Table 3.1). TOC values from the Sirte Shale Formation range between 0.18% and 5.50%, while TOC values obtained from the Tagrifet Formation range between 0.36% and 5.16%. Three grey-greenish Rakb Shale Formation samples (Amal Field) have TOC values ranging from 1.00% to 1.42% (Table 3.1). Nineteen samples from the Rachmat Shale have TOC values ranging from 0.60% to 1.90%. One sample from the Bahi Formation from M1-51 well (Nafoora Field) has a TOC of 0.90%. Eight samples from the Lower Cretaceous Nubian Formation have TOC values ranging from 0.23% to 0.69%, with the majority having < 0.5% TOC. The TOC values < 0.4% indicates of low source rock potential. Rock Eval pyrolysis data for all formations, including S_1 and S_2 (mg HC/g rock), Tmax (°C), production indices (PI), hydrogen indices (HI = mgHC/gTOC) and oxygen indices (OI = $mgCO_2$/gTOC) were measured. The HI versus OI (Fig. 3.3) and TOC versus S_2 (Fig. 3.4) cross-plots are used to determine the source rock quality (kerogen type) and richness. The majority of the source rocks contain Type II kerogen

(Peters and Moldowan, 1993), while the higher OI values of the Bahi and Nubian Formations indicate mixed Type II-III kerogen. The hydrocarbon potential of East Sirte Basin samples ranges from fair to excellent based on S_2 and TOC (Fig. 3.4). The Sirte and Tagrifet Formations exhibit the best (good to excellent) hydrocarbon potential. The high values (>1.0) for the S_1 peak (free hydrocarbons) and the abnormally high PI values (>0.2) might be indicative of migrated bitumen, as observed in other studies (e.g. Shaaban et al., 2006).

Table 3.1 Rock Eval/TOC data for selected formations from the East Sirte Basin

Formation	Samples	TOC	OI	HI	Tmax	S_2	S_1	PI
Kalash	6	0.21 to 0.28	n.d	n.d	n.d	n.d	n.d	n.d
Sirte	47	0.18 to 5.50	3 - 185	115 - 481	427 - 437	0.27 –21.40	0.16 – 49.60	0.07 – 1.55
Tagrifet	15	0.36 to 5.16	94 - 210	242 - 612	426 - 440	2.01 – 22.80	0.26 – 51.80	0.11 – 0.79
Rakb	3	1.00 to 1.42	91 - 129	208 -415	428 - 434	2.08 – 5.90	0.30 – 1.11	0.09 -0.20
Rachmat	19	0.60 to 1.90	49 - 221	126 - 702	428 - 434	1.18 – 11.46	0.20 – 31.04	0.09 – 0.43
Bahi	1	0.9	309	413	428	2.75	3.92	0.59
Nubian	8	0.23 to 0.69	262 - 280	419 - 433	425 - 426	2.22 – 2.91	3.05 – 3.79	0.54 – 0.58

TOC (wt %): total organic carbon; HI= Hydrogen Index (S_2*100/TOC) and OI= Oxygen Index (S_3*100/TOC); Tmax (^oC): maximum pyrolysis temperature yield; S_2: maximum temperature yield (mg HC/g rock); S_1: low temperature hydrocarbon yield (mg HC/g rock); PI: Production Index (S_1/S_1+S_2); n.d. not determined

3.3.2. Vitrinite reflectance (% R_o)

Vitrinite reflectance is the most extensively used thermal maturity indicator in petroleum geochemistry (e.g. Tissot and Welte, 1984; Hunt 1996). Thermal maturities of the studied samples were estimated from vitrinite reflectance measurements (%R_o). These measurements also show some correlation with the depths at which the samples were taken. Vitrinite reflectance data of representative samples from the deeper Sirte Formation range from 0.90 and 1.38 %R_o. Also two samples from the deeper Rachmat Fm have % R_o of 0.81 and 0.85. Both the Sirte and Rachmat Formation samples reached the oil window (Table 3.2). While samples from the shallower Tagrifet, Rakb, Bahi and Nubian Formations have % R_o values ranging between 0.46 and 0.58 supporting an early to mid stage of thermal maturity (Fig. 3.5).

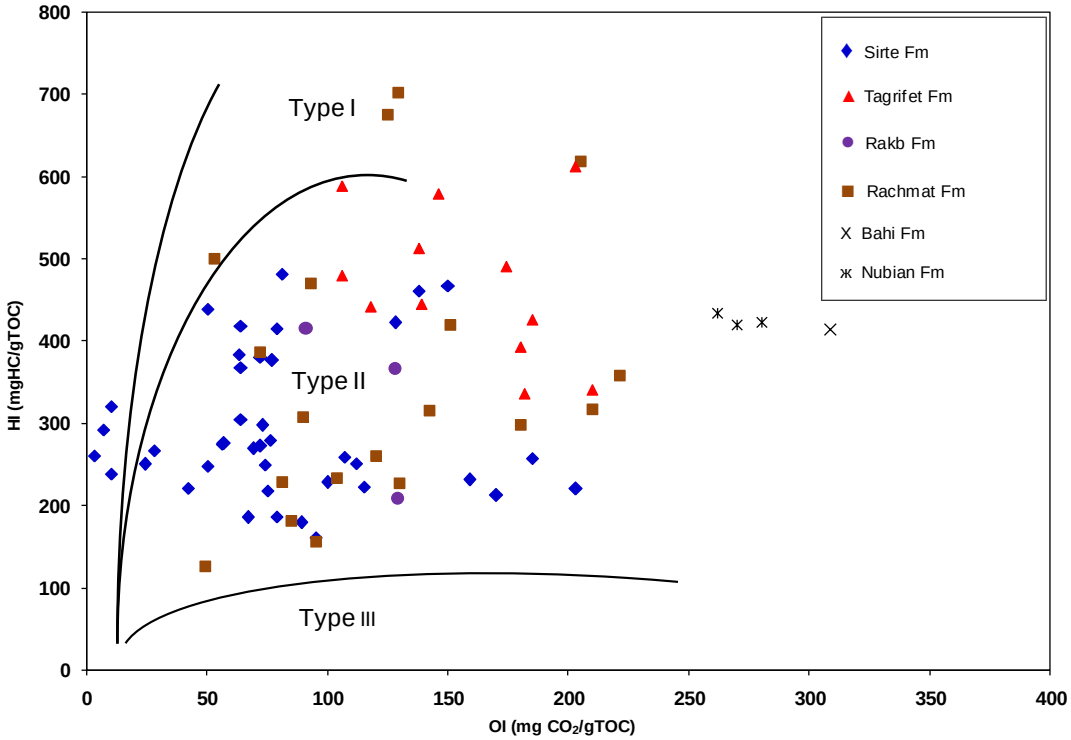

Fig. 3.3 Cross-plot of hydrogen index (HI) versus oxygen index (OI) illustrating the variation of kerogen type (I, II and III) in source rocks of the East Sirte Basin.

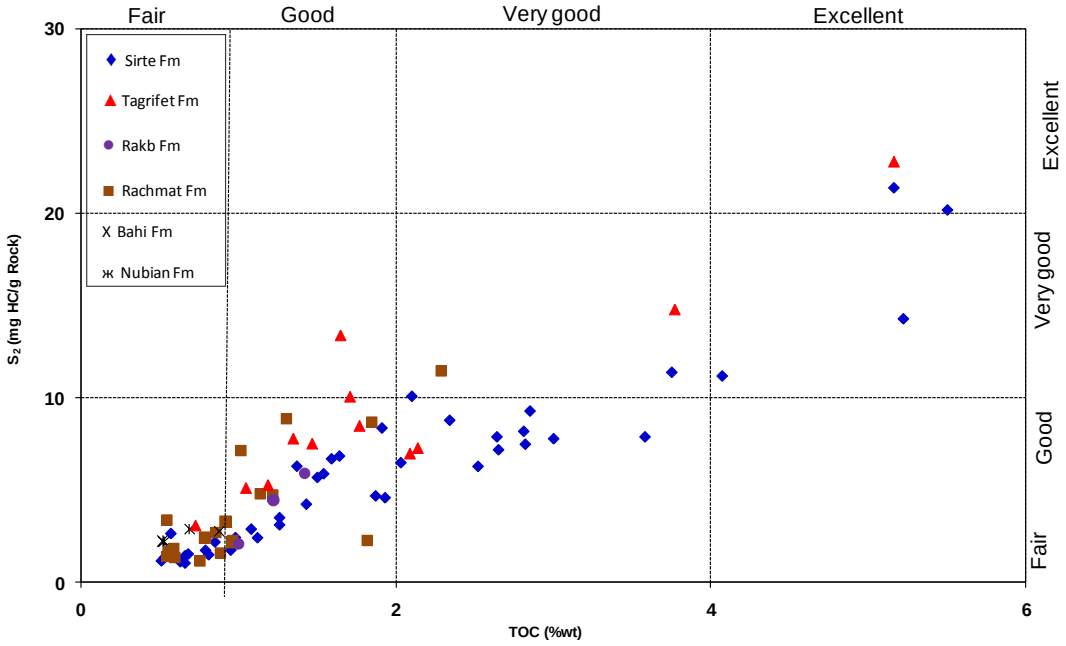

Fig. 3.4 Cross-plot of Rock Eval S_2 (mg HC/g rock) versus total organic carbon (TOC: wt. %) illustrating the variation of organic richness and petroleum generation potential in source rocks of the East Sirte Basin.

Table 3.2 Vitrinite reflectance and stable hydrogen and carbon isotopic data from the source-rocks of the East Sirte Basin

Field	Well	Formation	Depth (m)	%R_o	Pr (δD‰)	Ph(δD‰)	δD‰	$\delta^{13}C$‰	ΔD‰
Galio	6C1-59	Sirte	3051-54	1.29	-100	-101	-115	-29.2	15
Galio	6C1-59	Sirte	3600-03	1.33	-105	-100	-110	-30	8
Galio	6C1-59	Sirte	3087-90	1.30	-102	-105	n.d.	n.d.	n.d.
Galio	6J1-59	Sirte	3528-31	1.36	-102	-104	-109	-30.1	6
Galio	6J1-59	Sirte	3542	1.38	n.d.	n.d.	n.d.	n.d.	n.d.
Galio	6R1-59	Sirte	2967	1.24	-104	-107	n.d.	n.d.	n.d.
Sarir-C	KK1-65	Sirte	2670	1.05	n.d.	n.d.	n.d.	n.d.	n.d.
Sarir-C	OO2-65	Sirte	2478-81	0.90	n.d.	n.d.	n.d.	n.d.	n.d.
Nafoora	M1-51	Tagrifet	2882	0.58	-123	-116	-92	-31.8	-28
Sarir-C	KK1-65	Tagrifet	2745	0.51	-114	-114	-98	-33.1	-16
Sarir-C	KK1-65	Tagrifet	2760	0.55	n.d.	n.d.	-98	-32.8	n.d
Sarir-C	OO2-65	Tagrifet	2612	0.53	-112	-110	n.d.	-32.1	n.d
Amal	B-96	Rakb	2786	0.48	-118	-109	-92	n.d.	-20
Amal	B-95	Rakb	2725	0.46	-116	-113	n.d.	n.d.	n.d.
Nafoora	M1-51	Rachmat	3015	0.57	-118	-109	-96	-30.9	-18
Nafoora	M1-51	Rachmat	3000	0.53	-109	-110	n.d.	n.d.	n.d.
Sarir-C	OO2-65	Rachmat	2681	0.85	-115	-120	-98	-31.2	22
Sarir-C	OO2-65	Rachmat	2660	0.81	n.d.	n.d.	n.d.	n.d.	n.d.
Nafoora	M1-51	Bahi	3045	0.55	-118	-109	-96	-30.7	-18
Nafoora	M1-51	Nubian	3120	0.57	n.d.	n.d.	n.d.	n.d.	n.d.
Nafoora	M1-52	Nubian	3090-93	0.54	-116	-111	-99	-31	-15

R_o= vitrinite reflectance ; δD‰ = the average of D values of *n*-alkanes (C_{17} to C_{27}); $\delta^{13}C$‰ =the average of ^{13}C‰ values of *n*-alkanes (*n*-C_{16} to *n*-C_{27}) and ΔD‰ = Difference between average D values of Pr and Ph and average D values of *n*-alkanes (*n*-C_{17} to *n*-C_{27}); n.d. not determined.

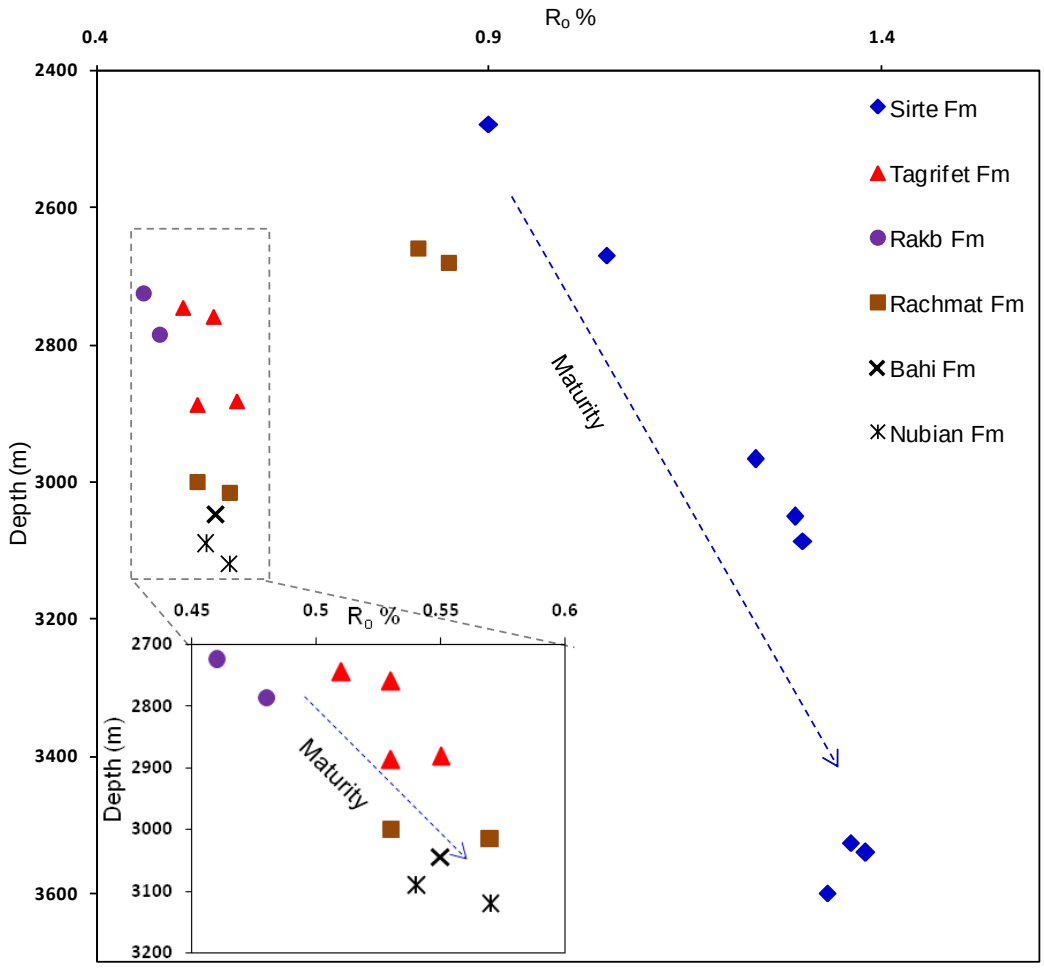

Fig. 3.5 Cross-plot of vitrinite reflectance versus vertical depth for selected source rock extracts from the East Sirte Basin.

3.3.3. Hydrogen and carbon isotopic composition

3.3.3.1. δD of *n*-alkanes and isoprenoids

Fig. 3.6 displays and compares the δD signatures of Pr and Ph measured in the various source rock intervals from the East Sirte Basin. Pr and Ph have been shown to become more enriched in δD with increasing thermal maturity (Dawson et al., 2005, 2007; Pedentchouk et al., 2006). The collected data (Table 3.2) show that δD values of isoprenoids are shown more positive than the *n*-alkanes. The δD enrichment in δD of Pr and Ph can attribute to a result of H/D exchange reactions, which favour the main and minor carbons adjacent to tertiary centres (Pedentchouk et al., 2006; Dawson et al., 2007). It is due to the isoprenoids tendency to undergo hydrogen exchange tertiary carbons more readily than straight-chain of *n*-alkanes because of their tertiary carbon centres.

The mechanism of hydrogen exchange led to D enrichment in Pr and Ph has known as rearrangement of chiral centres via structural changes in Pr and Ph isoprenoids (Dawson et al., 2007).

The observed enrichment of D in the Pr and Ph of these Libyan source rocks shows a strong correlation with various conventional thermal maturity parameters such as % R_o. Pr and Ph in Sirte Formation are relatively more enriched in D than the δD of isoprenoids in all the other formation, having δ values ranging from -100 to -105‰ for Pr and ranging from -100 to -104‰ for Ph. δD for the isoprenoids in the other formations range from -114 to -123‰ for Pr and -120 to -109‰ for Ph (Table 3.2). These δD data are consistent with the Sirte Formation being the most mature source rock of the East Sirte Basin.

The less mature rocks of the East Sirte Basin (Tagrifet, Bahi, Rakb and Rachmat Formations) contain Ph slightly more enriched in D relative to Pr (Fig. 3.6); possibly reflecting different sources (i.e. terrestrial plants versus algae) for Pr (cf. Dawson et al., 2007). The *n*-alkane D profiles of the aforementioned source rocks are shown in Fig. 3.7. The δD values of the higher-molecular-weight *n*-alkanes (C_{21}–C_{27}) from the Tagrifet, Bahi, Nubian, Rakb and Rachmat Formations are more positive (-94 to -91‰) than the lower-molecular-weight homologues in the same samples reflecting perhaps an input to the higher *n*-alkanes from land plants. The samples from the Bahi, Nubian, Rakb, Rachmat and Tagrifet Formations contain *n*-alkanes with average D values from -99 to -92‰, indicating a greater input of D-enriched terrestrial OM relative to the more distal (deeper) marine Sirte Formation, which has average D for *n*-alkanes of -115‰ to -109‰. Sedimentary OM in marine source rocks typically has δD values close to -150‰ if no significant isotopic exchange has occurred during thermal maturation (Santos Neto and Hayes, 1999).

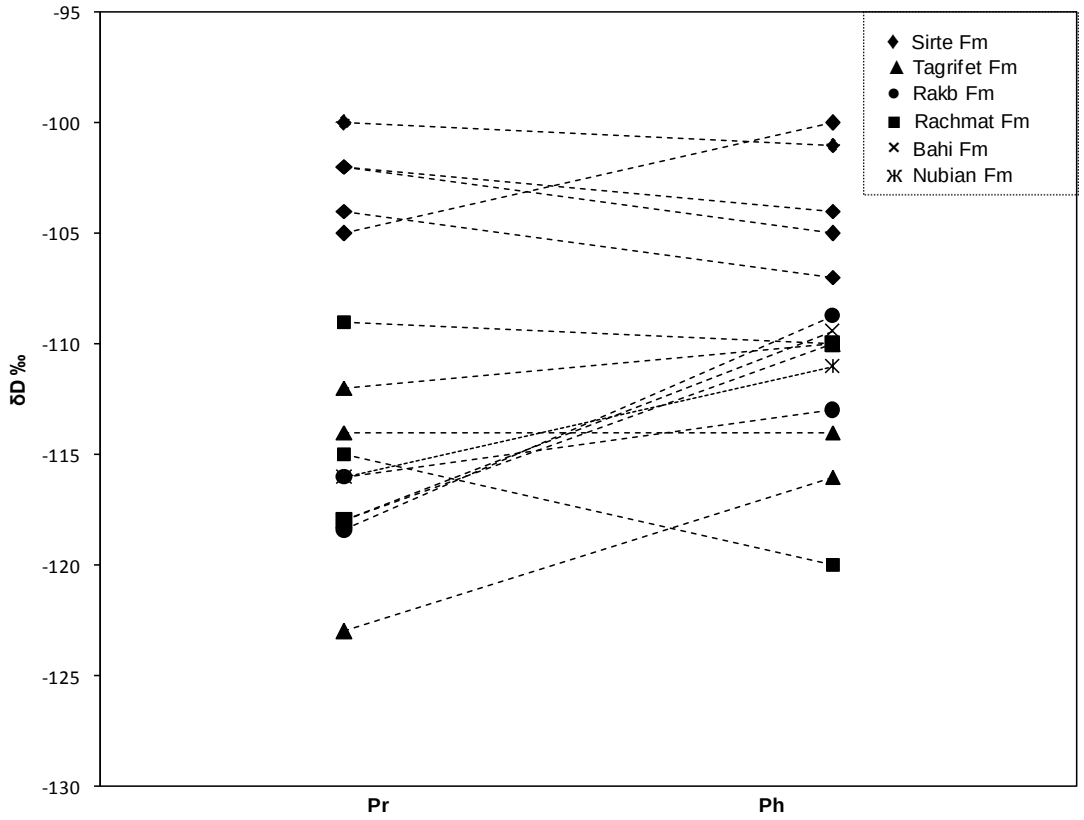

Fig. 3.6 Stable hydrogen isotopic compositions (δD ‰) of isoprenoid alkanes (Pr and Ph) in selected source rock extracts from the East Sirte Basin.

3.3.3.2. $\delta^{13}C$ of *n*-alkanes

The $\delta^{13}C$ values of the *n*-alkanes in the source rocks range from -29.2 to -33.1‰ (Table 3.2) and the *n*-alkane $\delta^{13}C$ profiles are shown in Figure 3.7. Stable carbon signatures of such hydrocarbons can be affected by many factors such as source of OM (Hayes, 1993; Peters and Cassa, 1993) and thermal maturation (Rigby et al., 1981; Clayton, 1991). In the Sirte Formation the average $\delta^{13}C$ values of the *n*-alkanes (C_{17}–C_{27}) are significantly heavier (-30.1 to -29.2‰) than those of the same *n*-alkanes in the other formations (-33.1to -30.7‰). These isotopic differences could be due to differences in maturation level and/or sources. The preferential generation and expulsion of ^{13}C-depleted hydrocarbons during source rock maturation leads to progressive enrichment of the residual kerogen in ^{13}C (Clayton, 1991). In the case of the Sirte Formation, the heavier $\delta^{13}C$ values of its residual *n*-alkanes are most likely due to its higher thermal maturity (Fig. 3.7).

3.3.4. Molecular composition

3.3.4.1. Thermal maturity parameters

Two well-established biomarker parameters (Peters and Moldowan, 1993) were used to assess the thermal maturity of selected samples (Table 3.3). Ts/Ts+Tm values range from 0.41 to 0.62 and 20*S*/20*S*+20*R* values from 0.22 to 0.58, spanning the onset of oil generation (immature to mature). The highest maturities are displayed by the Sirte Formation in the Galio field, in agreement with the findings of El-Alami (1996). The Sirte Formation likewise appears to be considerably more mature than other formations studied herein based on measurements of methylphenanthrene index (MPI-1) and calculated vitrinite reflectance (Rc = 0.60 MPI + 0.4: Radke and Welte, 1983). The elevated maturity of the Sirte Formation (R_c = 0.9–1%) in agreement vitrinite reflectance data (above) and from the adjacent Agedabia Trough (R_o ≈ 1.2–2%: Hallet, 2002). Although stratigraphically older, the Tagrifet, Rachmat, Rakb, Bahi and Nubian Formations within the Hameimat and Sarir Troughs (Fig. 3.1) are at the early stages of oil generation (R_c = 0.65–0.76%).

3.3.3.2. Ph/Ph and DBT/P values

The pristane to phytane (Ph/Ph) and dibenzothiophene to phenanthrene (DBT/P) values of the source rocks (Table 3.4) reveal the nature of their respective depositional settings. Their DBT/P values (0.04–0.47) are characteristic of marine shales whereas, in the majority of samples, the Pr/Ph ratio is <1 indicating deposition under anoxic conditions. The latter are commonly associated with hypersalinity. The slightly higher Pr/Ph values (1.01–1.25) of six shales from the Sirte, Tagrifet, Rakb and Rachmat Formations (Table 3.4) point to suboxic depositional conditions.

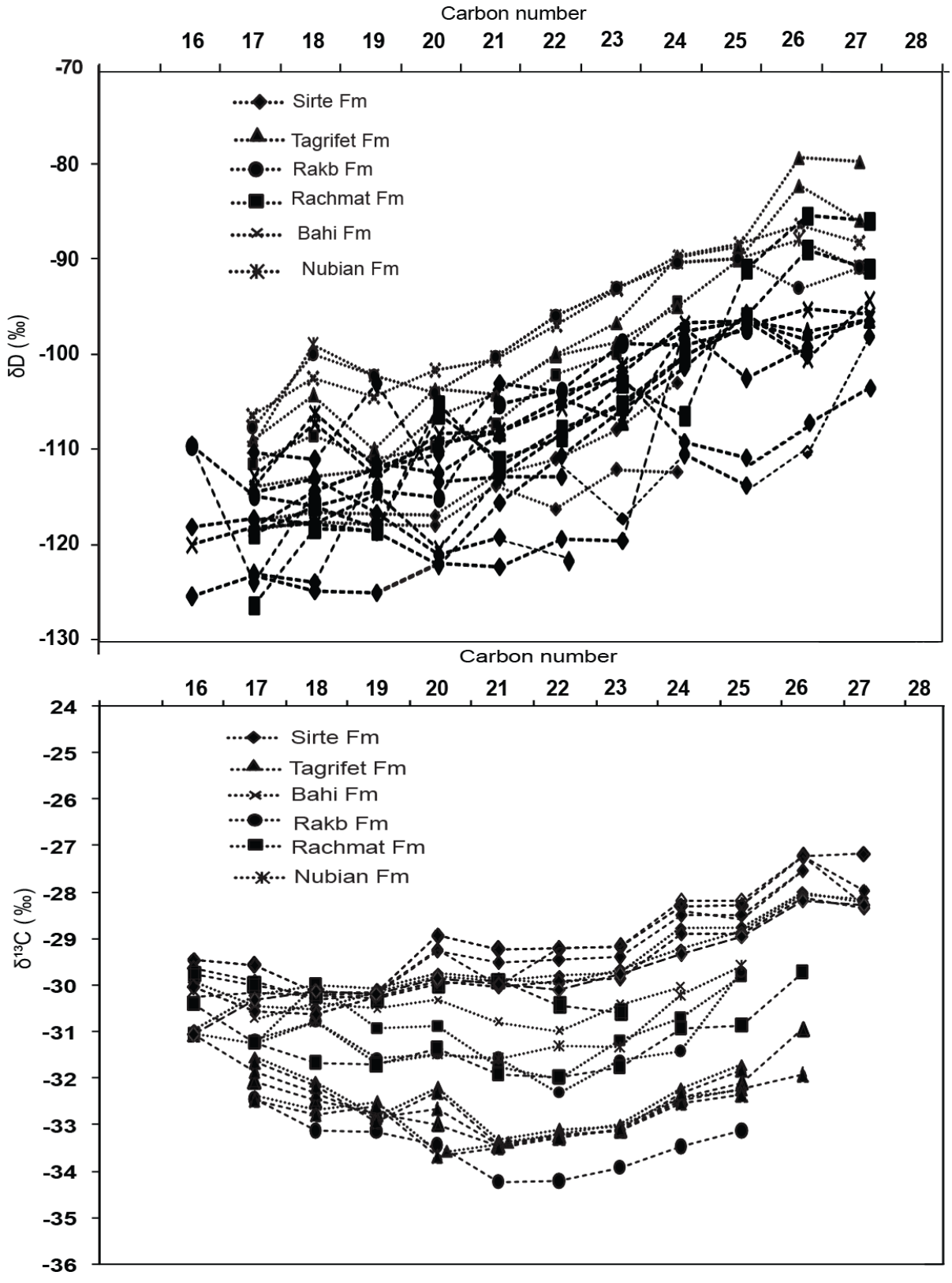

Fig. 3.7 Stable hydrogen isotopic (δD ‰) and stable carbon isotopic ($\delta^{13}C$ ‰) profiles of *n*-alkanes in selected source-rock OM from the East Sirte Basin.

Table 3.3 Geochemical parameters of thermal maturity calculated from the distribution and abundance of aliphatic biomarkers.

Field	Well	Formation	Depth (m)	Ts/Ts +T m	αααC_{29}S/S+R	C_{29} αββ/αββ + ααα
Galio	6C1-59	Sirte	3051-54	0.61	0.49	0.83
Galio	6C1-59	Sirte	3600-03	0.62	0.58	1.00
Galio	6C1-59	Sirte	3087-90	0.61	0.50	n.d.
Galio	6J1-59	Sirte	3528-31	0.62	0.50	1.05
Galio	6J1-59	Sirte	3542	0.62	0.50	n.d.
Galio	5R1-59	Sirte	2967	0.58	0.46	n.d.
Sarir-C	KK1-65	Sirte	2670	0.61	0.40	0.91
Sarir-C	OO2-65	Sirte	2478-81	0.50	0.36	n.d.
Nafoora	M1-51	Tagrifet	2882	0.45	0.24	0.24
Sarir-C	KK1-65	Tagrifet	2745	0.54	0.35	0.35
Sarir-C	KK1-65	Tagrifet	2760	0.53	0.36	0.36
Sarir-C	OO2-65	Tagrifet	2612	0.46	0.22	0.22
Amal	B-96	Rakb	2786	0.41	0.24	0.24
Amal	B-95	Rakb	2725	0.39	0.17	n.d.
Nafoora	M1-51	Rachmat	3015	0.47	0.24	0.55
Nafoora	M1-51	Rachmat	3000	0.50	0.35	n.d.
Sarir-C	OO2-65	Rachmat	2681	0.58	0.36	0.58
Sarir-C	OO2-65	Rachmat	2660	0.53	0.42	n.d.
Nafoora	M1-51	Bahi	3045	0.47	0.35	0.63
Nafoora	M1-51	Nubian	3120	0.47	0.33	n.d.
Nafoora	M1-52	Nubian	3090-93	0.48	0.34	0.35

Ts/Ts+Tm= 18α (H)-22,29,30-trisnorhopane/18α(H)-22,29,30-trisnorhopane+17α(H)-22,29,30-trisnorhopane; *S*/*S*+*R*=C_{29}ααα20*S*/C_{29}ααα20*S* + C_{29}ααα20*R*; C_{29} αββ/αββ+ααα= 5α,14β,17β-24-ethylcholstane 20*R*/ 5α,14α,17α24-ethylcholstane 20*R.*

3.3.4.2. Triterpanes and steranes

The hopane, tricyclic terpane and sterane distributions of the source rocks (Fig. 3.8) are far from uniform reflecting differences in the origin of their OM. For example, the relative abundance of C_{27}, C_{28} and C_{29} regular steranes will vary depending on the contributions of marine and lacustrine phytoplankton, green algae and/or land plants to their kerogen (Huang and Meinshein, 1979; Volkman, 2003). The sterane distributions of most of the samples are dominated by the C_{27} homologue, usually attributed to a marine algal source. The sample from the Tagrifet Formation in the Nafoora field is an exception, whereas the C_{28} sterane is co-dominant with the C_{27} and C_{29} steranes (Fig. 3.8). However, the Tagrifet Formation contains fossil planktonic foraminifera, bryozoans and inoceramid and rudist molluscs, clearly supporting a dominantly

marine environment. A high C_{23}/C_{19}TT ratio and a low relative abundance of C_{24}TeT are features commonly associated with marine shale and carbonate lithofacies (Aquino Neto et al., 1983). Thus, the low C_{19} TT/ (C_{19} TT + C_{23}TT) and C_{24}TeT/(C_{24}TT + C_{23}TT) in all the rock samples studied (Table 3.4) are consistent with their interpreted marine affinity.

Table 3.4 Geochemical parameters of palaeoenvironments from the distribution and abundance of aliphatic and aromatic isoprenoids for studied formations.

Field	Well	Formation	Depth (m)	Pr/Ph	DBT/P	C_{19}TT/C_{23}TT	C_{24}TeT/C_{23}TT
Galio	6C1-59	Sirte	3051-54	0.78	0.46	0.17	0.26
Galio	6C1-59	Sirte	3600-03	0.86	0.47	0.15	0.26
Galio	6C1-59	Sirte	3087-90	1.10	0.22	n.d.	n.d.
Galio	6J1-59	Sirte	3528-31	0.68	0.36	0.08	0.35
Galio	6J1-59	Sirte	3542	0.92	0.29	0.11	0.38
Galio	6R1-59	Sirte	2967	0.92	0.27	n.d.	n.d.
Sarir-C	KK1-65	Sirte	2670	0.86	0.31	n.d.	n.d.
Sarir-C	OO2-65	Sirte	2478-81	0.77	0.13	0.10	0.28
Nafoora	M1-51	Tagrifet	2882	0.86	0.16	0.19	0.26
Sarir-C	KK1-65	Tagrifet	2745	1.13	0.19	0.1	0.31
Sarir-C	KK1-65	Tagrifet	2760	1.25	0.11	0.09	0.31
Sarir-C	OO2-65	Tagrifet	2612	0.85	0.13	0.11	0.35
Amal	B-96	Rakb	2786	1.25	0.25	0.11	0.29
Amal	B-95	Rakb	2725	1.01	0.30	n.d.	n.d.
Nafoora	M1-51	Rachmat	3015	0.70	0.13	0.17	0.29
Nafoora	M1-51	Rachmat	3000	1.12	0.11	n.d	n.d.
Sarir-C	OO2-65	Rachmat	2681	0.80	0.21	0.1	0.29
Sarir-C	OO2-65	Rachmat	2660	0.68	0.30	n.d	n.d.
Nafoora	M1-51	Bahi	3045	0.68	0.04	0.09	0.3
Nafoora	M1-51	Nubian	3120	0.68	0.28	n.d.	n.d.
Nafoora	M1-52	Nubian	3090-93	0.65	0.31	0.1	0.31

Pr= pristane/Ph= phytane; DBT= dibenzothiophene/P= phenanthrene; C_{19}TT/ C_{23}TT= C_{19} tricyclic terpane /C_{19} tricyclic terpane + C_{23} tricyclic terpane; C_{24}TeT/ C_{23}TT= C_{24} tetracyclic terpane /C_{24} tricyclic terpane +C_{23} tricyclic terpane.

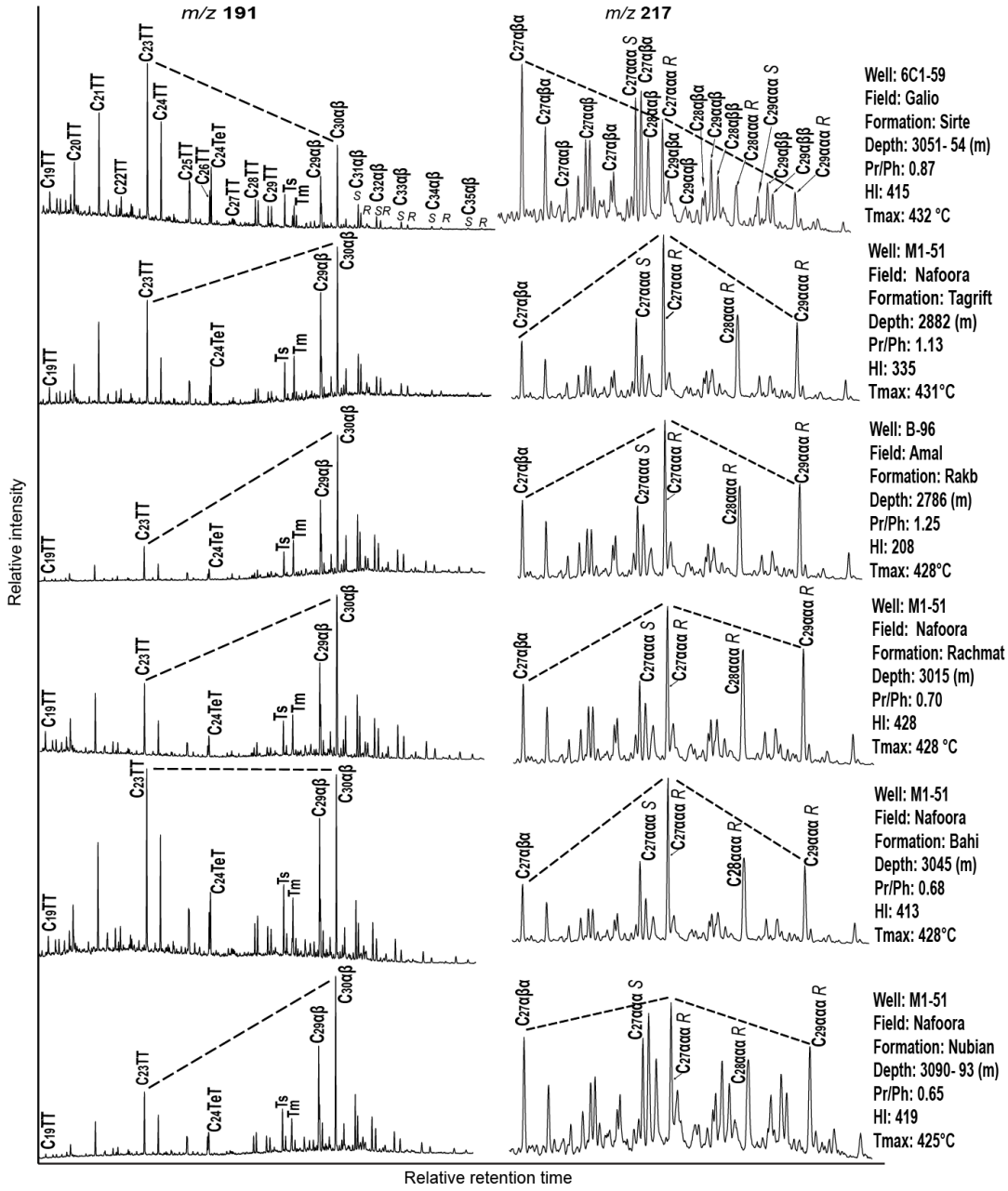

Fig. 3.8 Partial mass chromatograms showing distributions of tricyclic and tetracyclic terpanes and hopanes (*m/z* 191) and steranes (*m/z* 217) in various source rock units of the East Sirte Basin.

3.4. Conclusions

(i) A variety of organic geochemical analyses were applied to set of sediments extracts from the East Sirte Basin (Libya). The thermal maturity and palaeoenvironment of deposition was established, using Rock-Eval pyrolysis of source rocks, biomarker ratios and compound specific stable hydrogen and carbon isotopes of individual hydrocarbons from crude oils and source rock

extracts.

(ii) The thermal maturity of the source rocks from the Sirte Formation were found to be higher based on Ts/Ts+Tm (0.61 to 0.62) and αααC_{29} 20*S*/20*S*+20*R* (0.49 to 0.58) than the Tagrifet, Rakb, Rachmat, Bahi, and Nubian Formations. δD differences between *n*-alkanes and isoprenoids (Pr and Ph) are also consistent with higher levels of thermal maturity for the Sirte Formation.

(iii) Molecular composition of Ph/Ph, DBT/P, triterpanes and steranes indicate anoxic to sub oxic depositional environment and vary contributions OM of marine and lacustrine phytoplankton, green algae and/or land plants kerogen of rocks.

Acknowledgements

The authors thank Geoff Chidlow and Sue Wang for their assistance with GC-MS and GC-ir-MS analysis, respectively. We are grateful to the staff of the National Oil Corporation (NOC) in Tripoli and staff of the Libyan Petroleum companies (Waha, Veba and Gulf) for providing samples. We are also thanking Prof. David Mckirdy (*Adelaide University*) and Dr. Khaled R. Arouri (*The King Fahd University of Petroleum & Minerals in Dhahran)* about reviewing this work. Aboglila thanks Curtin University for a fee waiver and PhD scholarship

3.5. References

Abadi, A., 2002. Tectonics of the Sirte Basin. PhD Dissertation, Vrije Universiteit, Amsterdam, ITC, Enschede, p. 187.

Ahlbrandt, T.S., 2001. The Sirte Basin is Province of Libya-Sirte-Zelten Total Petroleum System. US Geological Survey Bulletin 2202-F. <http://geology.cr.usgs.gov/pub/bulletins/b2202-f/> (accessed 20.4.2009).

Aboglila, S., Grice, K., Trinajstic, K., Dawson, D., Williford, K., 2010a. Use of biomarker distributions and compound specific isotopes of carbon and hydrogen to delineate hydrocarbon characteristics in the East Sirte Basin (Libya). Organic Geochemistry. Presented at the 15th Australian Organic

Geochemistry Conference, Adelaide, September 2008. *In press*

Aquino Neto, F.R., Trendel, J.M., Restle, A., Connan, J., Albrecht, P., 1983. Occurrence and formation of tricyclic and tetracyclic terpanes in sediments and petroleum. In: Bjorøy, M. (Ed.), Advances in Organic Geochemistry 1981. John Wiley & Sons Ltd, Chichester, 659-667.

Baird, D.W., Aburawi, R.M., Bailey, N.J.L., 1996. Geohistory and petroleum in the central Sirte Basin. In: Salem, M.J., El-Hawat, A.S., Sbeta, A.M. (Eds.), Geology of Sirte Basin II, Elsevier, Amsterdam, 3–56.

Baric, G., Spanic, D., Maricic, M., 1996. Geochemical characterization of source rocks in the NC-157 block (Zaltan platform), Sirte Basin. In: Salem, M.J., El-Hawat, A.S., Sbeta, A.M. (Eds.). The Geology of Sirte Basin, II, Elsevier Amsterdam, 541–553.

Barr, F.T., Weegar, A.A., 1972. Stratigraphic Nomenclature of the Sirte Basin, Libya. Petroleum Exploration Society of Libya, Tripoli. P. 179.

Bastow, T.P., van Aarssen, B.G.K., Lang, D., 2007. Rapid small–scale separation of saturate, aromatic and polar components in petroleum. Organic Geochemistry, 38, 1235–1250.

Burwood, R., Redfern, J., Cope, M., 2003. Geochemical evaluation of East Sirte Basin (Libya) petroleum systems and oil provenance. Geological Society Special Publication, London, 203–213.

Clayton, C., 1991. Effect of maturity on carbon isotope ratios of oils and condensates. Organic Geochemistry, 17, 887–899.

Coward, M.P., Ries, A.C., 2003. Tectonic development of North African basins. In: Burnham, T., MacGregor, D.S., Cameron, N.R. (Eds.), Petroleum Geology of Africa: New Themes and Developing Technologies, 207. Geological

Society Special Publication, London, 61-83.

Dawson, D., Grice, K., Alexander, R., 2005. Effect of maturation on the indigenous δD signatures of individual hydrocarbons in sediments and crude oils from the Perth Basin (Western Australia). Organic Geochemistry, 36, 95–103.

Dawson, D., Grice, K., Alexander, R., Edwards, D., 2007. The effect of source and maturity on the stable isotopic compositions of individual hydrocarbons in sediments and crude oils from the Vulcan Sub-basin, Timor Sea, Northern Australia. Organic Geochemistry, 38, 1015–1038.

El-Alami, M., 1996. Habitat of oil in Abu Attiffel area, Sirte Basin, Libya. In: Salem, M.J., El-Hawat, A.S., Sbeta, A.M. (Eds.), The Geology of Sirte Basin II, Elsevier, Amsterdam, 337–348.

El-Alami, M., Rahouma, S., Butt, A., 1989. Hydrocarbon habitat in the Sirte Basin northern Libya. Petroleum Research Journal, 1, 17–28.

El-Hawat, A.S., Missallati, A.A., Bezan, A.M., Taleb, T.M., 1996. The Nubian Sandstone in Sirte Basin and its correlatives. In: Salem, M.J., El-Hawat, A.S., Sbeta, A.M. (Eds.). The Geology of Sirte Basin, II, Elsevier, Amsterdam, 3–30.

Ghori, K.A.R., Mohammed, R.A., 1996. The application of petroleum generation modelling to the eastern Sirte Basin, Libya. In: Salem, M.J., El-Hawat, A.S., Sbeta, A.M. (Eds.). The Geology of Sirte Basin, II, Elsevier, Amsterdam, 529–540.

Gras, R., 1996. Structural style of the southern margin of the Messlah High. In: Salem, M.J., El-Hawat, A.S., Sbeta, A.M. (Eds.). The Geology of Sirte Basin II, Elsevier, Amsterdam, 201–210.

Grice, K., de Mesmay, R., Glucina, A., Wang, S., 2008. An improved and rapid 5A molecular sieve method for gas chromatography isotope ratio mass spectrometry of *n*-alkanes (C_8-C_{30}). Organic Geochemistry, 39, 284-288.

Gruenwald, R., 2001. The hydrocarbon prospectivity of Lower Oligocene deposits in the Maragh Trough, SE Sirte Basin, Libya. Journal of Petroleum Geology, 24, 213-231.

Guiraud, R., Maurin, J.C., 1991. Early Cretaceous rifts of Western and Central Africa: an overview. Tectonophysics, 213, 153–168.

Hallett, D., 2002. Petroleum Geology of Libya. Elsevier, Amsterdam, p. 509.

Hallett, D., El-Ghoul, A., 1996. Oil and gas potential of the deep trough areas in the Sirte Basin, Libya. In: Salem, M.J., El-Hawat, A.S., Sbeta, A.M. (Eds.), The Geology of Sirte Basin II, Elsevier, Amsterdam, p. 455–483.

Hayes, J.M., 1993. Factors controlling the ^{13}C contents of sedimentary organic compounds: principles and evidence. Marine Geology, 113, 111–125

Huang, W. Y., Meinschein, G., 1979. Sterols and ecological indicators. Geochimica et Cosmochimica Acta, 43, 739-745.

Hunt, J.M., 1996. Petroleum Geochemistry and Geology. New York, 394-743.

Kroner, A., 1993. The Pan-African belt of northeastern and eastern Africa, Madagascar, southern India, Sri Lanka and east Antarctica; Terrane amalgamation during formation of the Gondwana Supercontinent. Geoscientific research in Northeast Africa. A.A. Balkema, Rotterdam, Netherlands, 3–9.

Pedentchouk, N., Freeman, K.H., Harris, N.B., 2006. Different response of D values of n-alkanes, isoprenoids, and kerogen during thermal

maturation. Geochimica et Cosmochimica Acta, 70, 2063–2072.

Peters, K.E., Cassa, M.R., 1993. Applied source rock geochemistry. In: Magoon, L.B., Dow, WG. (Eds.). The Petroleum System-from Source to Trap. American Association of Petroleum Geologists Memoir, 60, p.93–120.

Radke, M., Welte, D.H., 1983. The Methylphenanthrene Index (MPI): A maturity parameter based on aromatic hydrocarbons. In: Bjorøy, M. (Ed.), Advances in Organic Geochemistry 1981. John Wiley and Sons Ltd, Chichester, 504-512.

Rigby, D., Batts, B.D., Smith, J.W., 1981. The effect of maturation on the isotopic composition of fossil fuels. Organic Geochemistry, 3, 29–36.

Rusk, D.C., 2001. Libya: Petroleum potential of the underexplored basin centers: A twenty-first-century challenge. American Association of Petroleum Geologists Memoir, 74, 429–452.

Santos Neto, E.V., Hayes, J.M., 1999. Use of hydrogen and carbon stable isotopes characterizing oils from the Potiguar Basin (onshore), Northeastern Brazil. American Association of Petroleum Geologists Bulletin, 83, 496–518.

Shaaban, F., Lutz, R., Littke, R., Bueker, C., Odisho, K., 2006. Source rock evaluation and basin modelling in NE Egypt, (NE Nile Delta and Northern Sinai). Journal of Petroleum Geology, 29, 103–123.

Tissot B. P., Welte, D.H., 1984. Petroleum Formation and Occurrence. 2nd Edition. Springer Verlag. New York, p. 699.

Volkman, J. K., 2003. Sterols in microorganisms. Applied Microbiology and Biotechnology, 60, 495–506.

Chapter 4

The significance of 24-*nor*cholestanes, 4-methylsteranes and dinosteranes in oils and source-rocks from East Sirte Basin (Libya)

S. Aboglila, K. Grice, K. Trinajstic, C. Snape and K.H. Williford

Applied Geochemistry
In Press

Abstract

The present paper involves a detailed evaluation of various steroid biomarkers by gas chromatography- mass spectrometry (GC-MS) and GC-metastable reaction monitoring (MRM) analyses of several crude oils and source rocks from the East Sirte Basin. 24-*nor*cholestanes, dinosteranes, 4α-methyl-24-ethylcholestanes and triaromatic steroids have been identified in both source-rocks and crude oils of the East Sirte Basin. Diatoms, dinoflagellates (including those potentially associated with corals) and/or their direct ancestors are the proposed sources of these biomarkers. These biomarker parameters have been used to establish a Mesozoic oil-source correlation of the East Sirte Basin. Hydropyrolysis of an extant coral extract revealed a similar distribution (although immature) of dinosteranes and 4α-methyl-24-ethylcholestanes also observed in the Sirte oils and source-rocks. This is consistent with the presence of dinoflagellate cysts in the Numbian Formation of Lower Cretaceous age.

Keywords: Sirte Basin, dinosteranes, dinoflagellates, diatoms, corals, Mesozoic, Libya

4.1. Introduction

Eukaryotic steroids are the most commonly occurring polycyclic biomarkers in the geologic record. The most important components of Eukaryotic cell membranes include, sterols (e.g. cholesterol, ergosterol and sitosterol). Eukaryotes biosynthesise a wide range of sterols that are characterised by the number and position of functional moeities (from double bonds, hydroxy-, oxo- and alkylgroups to other complex, substituents) diagnostic to a wide range of algal assemblages (Volkman, 2003). There are however, a very limited range of diagenetically-altered steroids reported in sediments and petroleum (Table 4.1). A summary of the components diagnostic to various eukaryotic assemblages are shown in Table 4.1.

The most commonly reported steranes in organic matter and petroleum from the Late Neoproterozoic to the Cenozoic age are cholestane, ergostane, 24-methylcholestane and stigmastane. Natural product precursors of cholestane, ergostane and stigmastane are the most commonly occurring biomarkers found in almost every Eukaryotic assemblage (see Table 4.1 and Volkman, 1986; Volkman, 2003) and are thus non-specific. Some steroids have also been reported in three independent groups of bacteria and these include, *Myxococcales, Methylococcales*, and *Planctomycetales* (Pearson et al., 2003). Other steroids such as 24-*n*-propylcholestanes area diagnostic markers for marine algae of the order *Sarcinochrysidales* and brown tide algae (Moldowan et al., 1990). Dinosterane (4, 23, 24-trimethylcholestane) is also uniquely derived from dinosterol, and related compounds (Robinson et al., 1984) reported in many dinoflagellates. Dinosterane is thus a marker for dinoflagellates (Summons and Powell, 1987), although a diatom has been reported to contain similar sterols. In addition, dinoflagellates are probably the main origin of aromatic steroids bearing a methyl group at C-4 (4-methylcholestane, 4-methylergostane, and 4- methylstigmastane). The source of the 24-*nor*cholestane is unknown, but diatoms have been suggested as the main source by Holba et al. (1998a). 24-*nor*cholestanes have been found in crude oils associated with the proliferation of diatoms from the Jurassic to the Tertiary (Holba et al., 1998b). Other novel biomarkers for diatoms include the "highly

branched isoprenoid" (HBI) alkanes (e.g., Volkman et al., 1994). The natural product precursors of HBI alkanes are found in two diatom species (Table 4.1).

Sedimentary organic matter (SOM) of the East Sirte Basin (Libya) consists of several potential source(s) (Burwood et al., 2003). Geochemical data on SOM from the East Sirte Basin has shown two main petroleum groups and several potential source-rocks (see Aboglila et al. 2010a & b). The present paper involves a detailed evaluation of various steroid biomarkers by gas chromatography- mass spectrometry (GC-MS) and GC-metastable reaction monitoring (MRM) analyses of several crude oils and source rocks from the East Sirte Basin (Burwood et al., 2003; Aboglila et al., 2010a & b). 24-*nor*cholestanes, dinosteranes, and 4α-methyl-24-ethylcholestanes have been identified in both source-rocks and crude oils of the East Sirte Basin. Diatoms, dinoflagellates (including those potentially associated with corals) and/or their direct ancestors are the proposed sources of these biomarkers. These biomarker parameters have been used to establish an oil-source correlation and an age prediction of the source-rock of the oils in the East Sirte Basin.

4.2. Geological setting

The Sirte Basin is located in the northeast of Libya, extending from the 2000th meters bathymetric contour offshore in the Gulf of Sidra and bordered by the Haruj Uplift in the west, the Cyrenaica Platform and Al jaghbub Low in the east, and the Tazirbu and Sirte Arches in the south (Ahlbrandt, 2001) (Fig. 4.1). The geology of the Sirte Basin has been described previously (Parsons et al., 1980; El-Alami et al., 1989; Gras, 1996; Macgregor, 1996; Ghori and Mohammed, 1996), and research is ongoing (Burwood et al., 2003). The main evolution of the basin resulting in the current configuration occurred during the Cretaceous with the collapse of the Sirte arch (Rusk 2001; Hallett, 2002). Extensional faulting and subsidence of the basin continued into the Tertiary and maximum subsidence occurred in the Late to Middle Eocene. The Sirte Basin is divided into the West Sirte Basin and the East Sirte Basin by the Zelton Platform (Hallett, 2002).

Table 4.1 Biomarkers associated with Eukaryotes and their environments of deposition (after, Brocks and Grice, 2010 *in press*).

Organisms	Biomarkers	Depositional Environment and age	Other possible sources	References
Eukarya				
Eukaryotes (general)	Ergostane, stigmastane and their aromatic analogues	Most environments, Neoproterozoic to present		(Volkman et al., 1998; Volkman, 2003; Summons et al., 2006)
	Cholestane and aromatic analogues		Possible minor contribution from Myxococcales (myxobacteria)	(Kohl et al., 1983; Bode et al., 2003)
Pelagophyte algae ('brown tides' and Sarcinochrysidales)	24-*n*-propylcholestane	Common in marine environments		(Moldowan et al., 1990)
Dinoflagellates	4-Methylergostane, 4-methylstigmastane	Minor component in other eukaryotes		(Volkman, 2003)
	Dinosterane	Mostly Mesozoic and Cenozoic (minor concentrations in Paleozoic, possibly of 'protodinoflagellate' origin)	Rare in diatoms	(Robinson et al., 1984; Volkman et al., 1993; Moldowan and Talyzina, 1998; Grice et al., 1998a)
Diatoms	24-Norcholestane (C_{26})	Cretaceous to Cenozoic		(Holba et al., 1998b; Holba et al., 1998a)
Centric diatoms (genus *Rhizosolenia*)	C_{25} and C_{30} Highly Branched Isoprenoid (HBI) alkanes	Marine environments, Upper Turonian to present	C_{25} HBI in pennate diatoms (including epipytes)	(Nichols et al., 1988; Volkman et al., 1994; Sinninghe Damsté et al., 2004; Atahan et al., 2007)
Pennate diatoms (phylogenetic cluster including *Haslea*, *Pleurosigma*, *Navicula)*	C_{25} HBI alkanes	Marine environments	Centric diatoms (genus *Rhizosolenia*)	(Nichols et al., 1988; Sinninghe Damsté et al., 2004)
Prymnesiophyte algae	C_{37} - C_{39} di- to tetra-unsaturated alkenones		The degree of unsaturation changes with water temperature, and this is used in the photic zone temperature proxy Uk37	(Brassell et al., 1986; Grice et al., 1998b and references therein)
Botryococcus braunii (Chlorophyte alga)	Botryococcanes, cyclobotryococcanes, polymethylsqualanes	Fresh to brackish water, Tertiary		(Metzger et al., 1985; Huang et al., 1988; Metzger and Largeau, 1999; Summons et al., 2002; Grice et al., 1998c)
	Macrocyclic C_{15}-C_{34} alkanes without carbon number preference	Fresh to brackish water, Tertiary		(Grice et al., 2001; Audino et al., 2002)
Gloeocapsomorpha prisca (uncertain affinity, possibly an alga)	High concentrations of *n*-C_{15}, *n*-C_{17} and *n*-C_{19}	Cambrian to Devonian		(Fowler, 1992; Blokker et al., 2001)

The main faults, which divide the Sirte basin into a series of platforms and troughs, trend in a north-west to south-east direction except in the East Sirte Basin where fault trends occur in an east-west direction and it is this faulting which has contributed to the structural traps which have resulted in the East Sirte Basin being most productive for the petroleum industry of Libya (Rusk 2001; Ahlbrandt, 2001; Hallett, 2002). The post-rift sediments in the Sirte Basin comprise sequences of lacustrine and alluvial deposition as well as marine clastics and carbonates which range in thicknesses between 1000 m- 1500 m, the deeper area being in the east. The tendency for gas rather than oil to be produced in the northern part of the basin is thought to be depth related. Correlation of stratigraphic units between the sediments of the platform and troughs has proved to be difficult due to the rapid lateral changes in facies type and sediment thickness (Burwood et al. 2003).

The main petroleum system is the Sirte-Zelten located in the East Sirte Basin. The Cretaceous Sirte Shale comprises organic-rich dark shales and mudstones and is regarded as the major oil source rock for the East Sirte Basin (e.g. Barr and Weegar, 1972; Hallett, 2002; Burwood et al., 2003). Both oil and rock samples were taken from the East Sirte Basin for this study (Table 4.2). A rich fauna of benthic and planktonic foraminifera has been recovered from these sediments as well as from the slightly older Rachmat Formation (Hallett, 2002). The dinoflagellates *Lagenorhytis sp*. and *Odontoihina sp*. have been recorded from the Cretaceous Nubian Sandstone considered a minor source rock; however, this area is currently recognised as under-studied (Rusk, 2001; Hallett, 2002). Other potential source horizons have been recognised in Cretaceous, Triassic, Cambrian and Precambrian formations and been considered to have supplied a number of stratigraphically distinct reservoirs (Hallet, 2002, Burwood et al. 2003). Recent geochemical analyses of oils by Burwood et al, (2003) and Aboglila et al, (2010a) have indicated the presence of more source rocks than are currently identified.

4.3. Experimental

4.3.1. Samples

Oil and rock samples were collected by the National Oil Corporation (NOC) in Tripoli from eleven different wells (Fig. 4.1) from the East Sirte Basin. In total, twenty four petroleum samples were obtained from 7 oilfields (Fig. 4.1) and their depth and locations are summarised in Table 4.2.

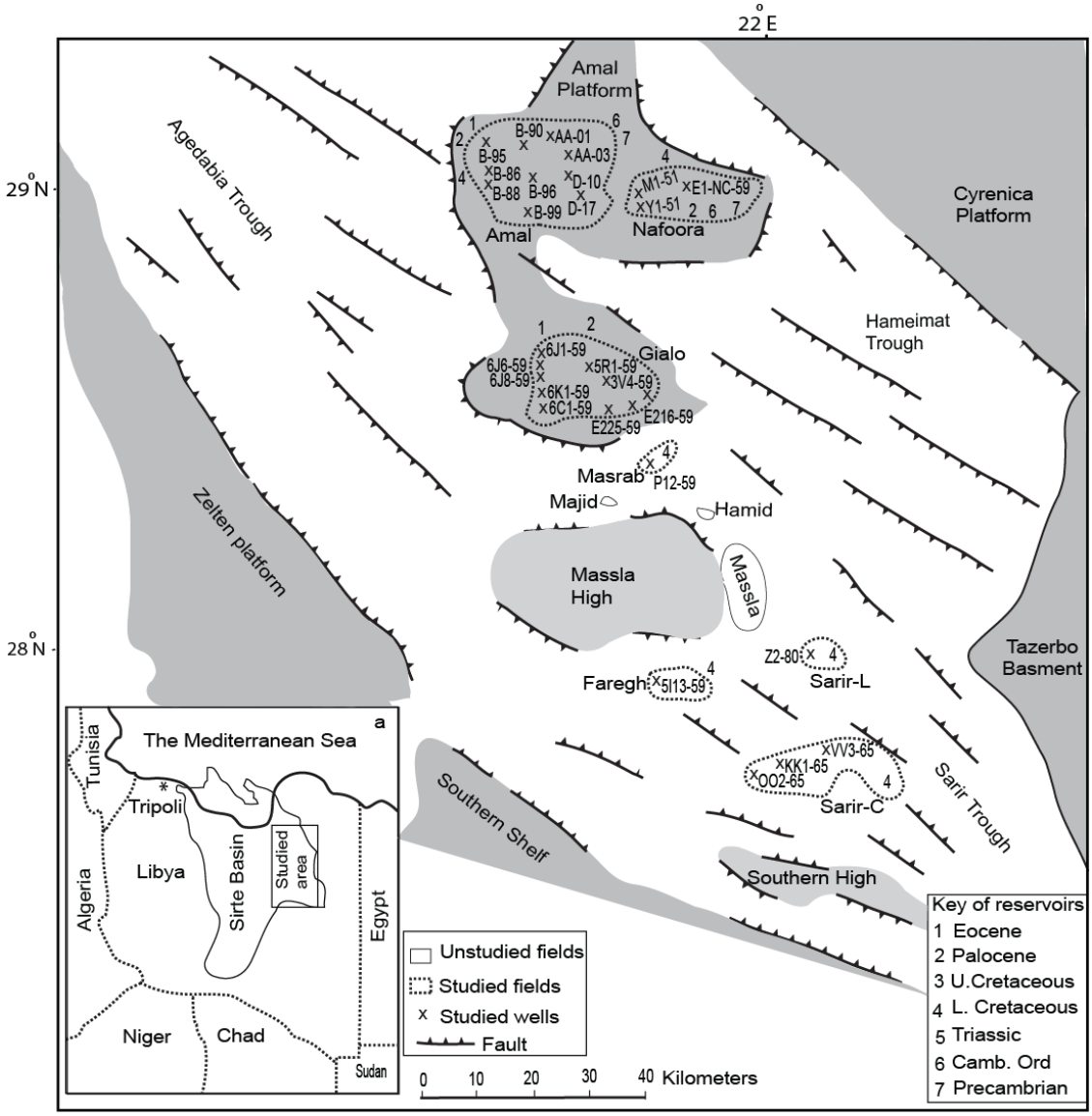

Fig. 4.1 Location of the Sirte Basin, the studied fields and selected oil wells in studied area (modified from Ahlbrandt, 2001; Burwood et al., 2003; Aboglila et al., 2010a).

Twenty one drill cuttings (Cretaceous in age) were provided from the following formations, 8 Sirte, 4 Tagrifet, 2 Rakb, 4 Rachmat, 1 Bahi and 2 from the Nubian Fm. Their depths and locations are shown in Table 4.2.

A coral sample was obtained from the Great Barrier Reef, Australia. The species collected was Porites that contained the alga zooxanthellae. The coral sample was finely ground and then extracted ultrasonically (2 hours), using a mixture of dichloromethane (DCM) and methanol (MeOH) (9:1 v/v). The solvent extract was filtered and excess solvent was removed by heating on a sand bath at 80° C, affording the extract. The extract obtained was subjected to Hydro-Pyrolysis (HY-PY), see below.

4.3.2. Rock extractions

The rocks were washed with double-distilled water to remove any surface contaminants. Rock samples were finely ground by a mechanical rock grinding machine (particle size of <150 μm), using a ring-mill (Rocklabs). All samples (10-20 g) were then extracted ultrasonically (2 hours), using a mixture of dichloromethane (DCM) and methanol (MeOH) (9:1 v/v). The solvent extract was filtered and excess solvent was removed by heating on a sand bath at 80°C, affording the extract.

Table 4.2 A list of the petroleum and rock samples analysed in this study.

Petroleum samples				**Rock samples**			
Well	**Field**	**Formation**	**Depth (m)**	**Field**	**Well**	**Formation**	**Depth (m)**
Y1-51	Nafoora	Nubian	3036	Gialo	6C1-59	Sirte	3051-54
AA-01	Amal	Sahabi	3824	Gialo	6C1-59	Sirte	3600-03
AA-03	Amal	Sahabi	3848	Gialo	6C1-59	Sirte	3087-90
B-90	Amal	Amal	3090	Gialo	6J1-59	Sirte	3528-31
B-95	Amal	Amal	3092	Gialo	6J1-59	Sirte	3542
B-99	Amal	Maragh	3053	Gialo	6R1-59	Sirte	2967
D-10	Amal	-	824	Sarir-C	KK1-65	Sirte	2670
D-17	Amal	-	808	Sarir-C	OO2-65	Sirte	2478-81
B-86	Amal	Amal	2996	Nafoora	M1-51	Tagrifet	2882
B-88	Amal	Amal	3000	Sarir-C	KK1-65	Tagrifet	2745
B-96	Amal	Amal	3261	Sarir-C	KK1-65	Tagrifet	2760
6J6-59	Gialo	Nubian	3430	Sarir-C	OO2-65	Tagrifet	2612
6J8-59	Gialo	Nubian	3290	Amal	B-96	Rakb	2786
3V3-59	Gialo	Lidam	3102	Amal	B-95	Rakb	2725
6K1-59	Gialo	Lidam	3364	Nafoora	M1-51	Rachmat	3015
5R1-59	Gialo	Lidam	3458	Nafoora	M1-51	Rachmat	3000
3V4-59	Gialo	Nubian	3121	Sarir-C	OO2-65	Rachmat	2681
6C1-59	Gialo	Galio	979	Sarir-C	OO2-65	Rachmat	2660
E225-59	Gialo	Jakhira	3290	Nafoora	M1-51	Bahi	3045
E216-59	Gialo	Augila	3182	Nafoora	M1-51	Nubian	3120
P-12	Masrab	Galio	3329	Nafoora	M1-52	Nubian	3090-93
Z2-80	Sarir-L	Nubian	3167				
5I13-59	Faregh	Nubian	3006				
VV3-65	Sarir-C	Nubian	2667				

4.3.3. Liquid chromatography

Crude petroleum and extracts were fractioned into saturate, aromatic, and polar fractions by using a small column (5.5 cm x 0.5 cm i.d.) of activated silica gel (120˚C, 8 h) (Bastow et al., 2007 method). Approximately 10 to 20 mg of sample was applied to the small column. The saturated hydrocarbon was obtained by eluting with *n*-pentane (2 mL); the aromatic hydrocarbon was obtained by eluting with a mixture of *n*-pentane and DCM (2 mL, 7:3 v/v,); and the polar (NSO) fraction was obtained by eluting with a mixture of DCM and MeOH (2 mL, 1: 1 v/v). The excess solvent was removed by heating the fractions on a sand bath at 80 ˚C.

4.3.4. Hydro-Pyrolysis (HYPY) of coral extract

The instrumental procedure for fixed bed HYPY has been described by Love et al., 1995 and Meredith et al., 2006. Prior to HYPY, the coral extract was mixed with a dispersed sulfidic molybdenum catalyst [$(NH_4)_2MoO_2S_2$ (10 mg), dissolved in a minimum of 20% methanol in water], and dried carefully and then placed into the pyrolysis reactor. The sample was then heated in a stainless steel tube (ambient temperature to 250˚C at 300˚C min^{-1}, then to 500˚C at 8˚C $min^{-1)}$. A constant hydrogen flow of 5 L min^{-1}, measured at ambient temperature and pressure, guaranteed rapid removal-of the volatile products from the reaction vessel. The product was collected on a silica gel-filled trap chilled with dry ice (see Meredith et al., 2004). The hydropyrolysate (adsorbed on silica gel) was fractioned into saturate, aromatic, and polar fractions by using a small column (5.5 cm x 0.5 cm i.d.) of activated silica gel as described above. GC-MS and GC-MRM analysis of the saturated hydrocarbon fraction was analysed as described below.

4.3.5. Biomarker analysis

Gas chromatography–mass spectrometry (GC-MS) using a Hewlett Packard (HP) 5973 mass-selective detector (MSD) interfaced to a HP6890 gas chromatograph (GC). A HP-5MS (J & W Scientific) GC column (5% phenylmethylsiloxane stationary phase) was used with helium as the carrier gas. Due to the low concentrations of the methylsterane isomers, GC-metastable

reaction monitoring (MRM) mode was used. The GC-MRM was performed on a Hewlett-Packard 5890 GC interfaced with a VG Autospec Ultima mass spectrometer operated at 70 eV with a mass range of *m/z* 50-600 and a cycle time of 1.8 h. The MRM mode for full scan (TIC) and the following *m/z* transitions of 358→217, 372→217, 386→217, 400→217 and 414→217 were monitored to obtain the C_{27}, C_{28}, C_{29} and C_{30} regular steranes in the saturated fractions respectively. The following *m/z* transitions of 386→231, 400→231, 414→231 and 414→98 were monitored to obtain the desmethylsteranes (C_{28}), desmethylsteranes (C_{29}), methylsteranes (C_{30}) and dinosteranes, respectively. The compounds were identified based on their mass spectra and previously reported data (Holba et al., 1998b; Grice et al., 1998b; Peters et al., 2005; Grosjean et al., 2009). The 245 ion was monitored in single ion monitoring (SIM) mode for the triaromatic steroids present in the aromatic fractions. The triaromatic steroids were identified by their relative retention times reported by (Wenzhi et al., 2005).

4.4. Results and Discussion

The oil samples analysed in this study have previously been characterised by a variety of organic geochemical analyses including stable carbon ($\delta^{13}C$), hydrogen (™D) isotopes of hydrocarbons (Aboglila et al., 2010a). From the latter study two main oil families (A and B) were identified with respect to variations in their source inputs and relative thermal maturity levels. The family A oils included the Sarir-L, Nafoora, Faregh and Sarir-C fields and were found to be relatively more mature and have a relatively higher terrigenous input than the family B oils. The family B oils included the Amal, Gialo and Masrab fields and showed a higher contribution of marine derived organic matter. In the East Sirte Basin, oils from the Nubian Formation (VV3-65 and 5I13-65 wells) are distinguished by a high relative abundance of hopanes to steranes. The oils from the Sahabi Formation (AA-01 and AA-03 wells) contained an abundant series of extended of tricyclic terpanes, whereas the other oils (see Table 4.2) contained a mixture of the various biomarkers identified in the two main groups [see Aboglila et al. (2010a) for more details].

Biomarker and $\delta^{13}C$ data was also obtained from a series of source rock extracts from the Sirte, Tagrifet, Rakb, Rachmat, Bahi and Nubian Formations [see Aboglila et al. 2010b for further details]. The source rocks were found to contain Type II/III kerogen. The source-rocks from the Sirte Formation showed a relatively higher thermal maturity than the Tagrifet, Rakb, Rachmat, Bahi, and Nubian Formations. Biomarker distributions supported an anoxic to a sub oxic depositional environment and varying contributions of OM from marine/lacustrine phytoplankton, green algae and/or land plants.

4.4.1. Crude oils

4.4.1.1. Sterane distributions

Representative parent-daughter (*m/z*) → ions of *m/z* 358→217 (C_{26}), 372→217 (C_{27}), 386→217 (C_{28}), 400→217 (C_{29}) and 414→217 (C_{30}) for oils from the East Sirte Basin are shown in Figure 4.2. All oils contain a complex distribution of C_{26}–C_{30} steranes with the exception of oils from the 5I13-59 and VV-65 wells, demonstrating a terrestrial depositional environment and oils from AA-01 and AA-03 wells, containing a high abundance of tricyclic components, which is consistent with study of Aboglila et al (2010a).

*Nor*cholestanes (C_{26} steranes) are commonly present in crude oils and rock extracts in low concentrations, compared with the more common C_{27}, C_{28} and C_{29} steranes, hence the need for GC-MRM analyses for identification. The *nor*cholestanes (C_{26} steranes) transitions were identified by their key fragment ions, their relative retention times by comparison of their mass spectra with published data (Holba et al., 1998b; Peters et al., 2005; Grosjean et al., 2009). The following sub-sections describe the specific sterane distributions identified in the crude oils and source-rocks from East Sirte Basin in further detail.

4.4.1.2. 24-Norcholestanes ratios (C_{26})

Biomarker of C_{26} steranes (24-*nor*cholestanes, 27-*nor*cholestane, and 21-*nor*cholestane isomers) have been previously recognised in geological samples (Moldowan et al., 1991).

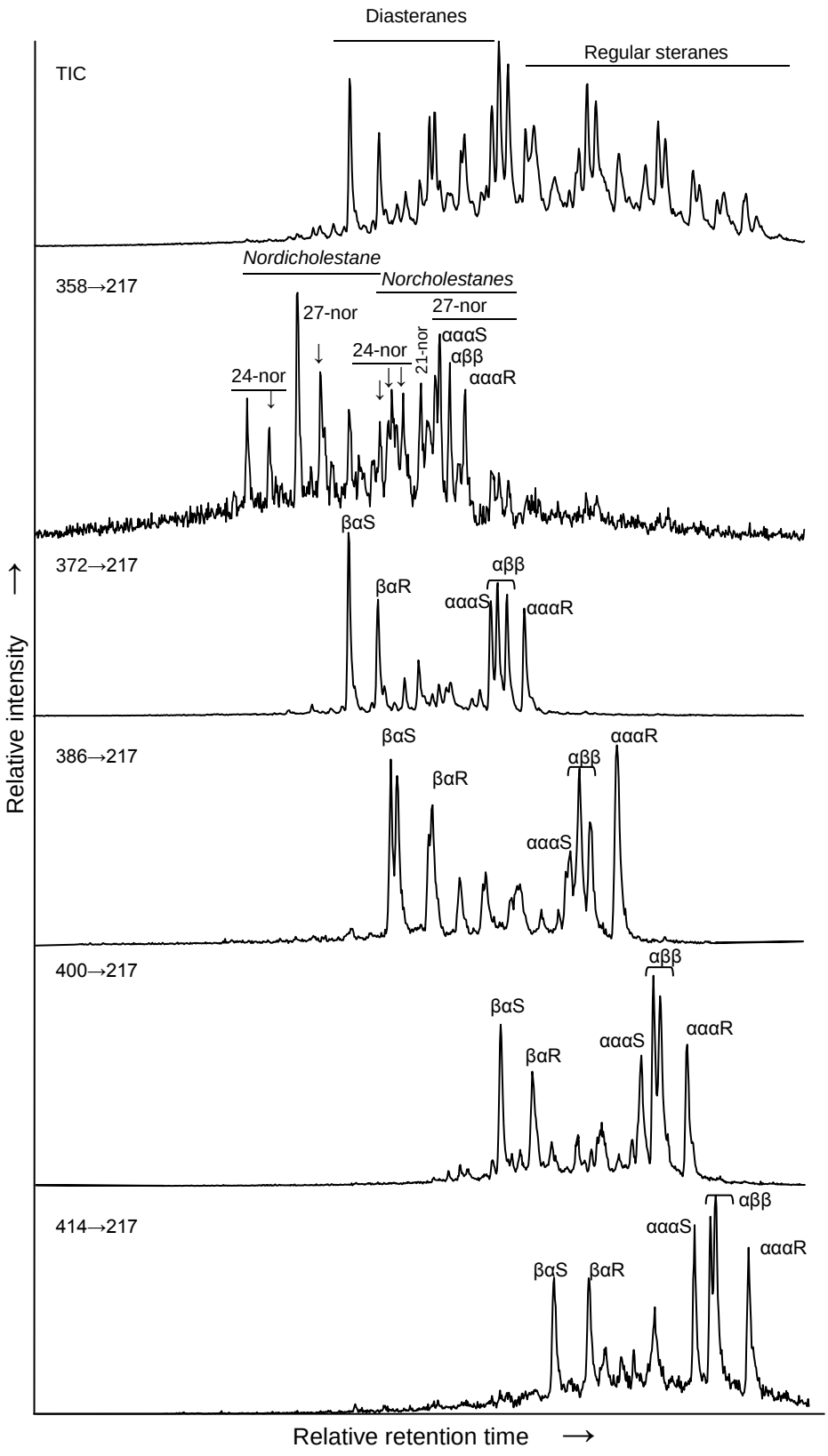

Fig. 4.2 MRM chromatograms show distributions of C_{26}–C_{30} steranes of crude oils (e.g. 6J1-59) from East Sirte Basin. βα, ααα and αββ indicate 13β (H),17α (H)-diasteranes, 5α (H),14α (H),17α (H)- and 5α (H),14β (H),17β (H)-steranes, respectively. Identification obtained from Holba et al. (1998b) Grosjean et al. (2009).

All the oil samples analysed in this study contain *nor*cholestanes (Fig. 4.2; C_{26} steranes identified based on the work of Holba et al. (1998b) and an abundance of C_{28} steranes, consistent with a diatomaceous facies (Grantham and Wakefield, 1988), except the oils from the 5I13-59, VV-65, AA-01 and AA-03 wells (Table 4.2). Holba et al. (1998b) observed a high abundance of 24-*nor*diacholestanes and 24-*nor*cholestanes in oils that were Cretaceous or younger compared with the abundance of their 27-*nor*cholestane analogs. A high abundance of 24-*nor*cholestanes to C_{28} steranes in oils has been attributed to a diatom source spanning the Jurassic to the Tertiary (Holba et al., 1998b). The *nor*cholestanes have been reported to occur in varying quantities in crude oils. Therefore the 24-*nor*diacholestane ratios (NDR) and 24-*nor*cholestanes ratios (NCR) were measured (Holba et al., 1998a, 1998b). The ratios of NDR and NCR vary between the Sirte oils (Table 4.3). For example, NDR > 0.20 points to a Jurassic or younger source, whereas NDR > 0.25 and NCR ≥ 0.40 corresponds to samples derived from Jurassic to Tertiary-aged deposits, consistent with the evolution of diatoms during the Cretaceous Era (Holba et al., 1998b). The variations of relative concentrations of 24- to 27-*nor*cholestanes between the Sirte oils (Table 4.3) may relate to relative effect of thermal maturity between samples (Moldowan et al., 1991). The relative abundance of the 21-*nor*cholestanes ccompared to the 24- and 27-*nor*cholestanes (Moldowan *et al.,* 1991) indicates that thermal maturity has had a negligible effect. The distributions of the 21-*nor*cholestane isomers are similar in all oil samples. None of the samples were found to contain the highly branched isoprenoid (HBI) alkanes, indicating the absence of centric diatoms (genus *Rhizosolenia*) (e.g. Volkman et al., 1994) (Table 4.1).

Dinosterol and associated sterols have been proposed as natural lipid precursors of dinosteranes and triaromatic dinosteroid biomarkers. They are largely produced by dinoflagellate organisms (Withers, 1987; Volkman et al., 1990; Moldowan and Talyzina, 1998). Biogeochemical evidence for dinoflagellate ancestors have been reported in the early Cambrian (Withers, 1987) and molecular evidence has provided a link of cyst-forming dinoflagellates with pre-Triassic ancestors (Moldowan and Talyzina, 1998), although other organisms have also been proposed since the Middle Triassic

(Volkman et al., 1990). These include, bacteria (*Methylococcus capsulatus*) (Bird et al., 1971) and some prymnesiophyte microalgae (Volkman et al., 1990). In this study GC-MRM analyses representative parent-daughter (*m/z*) → ions of 372→217 (C_{27}), 386→231 (C_{28}), 400→2231 (C_{29}), 414→231 (C_{30}) and 414→98 (dinosteranes) for oils from the East Sirte Basin are shown in Figure 4.3.

The 4α-methyl-24-ethylcholestanes and dinosteranes are abundant in all of the Sirte oils with the exception of four oils from the 5I13-59, VV-65, AA-01 and AA-03 wells.

Table 4.3 NDR= 24-*nor*diacholestane ratio and NCR = 24-n*or*cholestane ratio calculated from peaks (C_{26} steranes) of crude oils (Holba et al., 1998a, 1998b).

Well	Field	Formation	Depth (m)	NDR	NCR	3/3+5	3/3+4+6
B-90	Amal	Amal	3090	0.13	0.25	0.35	0.33
B-95	Amal	Amal	3092	0.15	0.25	0.34	0.35
B-99	Amal	Maragh	3053	0.16	0.26	0.37	0.31
D-10	Amal	-	824	0.08	0.12	0.36	0.34
D-17	Amal	-	808	0.20	0.28	0.34	0.32
B-86	Amal	Amal	2996	0.22	0.26	0.38	0.34
B-88	Amal	Amal	3000	0.11	0.16	0.36	0.35
B-96	Amal	Amal	3261	0.26	0.32	0.37	0.34
6J6-59	Galio	Nubian	3430	0.35	0.43	n.d.	n.d.
6J8-59	Galio	Nubian	3290	0.31	0.4	n.d.	n.d.
3V3-59	Galio	Lidam	3102	0.28	0.34	0.41	0.34
6K1-59	Galio	Lidam	3364	0.28	0.34	0.38	0.33
5R1-59	Galio	Lidam	3458	0.22	0.26	n.d.	n.d.
3V4-59	Galio	Nubian	3121	0.25	0.33	0.46	0.36
6C1-59	Galio	Galio	979	0.21	0.25	0.35	0.33
E225-59	Galio	Jakhira	3290	0.21	0.29	0.34	0.33
E216-59	Galio	Augila	3182	0.18	0.24	0.34	0.33
P-12	Masrab	Galio	3329	0.17	0.26	0.34	0.34
Y1-51	Nafoora	Nubian	3036	0.23	0.27	0.38	0.35
Z2-80	Sarir-L	Nubian	3167	0.18	0.25	0.41	0.35
AA-01	Amal	Sahabi	3824	n.d.	n.d.	n.d.	n.d.
AA-03	Amal	Sahabi	3848	n.d.	n.d.	n.d.	n.d.
5I13-59	Faregh	Nubian	3006	n.d.	n.d.	n.d.	n.d.
VV3-65	Sarir-C	Nubian	2667	n.d.	n.d.	n.d.	n.d.

NDR= 24-*nor*diacholestane ratios; NCR= 24-*nor*cholestanes ratios; n.d. not determined; Triaromatic dinosteroid ratios= 3/3+5 and 3/3+4+6 (Moldowan and Talyzina, 1998), 3= triaromatic steroid, 4= triaromatic steroid 3-methyl-24 ethylcholesteroid, 5= triaromatic 4-methyl-24-ethylcholesteroid and 6= triaromatic 2-methyl-24- ethylcholesteroid.

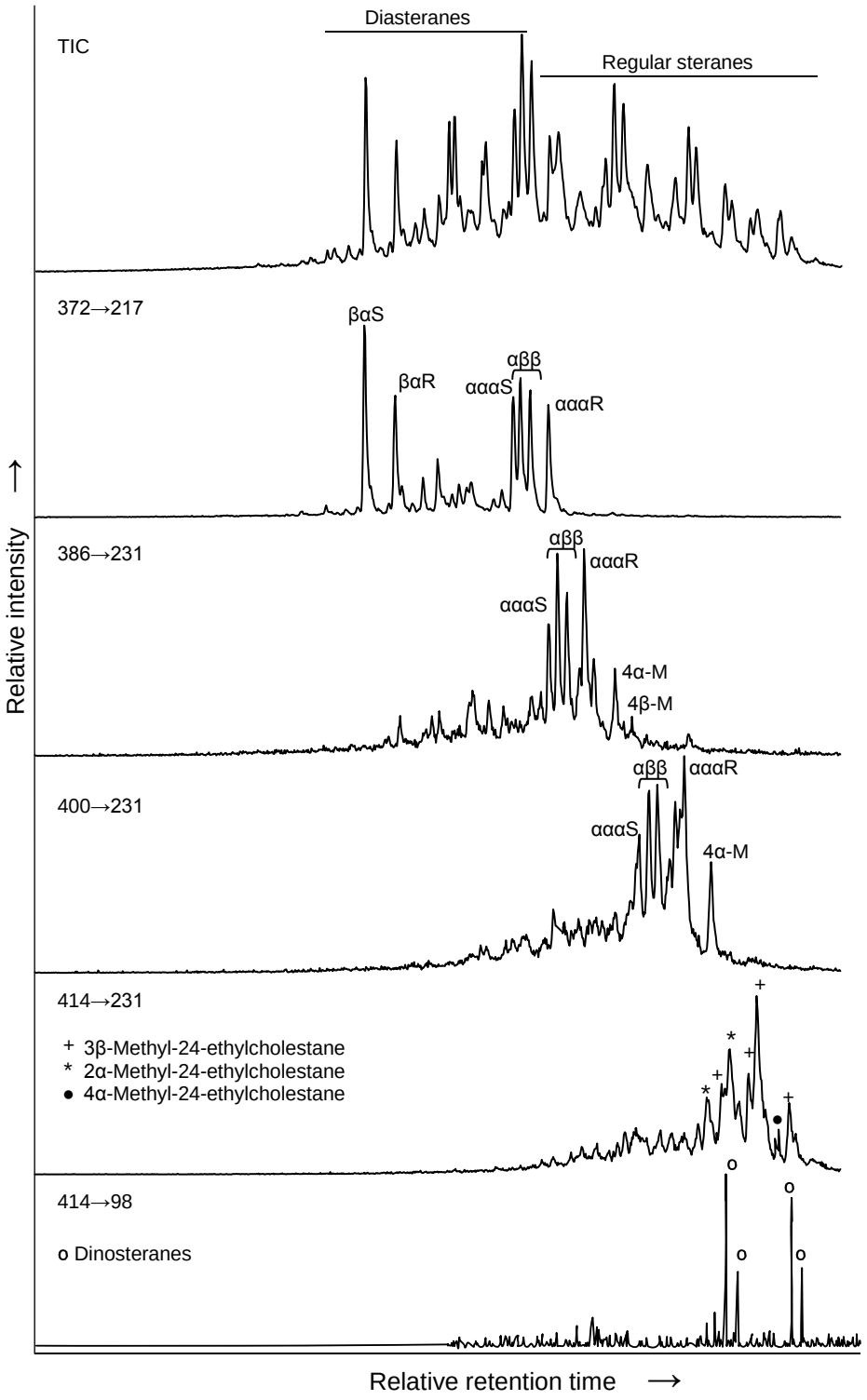

Fig. 4.3 MRM chromatograms show methylsteranes distributions of C_{27}–$C_{30,}$ including dinosteranes and 4α-methylsteranes (4α-M), in crude oils (e.g. D-17) from East Sirte Basin. Identification from Grice et al. (1998b); Peters et al. (2005); Grosjean et al. (2009).

The abundance and presence of dinosteranes and 4α-methyl-24-ethylcholestanes in the Sirte oils can be considered as evidence for dinoflagellates deposited during the Middle Triassic to Cretaceous (Mesozoic). The HYPY products of the extant coral extract analysed in this study by GC-MRM analyses (Fig. 4.4) also revealed a similar distribution of dinosteranes and 4α-methyl-24-ethylcholestanes as observed in the Sirte oils (above) supporting a source from dinoflagellates (zooxanthellae) in the coral. However, the dinosteranes and 4α-methyl-24-ethylcholestanes show isomers with their original biological configuration (dominated by the ααα C_{28}R sterane). This is one of the unique features of HYPY i.e. the original biological configuration is retained during the pyrolysis process (c.f. Love et al., 1995). The triaromatic dinosteroids derived from dinoflagellate precursors have also been considered as age diagnostic markers (Moldowan and Talyzina, 1998). The ratios of the triaromatic steroids in the Sirte oils range between 0.31 and 0.46. These ratios are consistent with a contribution of organic matter (Mesozoic in age). This is also consistent with the presence of dinoflagellate cysts in the Numbian Formation of Lower Cretaceous age (Hallett, 2002).

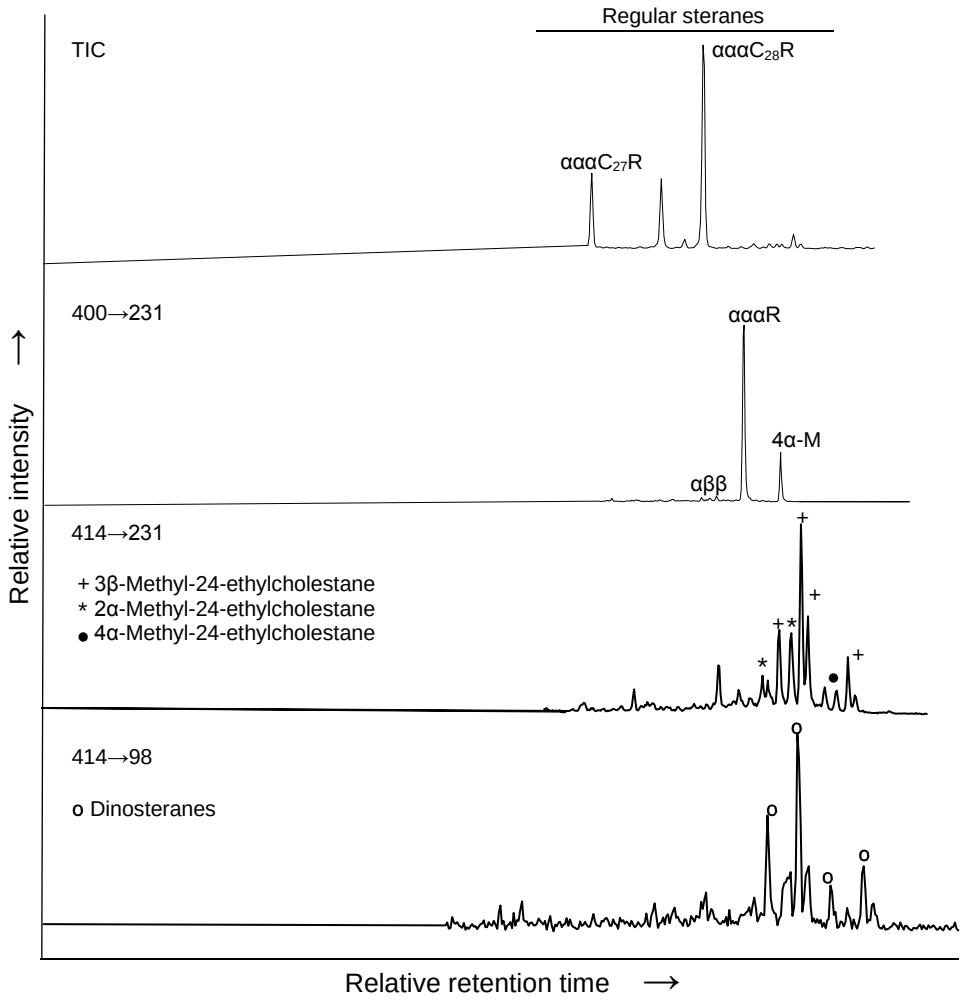

Fig. 4.4 The coral extract analysed by GC-MRM analyses, includes dinosteranes and 4α-methyl-24-ethylcholestanes. Identification from Grice et al. (1998b); Peters et al. (2005); Grosjean et al. (2009).

4.4.2. Source rocks

4.4.2.1. Sterane distributions

Representative parent-daughter (*m/z*) → ions of *m/z* 358→217 (C_{26}), 372→217 (C_{27}), 386→217 (C_{28}), 400→217 (C_{29}) and 414→217 (C_{30}) for source-rock extracts from the East Sirte Basin are shown in Figure 4.5 (e.g. Rachmat Fm; M1-51; 3015 m). All of the extracts contained steranes, diasteranes, *nor*cholestanes and 4α-methyl-24-ethylcholestanes and dinosteranes.

4.4.2.2. 24-*nor*cholestanes ratios (C_{26} steranes)

All of the bitumens contain abundant C_{26} steranes (Fig. 4.5; e.g. Rachmat Fm; M1-51; 3015 m). The NDR and NCR ratios (Table 4.4), are much higher than NDR and NCR ratios in the oils (Table 4.3). The 24- and 27- *nor*cholestane, 21-*nor*cholestane are higher in abundance ccompared to the other steranes in thermally mature sediments (Moldowan et al., 1991). The NDR and NCR ratios vary between the formations (Table 4.4). The Sirte Formation show high abundances of 24-*nor*cholestanes relative to 27-*nor*cholestanes, which is in agreement with a higher thermal maturity for the Sirte Formation compared to the other formations as observed previously Aboglila et al. (2010b).

Table 4.4 NDR= 24-Nordiacholestane ratio and NCR= 24-Norcholestane ratio calculated from peaks (C_{26} steranes) of rock extracts (Holba et al., 1998a, 1998b).

Field	Well	Formation	Depth (m)	NDR	NCR	3/3+4+6	3/3+5
Gialo	6C1-59	Sirte	3051-54	0.36	0.43	0.33	0.32
Gialo	6C1-59	Sirte	3600-03	0.29	0.47	0.35	0.34
Gialo	6C1-59	Sirte	3087-90	0.30	0.41	0.33	0.26
Gialo	6J1-59	Sirte	3528-31	0.27	0.42	n.d.	n.d.
Gialo	6J1-59	Sirte	3542	0.31	0.40	0.30	0.35
Gialo	6R1-59	Sirte	2967	0.34	0.44	0.33	0.26
Sarir-C	KK1-65	Sirte	2670	0.27	0.41	0.33	0.26
Sarir-C	OO2-65	Sirte	2478-81	0.26	0.39	n.d.	n.d.
Nafoora	M1-51	Tagrifet	2882	0.37	0.45	0.33	0.24
Sarir-C	KK1-65	Tagrifet	2745	0.26	0.46	0.31	0.24
Sarir-C	KK1-65	Tagrifet	2760	0.28	0.42	n.d.	n.d.
Sarir-C	OO2-65	Tagrifet	2612	0.29	0.48	0.32	0.28
Amal	B-96	Rakb	2786	0.26	0.42	0.36	0.36
Amal	B-95	Rakb	2725	n.d.	n.d.	0.37	0.35
Nafoora	M1-51	Rachmat	3015	0.33	0.45	0.34	0.22
Nafoora	M1-51	Rachmat	3000	n.d.	n.d.	0.33	0.24
Sarir-C	OO2-65	Rachmat	2681	0.29	0.43	0.34	0.23
Sarir-C	OO2-65	Rachmat	2660	n.d.	n.d.	n.d.	n.d.
Nafoora	M1-51	Bahi	3045	0.25	0.33	0.34	0.27
Nafoora	M1-51	Nubian	3120	0.25	0.36	0.33	0.28
Nafoora	M1-52	Nubian	3090-93	0.26	0.41	n.d.	n.d.

NDR= 24-nordiacholestane ratios; NCR= 24-norcholestanes ratios; n.d. not determined (i.e. samples were not analysed); Triaromatic dinosteroid ratios= 3/3+5 and 3/3+4+6 (Moldowan and Talyzina, 1998), 3= triaromatic steroid, 4= triaromatic steroid 3-methyl-24 ethylcholesteroid, 5= triaromatic 4-methyl-24-ethylcholesteroid and 6= triaromatic 2-methyl-24- ethylcholesteroid.

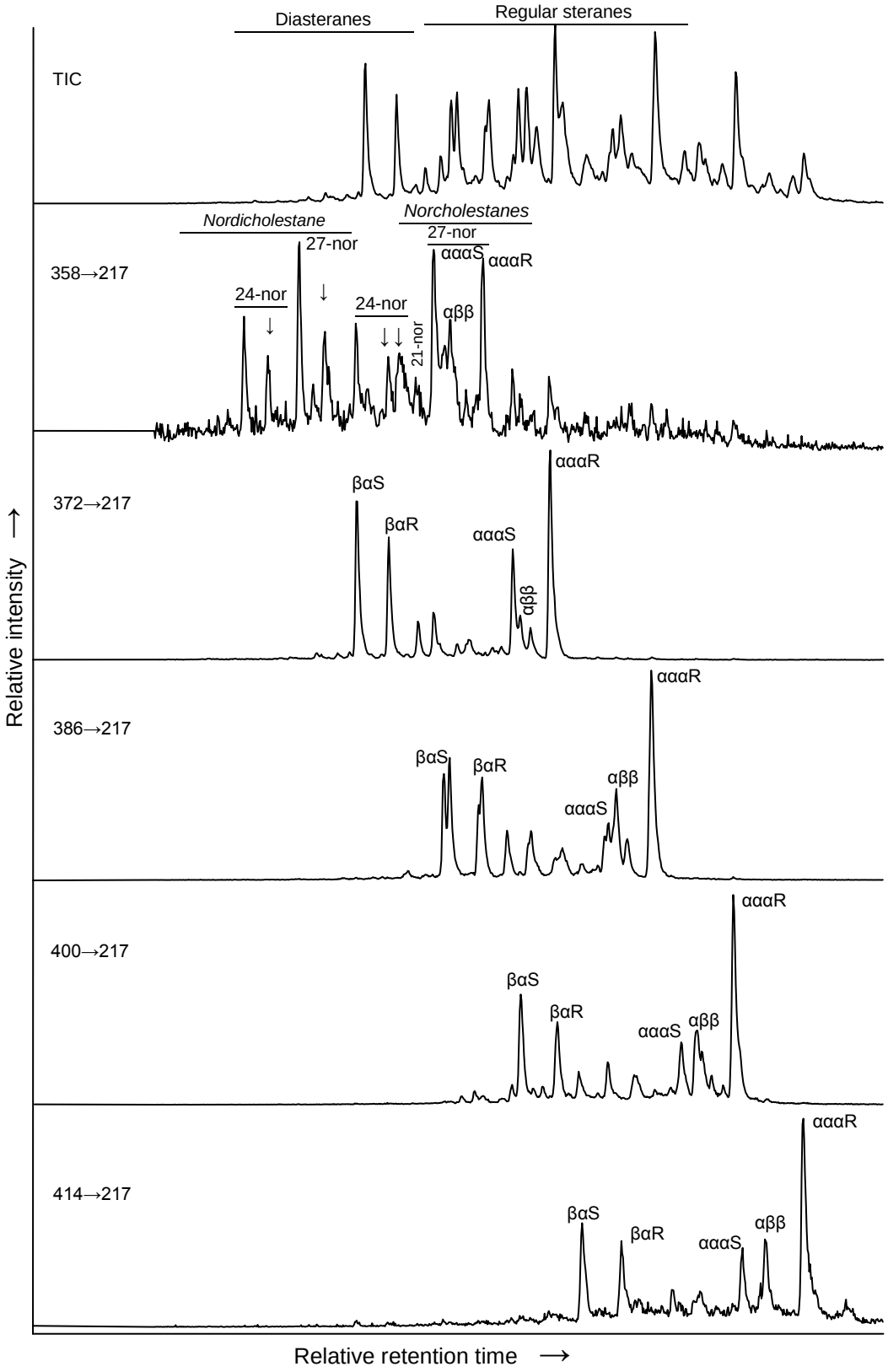

Fig. 4.5 MRM chromatograms show distributions of C_{26}–C_{30} steranes in source rock (e.g. Rachmat Fm; M1-51; 3015 m) based on transitions to *m/z* 217. Identification obtained from Holba et al. (1998b) Grosjean et al. (2009).

The NDR ratios range from 0.25 to 0.37 and NCR ratios range from 0.33 to 0.48 consistent with a Mesozoic age (Holba et al., 1998a & b). Depositions of the Sirte Cretaceous source-rocks are coincident with the evolution of diatoms (Holba et al., 1998b). C_{30} methyl steranes were identified in all extracts (Fig. 4.6; e.g. Sirte Fomation (OO2-65; 2478-81 m), indicating a source of OM from a marine environment (c.f. Peters et al., 2005).

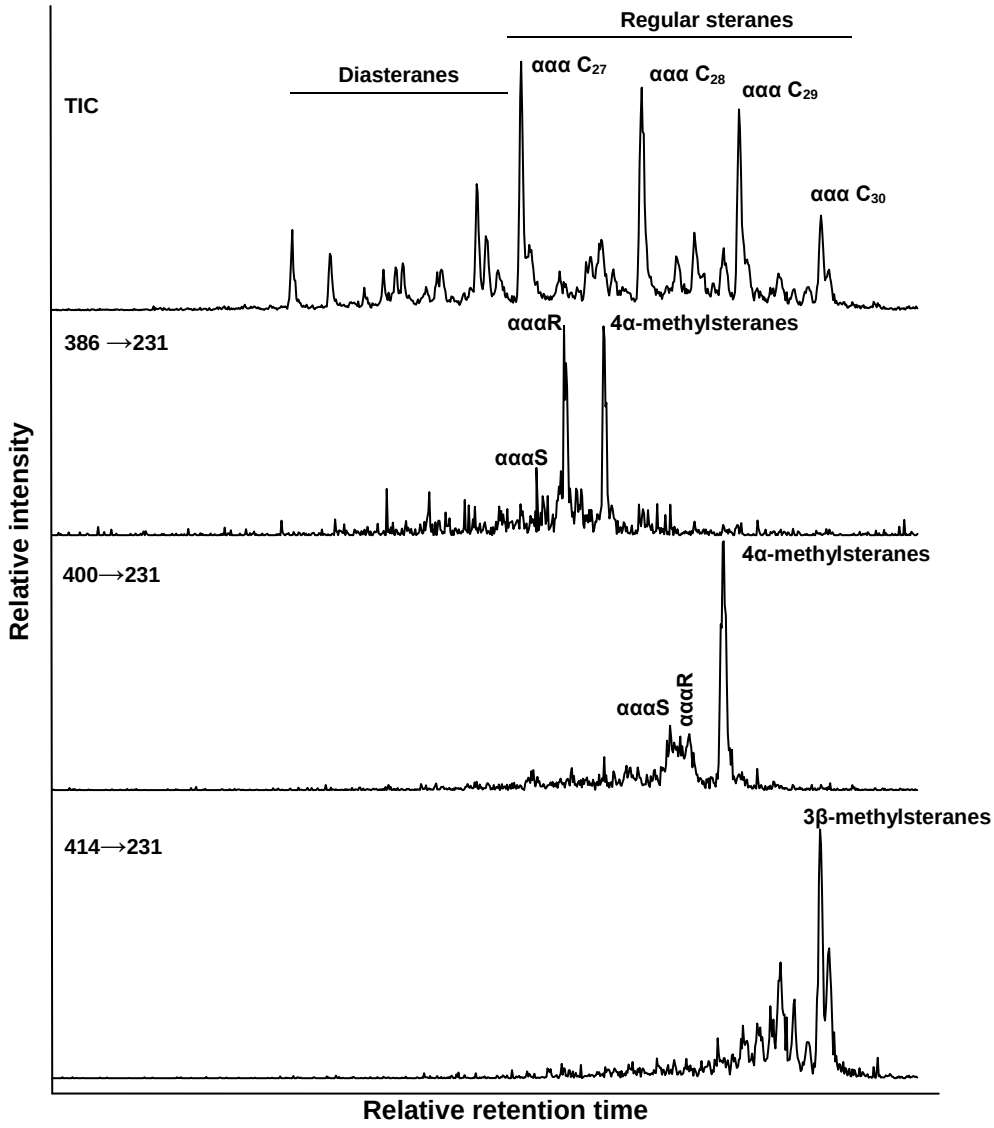

Fig. 4.6 MRM chromatograms showing methylsteranes distributions of C_{27}–C_{30} (e.g. Sirte Fm; OO2-65; 2478-81 m), based on transitions to *m/z* 231.

4.4.2.3. 4α-methyl-24-ethylcholestane and Dinosteranes

TIC and parent-daughter (*m/z*) → ions of 372→217 (C_{27}), 386→231 (C_{28}), 400→2231 (C_{29}), 414→231 (C_{30}) and 414→98 (dinosteranes) for the bitumens from the East Sirte Basin are shown in Figure 4.7 (e.g. M1-51; Tagrifet Fm; 2882 m). All samples contain 4α-methyl-24-ethylcholestane and dinosteranes, derived from 4-methyl-24-ethylsterol and dinosterol precursors produced by dinoflagellate organisms in marine or lacustrine environments (e.g. Summons et al., 1992). The enrichment of such biomarkers throughout the East Sirte shale supports a Cretaceous aged-source. Triaromatic dinosteroids (Table 4.4) were observed in some of the extracts analysed from the studied Sirte formations. The triaromatic ratios varied between 0.22 and 0.37 (Hallett, 2002). These ratios are consistent with a Mesozoic age contribution to the source-rocks.

4.4.3. Oil-source rocks correlations

Oils from the East Sirte Basin show abundant and similar distributions of 24-*nor*cholestanes, dinosteranes, 4α-methyl-24-ethylcholestanes and triaromatic steroids to the bitumens extracted from various formations of the East Sirte Basin providing evidence for a source contribution from dinoflagellates and diatoms deposited during the Mesozoic. The presence of various steroid biomarkers of oils and bitumens and their fractions permit the genetic correlation between the analysed oils and the Cretaceous source rocks. Despite the absence of steroids in oils from the 5I13-59, VV 65 AA-01 and AA-03 wells may suggest that these oils can attribute a different genetic correlation. A various correlation between hydrocarbon from the East Sirte Basin is worth interesting, with a further research should be carried out to identify this additional correlations.

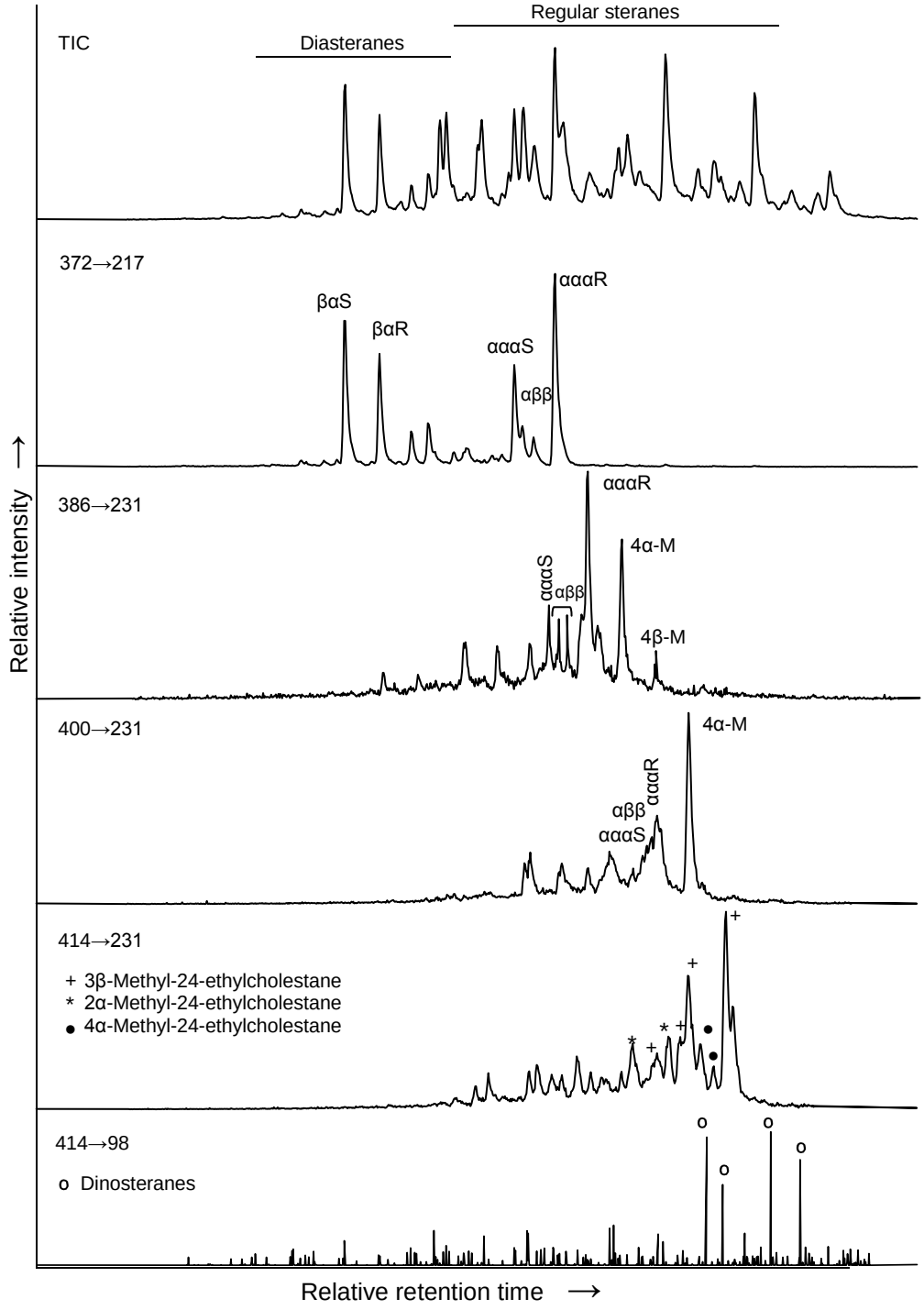

Fig. 4.7 MRM chromatograms show methylsterane distributions including 4α-methylsteranes (4α-M) and dinosteranes in source rocks (e.g. M1-51; Tagrifet Fm; 2882 m), based on transitions to *m/z* 231. Identification made from Grice et al., 1998b; Peters et al., 2005 ; Grosjean et al., 2009.

4.5. Conclusions

All oils and source-rocks from the East Sirte Basin analysed contain a complex distribution of C_{26}–C_{30} steranes with the exception of oils from the 5I13-59 and VV 65 wells. All the samples were found to contain *nor*cholestanes and an abundance of C_{28} steranes, consistent with a diatomaceous facies. The ratios of NDR and NCR varied between the Sirte oils. NDR > 0.20 supports a Jurassic or younger source, whereas NDR > 0.25 and NCR ≥ 0.40 corresponds to samples derived from Jurassic to Tertiary-aged deposits, consistent with the evolution of diatoms during the Cretaceous. Abundant dinosteranes, 4α-methyl-24-ethylcholestanes and various triaromatic steroids provided evidence for a source contribution from dinoflagellates deposited during Mesozoic. This is consistent with the presence of dinoflagellate cysts in the Nubian Formation of Lower Cretaceous age. HYPY of an extant coral revealed a similar distribution (although immature) of dinosteranes and 4α-methyl-24-ethylcholestanes also observed in the Sirte oils and source-rocks).

Acknowledgements

The authors thank Geoff Chidlow for his assistance with GC-MS and GC-MS MS analysis, respectively. We are grateful to the staff of the National Oil Corporation (NOC) in Tripoli, and staff of the Libyan Petroleum companies (Waha – Veba - Gulf) for providing samples. KG acknowledges the ARC for a Discovery grant.

4.6. References

Aboglila, S., Grice, K., Trinajstic, K., Dawson, D., Williford, K., 2010a. Use of biomarker distributions and compound specific isotopes of carbon and hydrogen to delineate hydrocarbon characteristics in the East Sirte Basin (Libya). Organic Geochemistr*y.* Presented at the 15th Australian Organic Geochemistry Conference, Adelaide, September 2008. *In press*

Aboglila, S., Grice, K., Trinajstic, K., Dawson, D., Williford, K., 2010b. A geochemical evaluation of thermal maturity and depositional

palaeoenvironments of seven Cretaceous formations from the East Sirte Basin (Libya). LPI Petroleum Research Journal. *In press*

Ahlbrandt, T.S., 2001. The Sirte Basin Province of Libya – Sirte-Zelten Total Petroleum System. US Geological Survey Bulletin 2202-F. http://geology.cr.usgs.gov/pub/bulletins/b2202-f/ (accessed 20.4.2009)

Atahan P., Grice K., Dodson J., 2007. Human influence on Holocene environmental change in the Yangtze River delta: a combined biomarker, $\delta^{13}C$, 14C, pollen and charcoal approach. The Holocene, 17, 507-515.

Barr, F.T., Weegar, A.A., 1972. Stratigraphic Nomenclature of the Sirte Basin, Libya. Petroleum Exploration Society of Libya, Tripoli, p. 179.

Bastow, T.P., van Aarssen, B.G.K., Lang, D., 2007. Rapid small–scale separation of saturate, aromatic and polar components in petroleum. Organic Geochemistry, 38, 1235–1250.

Bird, C.W., Lynch J.M., Pirt F.J., Reid W. W., Brooks C. J.W., Middleditch B.S., 1971. Steroids and squalene in *Methylococcus capsulatus* grown on methane. Nature, 230, 473-474.

Blokker, P., Van Bergen, P. F., Pancost, R.D., Collinson, M.E., Sinninghe Damsté, J. S., De Leeuw J. W., 2001. The chemical structure of *Gloeocapsamorpha prisca* microfossils: implication for their origin. Geochimica et Cosmochimica Acta, 65, 885-900.

Bode, H. B., Zeggel B., Silakowski B., Wenzel S.C., Hans, R., Müller R., 2003. Steroid biosynthesis in prokaryotes: identification of myxobacterial steroids and cloning of the first bacterial 2,3(S)-oxidosqualene cyclase from the myxobacterium Stigmatella aurantiaca. Molecular Microbiology, 47, 471–481.

Brassell, S.C., Eglinton, G., Marlowe, I. T., Pflaumann, U., Sarnthein, M., 1986. Molecular stratigraphy: a new tool for climatic assessment. Nature, 320, 129-133.

Brocks J.J., Grice K., 2010. Biomarkers (Ancient biomolecules end evolution) Encyclopedia of Geobiology. *in press*.

Burwood, R., Redfern, J., Cope, M., 2003. Geochemical evaluation of East Sirte Basin (Libya) petroleum systems and oil provenance. In: Burnham, T., MacGregor, D.S., Cameron, N.R. (Eds.), Petroleum Geology of Africa: New Themes and Developing Technologies, 207. Geological Society Special Publication, London, p.203–214.

El-Alami, M., Rahouma, S., Butt, A., 1989. Hydrocarbon habitat in the Sirte Basin northern Libya. Petroleum Research Journal, 1, 17–28.

Fowler, M.G., 1992. The influence of Gloeocapsomorpha prisca on the organic geochemistry of oils and organic-rich rocks of Late Ordovician age from Canada. In Early Organic Evolution: Implications for Mineral and Energy Resources (eds. M. Schidlowski et al.), p.336-356.

Ghori, K.A.R., Mohammed, R.A., 1996. The application of petroleum generation modelling to the eastern Sirte Basin, Libya. In: Salem, M.J., El-Hawat, A.S., Sbeta, A.M. (Eds.), the Geology of Sirte Basin II, Elsevier, Amsterdam, p. 529–540.

Grantham, P.J., Wakefield, L.L., 1988. Variations in the sterane carbon number distributions of marine source rock derived crude oils through geological time. Organic Geochemistry, 12, 61–73.

Gras, R., 1996. Structural style of the southern margin of the Messlah High. In: Salem, M.J., El-Hawat, A.S., Sbeta, A.M. (Eds.). The Geology of Sirte Basin II, Elsevier, Amsterdam, 201-210.

Grice K., Schouten S., Peters K. E., Sinninghe Damsté J. S., 1998a. Molecular isotopic characterisation of hydrocarbon biomarkers in Palaeocene-Eocene evaporitic, lacustrine source rocks from the Jianghan Basin, China. Organic Geochemistry, 29, 1745-1764.

Grice K., Klein Breteler, W.C, Schouten, S., Grossi, V., De Leeuw, J.W., Sinninghe-Damste, J.S., 1998b. The effects of zooplankton herbivory on biomarker proxy records. Paleoceanography, 13, 686-693.

Grice, K., Schouten, S., Nissenbaum, A., Charach, J., Sinninghe-Damste, J.S., 1998c. A remarkable paradox: freshwater algal (*Botryococcus braunii*) lipids in an ancient hypersaline euxinic ecosystem. Organic Geochemistry, 28, 195-216

Grosjean, E., Love G.D., Stalvies, C., Fike, D.A., Summons, R.E., 2009. Origin of petroleum in the Neoproterozoic–Cambrian South Oman Salt Basin. Organic Geochemistry, 40, 87–110.

Hallett, D., 2002. Petroleum Geology of Libya. Elsevier, Amsterdam, 1.

Holba, A.G., Dzou, L. I. P., Masterson, W. D., 1998a. Application of 24-norcholestanes for constraining the age petroleum. Organic Geochemistry, 29: 1269-1283.

Holba, A.G., Tegelaar, E.W., Huizinga, B.J., Moldowan, J.M., Singletary, M.S., McCaffrey, M.A., Dzou, L.I.P., 1998b. 24-*Nor*cholestanes as age sensitive molecular fossils. Geology, 26, 783–786.

Huang, Z., Poulter C. D., Wolf, F.R., Somers, T.C., White J. D., 1988. Braunicene, a novel cyclic C_{32} isoprenoid from *Botryococcus braunii*. Journal of the American Chemical Society, 110.

Kohl, W., Gloe, A., Reichenbach, H., 1983. Steroids from the myxobacterium Nannocystis exedens. Microbiology, 129, 1629-1635.

Love, G.D., Snape, C.E., Carr, A.D., Houghton, R.C., 1995. Release of covalently-bound alkane biomarkers in high yields from kerogen via catalytic hydropyrolysis. Organic Geochemistry, 23, 981–986.

Macgregor, D.S., 1996. The hydrocarbon systems of North Africa. Marine and Petroleum Geology, 13, 32-340.

Meredith, W., Russel, C.A., Snape, C.E., Fabbri, D., Vane, C.H., Love, G.D., 2004. The thermal desorption of hydropyrolysis oils from silica to facilitate rapid screening by GC-MS. Organic Geochemistry, 35, 73-89.

Meredith, W., Sun, C.G., Snape, C.E., Sephton, M.A., Love, G.D., 2006. The use of model compounds to investigate the release of covalently bound biomarkers via hydropyrolysis. Organic Geochemistry, 37, 1705-1714.

Metzger P., Casadevall E., Pouet M. J., Pouet Y., 1985. Structures of some botryococcenes: branched hydrocarbons from the B-race of the green alga *Botryococcus braunii*. Phytochemistry, 24, 2995-3002.

Metzger P., Largeau C., 1999. Chemicals of *Botryococcus braunii*. In Chemicals from Microalgae (ed. Z. Cohen), p. 205-260. Taylor and Francis

Moldowan J. M., Fago F. J., Lee C. Y., Jacobson S. R., Watt D. S., Slougui N.-E., Jeganathan A., Young D. C., 1990. Sedimentary 24-*n*-propylcholestanes, molecular fossils diagnostic of marine algae. Science, 247, 309-312.

Moldowan, J. M., Talyzina, N. M., 1998. Biogeochemical evidence for dinoflagellate ancestors in the Early Cambrian. Science, 281, 1168-1170.

Moldowan, J.M., Lee, C.Y., Watt, D.S., Jeganathan, A., Slougui, N.-E., Gallegos, E.J., 1991. Analysis and occurrence of C_{26} steranes in petroleum and source rocks. Geochimica et Cosmochimica Acta, 55, 1065-1081.

Nichols, P.D., Volkman, J.K., Palmisano, A.C., Smith, G.A., White, D.C., 1988. Occurrence of an isoprenoid C_{25} di-unsaturated alkene and high neutral lipid content in Antarctic Sea-ice diatom communities. Journal of Phycology, 24, 90-96.

Pearson, A., Budin, M., Brocks, J.J., 2003. Phylogenetic and biochemical evidence for sterol synthesis in the bacterium Gemmata obscuriglobus. Proceedings of the National Academy of Science, 100, 15352–15357.

Parsons, M.G., Zagaar, A.M., Curry, J.J., 1980. Hydrocarbon occurrence in the Sirte Basin, Libya. Canadian Society of Petroleum Geologists Memoirs, 6, 723-732.

Peters, K.E., Walters, C.C., Moldowan, J.M., 2005. The biomarker guide vol 1: biomarkers and isotopes in the environment and human history. Cambridge University Press, Cambridge, p. 488.

Robinson, N., Eglinton, G., Brassell, S. C., Cranwell, P. A., 1984. Dinoflagellate origin for sedimentary 4α-methylsteroids and 5α(H)-stanols. Nature, 308, 439-442.

Rusk, D.C., 2001. Libya: Petroleum potential of the underexplored basin centers. A twenty-first-century challenge. In: Downey, M.W., Threet, J.C., Morgan, W.A. (Eds.), Petroleum Provinces of the Twenty-first Century. American Association of Petroleum Geologists Memoir, 74, 429–452.

Sinninghe Damsté, J. S., Muyzer, G., Abbas, B., Rampen, S.W., Massé, G., Allard, W.G., Belt, S.T., Robert, J.M., Rowland, S.J., Moldowan, J.M., Barbanti, S.M.,

Fago, F.J., Denisevich, P., Dahl, J., Trindade, L.A.F., Schouten, S., 2004b. The rise of the rhizosolenid diatoms. Science, 304, 584-587.

Summons, R. E., Powell, T.G., 1987. Identification of aryl isoprenoids in source rocks and crude oils: biological markers for the green sulphur bacteria. Geochimica et Cosmochimica Acta, 51, 557-566.

Summons, R. E., Thomas J., Maxwell J. R., Boreham C. J., 1992. Secular and environmental constraints on the occurrence of dinosterane in sediments. Geochimica et Cosmochimica Acta, 56, 2437-2444.

Summons, R. E., Bradley A. S., Jahnke L. L., and Waldbauer J. R., 2006. Steroids, triterpenoids and molecular oxygen. Philosophical Transactions of the Royal Society B: Biological Sciences, 361- 951.

Summons, R. E., Metzger P., Largeau, C., Murray A. P., and Hope J. M., 2002. Polymethylsqualanes from Botryococcus braunii in lacustrine sediments and oils. Organic Geochemistry, 33, 99-109.

Volkman, J. K., 1986. A review of sterol markers for marine and terrigenous organic matter. Organic Geochemistry, 9, 83-99.

Volkman, J. K., 2003. Sterols in microorganisms. AppliedMicrobiology Biotechnology, 60, 496-506.

Volkman, J. K., Barrett, S. M., Dunstan, G. A., 1990. A new source of 4-methyl sterols and 5α(H)-stanols in sediments: Prymnesiophyte microalgae of the genus Pavlova. Organic Geochemistry, 15, 489-497.

Volkman, J.K., Barrett S.M., Blackburn, S.I., Mansour, M.P., Sikes, E.L., Gelin, F., 1998. Microalgal biomarkers: a review of recent research developments. Organic Geochemistry, 29, 1163-1179.

Volkman, J.K., Barrett, S.M., Dunstan, G.A., 1994. C_{25} and C_{30} highly branched isoprenoid alkanes in laboratory cultures of two marine diatoms. Organic Geochemistry, 21, 407-413.

Volkman, J.K., Barrett S.M., Dunstan G.A., Jeffrey, S.W., 1993. Geochemical significance of the occurrence of dinosterol and other 4-methyl sterols in a marine diatom. Organic Geochemistry, 20, 7-15.

Wenzhi, Z., Shuichang, Z., Feiyu, W., Jianping, C., 2005. Gas accumulation from oil cracking in the eastern Tarim Basin: A case study of the YN2 gas field. Organic Geochemistry, 36, 1602-1616.

Withers, N., 1987. Dinoflagellate sterols, in The Biology of Dinoflagelltes. (ed. Taylor, F. J. R.), Oxford: Blackwell Scientific, p. 316-359.

Chapter 5

Conclusions and recommendations for future work

5.1. Conclusions

In Chapter 2 a variety of organic geochemical analyses were applied to large a set of oils from the East Sirte Basin (Libya). The thermal maturity and palaeoenvironment of deposition was established, using biomarker ratios and compound specific hydrogen and carbon isotopes of individual hydrocarbons. Various biomarker maturity parameters separated the oils from the East Sirte Basin into two families (A and B). The family A oils (Sarir-L, Nafoora, Faregh and Sarir-C fields) were found to be relatively more mature. The D values of Pr and Ph were found to be significantly more enriched in D for the family A oils, compared to the family B oils because of the higher thermal maturity of family A oils. Family A oils have relatively more positive ^{13}C values of *n*-alkanes than family B oils, also consistent with the higher thermal maturity of family A oils and their derivation from a terrestrial source rock. The more negative ^{13}C values for the family B oils are typical of a marine source.

In Chapter 3 a number of organic geochemical analyses were applied to set of sediments extracts from the East Sirte Basin (Libya). The thermal maturity of the source rocks from the Sirte Formation were found to be higher based than the Tagrifet, Rakb, Rachmat, Bahi, and Nubian Formations. δD differences between *n*-alkanes and isoprenoids (Pr and Ph) are also consistent with higher levels of thermal maturity for the Sirte Formation.

In Chapter 4 all the oils and source-rocks from the East Sirte Basin analysed were found to contain a complex distribution of C_{26}–C_{30} steranes with (except oils from the 5I13-59 and VV 65 wells). All the samples were found to contain *nor*cholestanes and an abundance of C_{28} steranes, consistent with a diatomaceous facies. The ratios of NDR and NCR varied between the Sirte oils. NDR > 0.20 supports a Jurassic or younger source, whereas NDR > 0.25 and NCR ≥ 0.40 corresponds to samples derived from Jurassic to Tertiary-aged deposits,

consistent with the evolution of diatoms during the Cretaceous. Abundant dinosteranes, 4α-methyl-24-ethylcholestanes and various triaromatic steroids provided evidence for a source contribution from dinoflagellates deposited during Mesozoic. This is consistent with the presence of dinoflagellate cysts in the Nubian Formation of Lower Cretaceous age.

5.2. Recommendations for future work

Novel results are offered within this dissertation and much additional research can be suggested.

- Overall, our findings confirm the complexity of the East Sirte Basin hydrocarbon habitat.
- An additional focus on other potential source horizons and on areas such as Jurassic – Triassic ages or older, restricted rift basins could identify the potential new petroleum sources of the area.
- Combine geological data with basin modeling information of the Sirte Basin.
- Establish if the dinoflagellates and diatoms are from a different source to other hydrocarbons in the Sirte Basin oils.